A Simulation Method for Design and Development of Magnetic Shape Memory Actuators

Thomas Schiepp

A thesis submitted to
The University of Gloucestershire
in accordance with the requirements of the degree of
Doctor of Philosophy
in the Faculty of Media, Arts and Technology

April 2015

Abstract

The systems/products and their design processes have become more and more complicated due to the fact that their requirements in terms of function, durability, reliability and energy efficiency have been increased significantly and that their leading time has to be short and their materials cost has to be low. To meet these requirements, individual parts and subsystems have to offer increased functionality and efficiency themselves. It has been found that smart materials, such as piezo ceramics or various shape memory alloys as well as less known dielectric elastomers or magnetic shape memory alloys, offer ideal preconditions to fulfil such requirements. Among the various shape memory alloys, the Magnetic Shape Memory (MSM) alloy is a kind of smart material that can elongate and contract in a magnetic field. Based on the MSM alloy a new type of smart electromagnetic actuators have been designed and developed. This kind of actuator exhibits the features above. Typically, the MSM material is a monocrystalline Ni-Mn-Ga alloy, which has the ability to change its size or shape very fast and many million times repeatedly. State-of-the-art alloys are able to achieve a magnetic field induced strain of up to 12%. The magneto-mechanical characteristic of MSM alloys is being constantly improved. However, as far as the author is aware, there are no efficient and commercially available tools for engineers to design MSM-based actuators. To achieve this, simulation tools for design are indispensable. This thesis is dedicated to this task.

In this PhD thesis, new design and simulation techniques for MSM-based actuators have been studied. In particular, three simulation methods have been proposed. These three methods extend standard magneto-static FEM simulation techniques by taking into account the magneto-mechanical coupling and the magnetic anisotropy of the MSM materials. They differ in terms of the necessary a priori alloy characterisation (i.e., measurement effort), computational complexity and consequent computing time. The magneto-mechanical characteristics of the MSM material are a necessary and fundamental ingredient for this type of simulation. However, the characterisation of the MSM materials is a very challenging task and requires specific modifications to standard measurement approaches. So, in this thesis, some specific measurement methods of the magneto-mechanical characteristics of the MSM materials have been proposed, designed and developed. It is described how existing measurement instruments can be modified to measure the unique magneto-mechanical characteristics of MSM, so they are applicable and with practical values. Various tests have been carried out to validate the new methods and the necessary characterisations of the properties of MSM materials have been performed, such as the measurement of the permeability of MSM under a defined stress during elongation. The new measurement results have been analysed and the findings have been used to design and develop the simulation methods. The three simulation methods can be used to predict and optimise the current-elongation behaviour of an MSM element under the load of a mechanical stress while excited by a magnetic field. Extensive experiments have been carried out to validate these three simulation methods. The results show that the three methods are relatively simple but, at the same time, very effective means to model, predict and optimise the properties of an MSM actuator using finite element tools. In addition, the experiment results have also shown that the simulation methods can be used to gain some deep insights into the magneto-mechanical interaction between the MSM element and the electromagnetic actuator. In this thesis an evolutionary algorithm which works together with the simulation methods has been developed to achieve individual optimised solutions in very short times.

In summary, from the experiment results, it has been found that the measurements and simulation methods proposed and developed in this thesis; enable designers to perform simulations for a high-quality actuator design based on the magneto-mechanical properties of MSM alloys. This is the first time that a MSM can be characterised for simulation purposes in a fast and precise way to predict

MSM and electromagnetic actuator interactions and identify and optimise the design parameters of such actuators.

However, these simulation methods are strongly dependent on the measurement of the magneto-mechanical characteristics of magnetic shape memory alloys, whose precision can be further improved. To reach commercial success as well higher precision in the simulation prediction, further achievements in the field of material science (e.g. smoothness of mechanical curves) are also necessary.

Declaration of Original

I declare that the work in this thesis was carried out in accordance with the regulations of the University of Gloucestershire and is original except, where indicated by specific references in the text. No part of the thesis has been submitted as part of any other academic award. The thesis has not been presented to any other education institution in the United Kingdom or overseas.

Any views expressed in the thesis are those of the author and in no way represent those of the University

Signed: 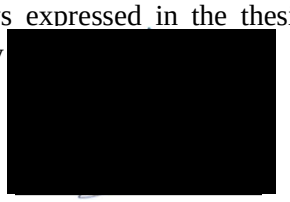 Date: 24.04.2015

Acknowledgements

A successful work is never a one person job and therefore I would like to give very special thanks and my profound gratitude to the following people who brought their own contribution either mentally, physically or psychologically to help in the construction and the accomplishment of this work.

Dr. Shujun Zhang and Prof. Dr. Andreas Schlüter
My supervisors consistently and helpfully advised me with many important suggestions for my research and publications. At many stages of this research I benefited from their advice and it has been a great experience for me to work with you. Thank you for improving my work in many ways.

Dr. Kevin Haphesi
I also would like to thank my advisor for his support and suggestions. He gave me some good advices and helped me to complete my thesis at the University of Gloucestershire.

The staff of Faculty of Media, Arts and Technology of the University of Gloucestershire
Thank you for your help, encouragement, technical, and moral support.

Dr. Michael Schwabe
Thanks to the CEO of ETO MAGNETIC, by giving me an opportunity to do research in this company, I got a chance to benefit from the possibilities and also discovered how important and fruitful it is to work as a team member of such an innovative company.

Dr. Markus Laufenberg and Oliver Thode
Thanks for your enormous support and encouragement before and during this project. Especially Markus was one of the important columns in many stages in the course of this research project and I benefited from his advice, particularly when exploring new ideas.

Dr. Markus Straub
Every Hero needs a sidekick and on our way to the dissertation we both had each other, thank you for constructive ideas, which improved my PhD thesis in so many ways.

Dr. Leonardo Riccardi
I'd like thanking Leo for fruitful discussions during the final phases of the writing process and for improving my writing.

Colleagues
I will also like to acknowledge a number of colleagues at ETO, without whom this experience would have been incomplete. I´d like to thank Manuel Maier for supporting me by building prototypes and doing all the measurements as well as Michael Helmer who helped by realising electronics. Special thanks to Melanie Ulke for producing so many ambitious precision parts by only having schemes. René Schnetzler and Ralf Heist for supporting me during the last phase of my thesis, thank you all. Furthermore I'd like to thank Dr. Walter Zimmermann and Dr. Emmanuel Pagounis for fruitful discussions at several stages of this research. I would like to acknowledge Sandra Schäfer for her brilliant work as my master student. I also liked to thank Jörg Bürssner for fruitful discussions over all the years. As well as Volker Burger who encouraged and supported me to do this kind of research.

My Friends

I thank Gregor Buckenmaier and Sasha Sander for their support in any IT needs in the last decade for realising so many workarounds so that I can reach my targets.

A very special thank to Michael Wider who is since we visited school for master craftsman one of my best friends, without your support I had not come far. I also want to thank Mathias Draxler who encouraged me to do a significant course change in my life and made me prosing to visit the university after I already worked as car mechanic.

My Family
I like to thank my parents by supporting me my whole life, also when I decided leave a good paid job for an uncertain future in trying to study engineering. My parents-in-law Albrecht and Beatrice Strohm, they supported me since my first academic steps by giving me a home without any questions just by a trust in a young guy.

I must express my gratitude to my family, especially my daughter Isabella and my wife Nadine for the continue support and encouragement. Their love and support provided me the energy to attain my work and study.

The list is far from being extensive and I hereby express my profound apologies to those that I forgot to mention by name.

Table of Contents

List of Abbreviations

Variables	Meanings	Unit
5M	Modulation types of unit cells	
7M	Modulation types of unit cells	
10M	Modulation types of unit cells	
14M	Modulation types of unit cells	
NM	Modulation type of unit cells	
A	Surface area	[mm²]
AC	Alternating current	[V]
B	Magnetic flux density	[T]
B_0	Magnetic flux density in vacuum	[T]
B_R	Remanence	[T]
D	Diameter	[mm]
DC	direct current	[V]
DMC	Dynamic magnetisation curve	
EA	Evolutionary Algorithm	
FEA	Finite element analysis	
FEM	Finite element method	
FEMM	Finite element method magnetic	
FSMA	Ferromagnetic shape memory alloy	[-]
H	magnetic field strength	[A/m]
I	Electrical current	[A]
K_1	Anisotropy constant	[-]
l	length of a specimen	[mm]
l_0	initial length of a specimen	[mm]
MSME	magnetic shape memory element	
MSMA	magnetic shape memory alloy	
MNM	Magnetic network method	
n	amount of coil windings	[-]
NOL	Naval Ordnance Laboratory	
Q_s	Quality value for actuator size	[-]
Q_p	Quality value for consumption	[-]
Q_m	Quality value for Maxwell forces	[-]
Q_f	Quality value for desired magnetic flux	[-]
Q_g	Quality value for mechanical stability	[-]
Q_{all}	Summed up to overall quality value with	[-]
R	Correlation coefficient	[-]
R^2	Coefficient of determination	[-]
SBS	Stress bases simulation	
SDM	Stress based magnetisation curve	
SMA	Shape memory alloy	
T	Temperature	[K]
T_c	Curie temperature	[K]
x; y; z	Cartesian coordinates	[-]
ε_0	Maximum strain	[%]
σ_{ext}	External-stress	[N/mm²]
σ_t	Twinning-stress	[N/mm²]
σ_{mag}	Magneto-stress	[N/mm²]
μ_0	Permeability of vacuum (air)	[N/A²]
μ_r	Relative permeability	[-]
φ	Magnetic Flux	[Wb]

List of Figures

List of Tables

1 Introduction

1.1 Project Background

Increased product requirements with respect to functionality, durability, and energy efficiency lead to more and more complex systems and design processes. These requirements, however, have to be fulfilled at competitive system and life-cycle costs. In consequence, individual parts and subsystems have to have more functions and work with high efficiency. The broad class of smart materials, including prominent examples such as piezo ceramics or shape memory alloys as well as less known magnetic shape memory (MSM) alloys, offer ideal preconditions to fulfil such requirements. Therefore, they have a great potential to play an important role in future actuation technologies.

MSM actuators represent a new type of smart electromagnetic actuators where the magnetic shape memory element (MSME) elongates and contracts in a magnetic field. Typically, the MSM material is a monocrystalline alloy that consists of Nickel (Ni), Manganese (Mn) and Gallium (Ga), which has the ability to change its size or shape very fast (Marioni, O'Handley, & Allen, 2003) and many million times repeatedly (Aaltio, Soroka, Ge, Söderberg, & Hannula, 2010). As shown in Figure 1.1, MSM actuators exhibit unique advantages such as fast switching with large work output that could open a new area for various applications. Furthermore MSM actuators offer an ecological advantage, when they are designed as multistable actuators with near-zero current consumption in any stable position (Gauthier, Hubert, Abadie, Lexcellent, & Chaillet, 2006), (Pagounis & Schmidt, 2012). At the moment standard material is available and ready to be used successfully in actuators. However, the MSM technology is still in a research state and further improvements in the material are expected.

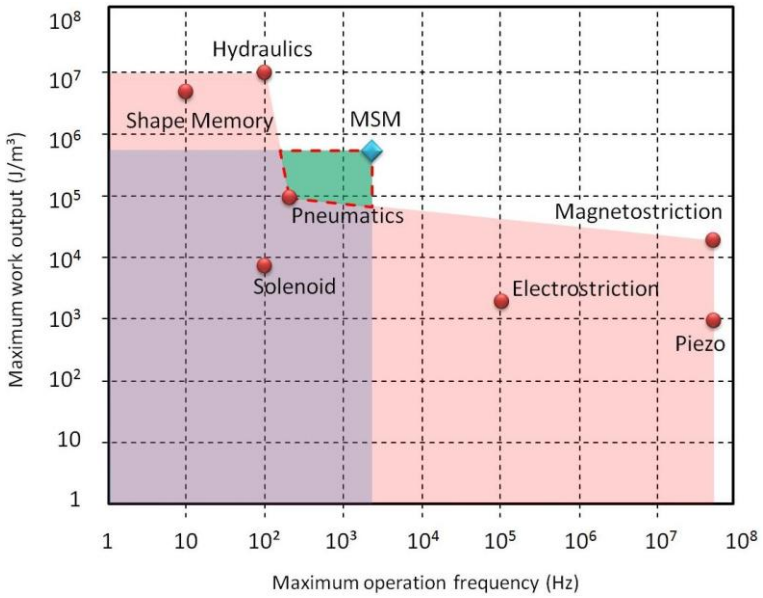

Figure 1.1: Work output vs. operation frequency of actuator types (Benon, 2001)

The market of electromagnetic actuators is a competitive environment in which some technologies are known since the Englishman William Sturgeon invented the first electromagnet in 1825 (Watkins, 1833). To be able to enter this market it is necessary to have a unique selling proposition (USP) and offer an economical advantage. So it is advantageous to start in niche markets, where cost pressure is lower. But in the case of actuator technology the costs are of interest as well and it is necessary to design actuators on customer demand fast and easy to reduce costs already in the design stage and also to be able to compete with established actuator technologies. Therefore MSM requires modified approaches in the complete design process. Simulation tools like the finite element method (FEM),

also known as finite element analysis (FEA) (Kallenbach, et al., 2012), are indispensable in many areas of today engineering. With these tools, engineers can test their designs at an early stage of the design cycle. They determine causes of premature failure in subsequent use; furthermore they can check fast design changes to reduce cost and weight as well as to determine the safety factor of products. Analysis tools for mechanical engineers are of particular value since they can help identifying design problems, which might otherwise not be recognised due to complexity of the developed systems, due for instance to the dynamics of many moving parts of machinery in the construction assessment (Bungartz, Zimmer, Buchholz, & Pflüger, 2009). In the area of MSM, simulations were used for several issues such as the optimisation of the casting procedure or of the material composition. Indeed, electromagnetic simulation was also done with the intention to produce demonstrators to proof functionality of the MSM effect, or for characterisation purposes of the MSM technology. But the improvement of the interaction with an electromagnetic actuator and design optimisation in dependence on a specific customer requirement was subordinated.

1.2 Motivation

To be able to reach commercial success with the MSM technology these simulation tools are indispensable. Because of the specific behaviour of the MSME in combination with the fact that MSM is a young class of material, there is no commercially available software that offers the calculation of an MSM-based actuator. This work investigates such simulation techniques applied to the MSM technology, to allow designing MSM actuators in a fast and precise way and additionally identify and optimize the design parameters of such actuators.

Researchers from different areas were working on MSM and successfully used several simulation techniques with the target to optimise and characterise the material properties. But still no sufficient simulation approach is known, which is adequate for the engineering of a complete actuator and a successful product. The final customers usually provide the desired electrical requirements (e.g., max. voltage and max. current) and are more interested in the overall mechanical properties of the final system. Thus, the main focus of this thesis is to offer tools for the precise prediction of the electro-magneto-mechanical behaviour of an MSM actuator.

1.3 Research Questions, Overall Aim and Objectives

The overall aim of this thesis is to develop simulation methods for the design of MSM actuators, to enable engineers to apply this technology in several application areas. In the case of commercialisation a method is needed that is as fast as possible, as precise as necessary and applicable for product engineers. In contrast, for research purposes it is desired to get a deeper understanding of the effect itself and calculation time is secondary. In any case it is necessary to describe the MSM actuator as a system to receive realistic results. This leads to the following research questions:

- Which simulation model can be used to predict the behaviour of a MSM actuator system?
- Which input data are necessary to perform a simulation with the researched methods?
- Are the researched models adequate for simulation purposes?

Out of these questions arise the following objectives:

- Investigation on simulation models that can represent the MSM behaviour in the FEA/FEM simulation environment.
- Research relevant material properties of MSM and modification of measurement methods for magnetic simulation purposes.
- Validation of the simulation methods.

In the first objective the emphasis is on the simulation model that should describe the magneto-mechanic behaviour of an MSM actuator as a whole system. The model has to consider the macroscopic behaviour of the magnetic circuit and to emulate the behaviour of the MSME as detailed as useful in adequate computing time. Therefore, three simulation methods are developed with varying complexity in terms of preparation (measurement) and execution (calculation).

In magnetic simulations data like magnetisation curves of all ferromagnetic materials are necessary but in this research the properties of all ferromagnetic materials other than MSM play a minor role. But as this has an impact on the simulation results, it should be mentioned here that these are taken into account. Hence in the second objective MSM alloy properties are in focus. The material itself is in research state and ongoing work in this area has continuous impact on the magnetisation curve or on the value of the twinning stress for example. This influences the actuation behaviour and enables further possibilities for customer needs. It is target to research the relevant characteristics of MSM as deep as necessary to receive all ingredients for a working simulation model. Therefore the standard measurement devices have to be modified. This necessary because of the current research state of MSM are no standard measurement devices as well as procedures for particular this kind of material established.

To achieve the third objective, the characteristics of actuator designs have to be evaluated to validate the simulation results. Therefore, 8 MSM samples are characterised with modified measurement methods. Afterwards the samples are implemented in a prototype actuator and the switching behaviour is compared with the simulated behaviour to evaluate the preciseness of each simulation model.

1.4 Contributions to the New Knowledge Generation

The contribution of this PhD thesis to the new knowledge generation would be:

- Simulation methods
    - The Stress Based Simulation (SBS) is very precise model that represents the physical phenomena as reasonable for FEM
    - The Dynamic Magnetisation Curve (DMC) is a quite fast method that need relatively low amount of measurement
    - The Stress Dependent Magnetisation curve (SDM) can estimate functionality in only one simulation run
- Magnetic measurement technique
    - Magnetisation curves of hard and easy axis of MSME
    - Magnetisation curve of MSME at several levels
    - Magnetisation curve in combination of external stress

1.5 Thesis Structure

The structure of the thesis follows basically the chronological course of actions. It starts with the following literature review to get an overview of current work in the area of smart materials and particular with MSM. Chapter 3 describes the research methods. Because MSM is a young class of material and the simulation of such an actuator requires techniques developed in different technical areas, also the methods that are discussed here are from different areas. The researched simulation methods are presented in Chapter 4. It is shown how the model interacts with the magnetic simulation tool as well the simulation procedures and which type of input data is necessary. Especially, the input data are the basis for Chapter 5, which describes how the measurement devices are modified to receive such input data. All measurement results which are necessary to perform the simulation of all three proposed methods as well as the measurements on a MSM prototype are shown in Chapter 6.

Chapter 7 presents the simulation and the benchmark results that compare the performance or even computing time and preciseness of the methods. In Chapter 8 several examples are shown where these methods are used for research issues as well as first steps for commercialisation.

2 Literature Review

2.1 Introduction

An actuator is a device that can be used to act upon a environment. This kind of device is driven typically by electric current, hydraulic fluid pressure, or pneumatic pressure, and converts this energy into motion and can also be used to apply a force (Sclater, 2011). In particular, an electrical actuator is characterised by the fact that it is driven electrically with current or voltage, ideally by low power (Janocha, 2013). Such a device transduces the electrical power into a magnetic field and finally this field into mechanical energy (Kallenbach, et al., 2012). It is typically used in manufacturing or industrial applications such as pumps, switches, combustion engines and valves. Many of those devices are using the reluctance principle, which is based on the behaviour of the magnetic circuit that tends to achieve the state of lowest energy. As a consequence, every moveable part of the circuit will be displaced by a magnetic force to reduce air gaps and minimize the magnetic energy. Among the various actuators, a Magnetic Shape Memory Actuator (MSMA) is a new type of actuator that employs a shape memory alloy to respond to magnetic fields.

2.2 Smart Materials

Smart Materials are a class of materials that can change their properties or characteristics such as shape, size, colour or stiffness depending on an external stimulus like temperature, pressure, electric or magnetic field etc. These materials can be solids, liquids or gases. (Addington & Schodek, 2007). Smart materials have been known since the 19th century, when J.P. Joule discovered magnetostriction (Joule, 1847). Since then, the properties of smart materials have been continuously improved and various new materials have been discovered. Some of these like piezo, or thermal shape memory alloys, have already been successfully commercialised. Further property improvements and more new types of smart materials can be expected in the future. In this section, some of the materials shown in Table 2.1 will be reviewed.

Smart material	Stimulus	Variation
Electrorheologic fluids	electric field	viscosity
Electrostrictive	electric field	force/stroke
Photomechanical	light	force/stroke
Piezo	electric field	force/stroke
Magnetorheologic fluids	magnetic field	viscosity
Magnetic shape memory	magnetic field	force/stroke
Magnetostrictive	magnetic field	force/stroke
Shape memory	heat	force/stroke

Table 2.1: Selection of smart materials

2.2.1 Piezoelectricity

Piezoelectricity is a smart material that is already in the market. This material was already discovered in 1880 from the brothers Jacques and Pierre Curie (Janocha, 2013). As shown in Figure 2.1, they identified, that a deformation, for example of quartz, caused by an applied mechanical stress, polarises this material in a way that the surfaces are charged and an electric field is created. If the surfaces (electrodes) were short-circuited, the surface charges are equalised by a current. This behaviour is called the direct piezoelectric effect. In contrast, the inverse piezoelectric effect, i.e. a material deformation due to an applied voltage, was forecasted by Gabriel Lippmann in the following year due to thermodynamic considerations and confirmed by the Curie brothers experimentally (Janocha,

2013). The piezoelectric effect in natural monocrystalline materials such as quartz and tourmaline is very small. The discovery of polycrystalline ceramics such as barium titanate ($BaTiO_3$), during the second world war (Lee & Aksay, 2001), as well as the findings of their ferroelectric properties (von Hippel, 1950) and the discovery of lead zirconate titanate (PZT) was a breakthrough for the piezoelectric effect (APC International Ltd., 2011).

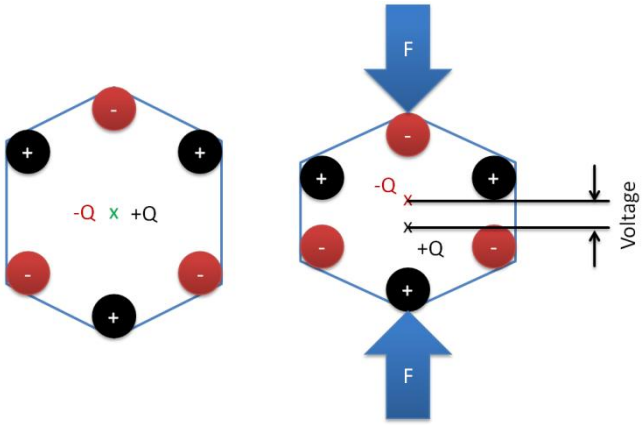

Figure 2.1: Schematic of the piezo effect

This discovery in combination with increasing demands on positioning resolution and actuator dynamics moved the piezo actuators in the focus of interest. Besides the material composition, the main influence on stroke and force is based in the design of the actuator. The most common actuators are the stack actuator and the bending transducer.

The stack actuators are composite structures as shown in Figure 2.2. They are made by stacking separately finished piezoelectric ceramic discs or rings with alternating polarity and metal electrode foils to drive all these actuator elements (green). With this construction, they are connected mechanically in series and electrically in parallel. The changes in length of the individual ceramic layers are finally resulting in an elongation of the stack. Today such piezoelectric actuators show very large forces up to several kN and can reach strokes from nanometres up to several hundred micrometres. Furthermore they are very quick with a response time of a few microseconds (APC International Ltd., 2011). The large forces are an advantage of this technology, but state of the art elongation is often insufficient for applications. To reach a stroke of 1 mm a stack of more than 100 mm in length is necessary. Such a stack actuator is from the costs perspective as well as from the size rather unattractive. Therefore the customer has to modify his system or to transform the force and elongation with a gear mechanism.

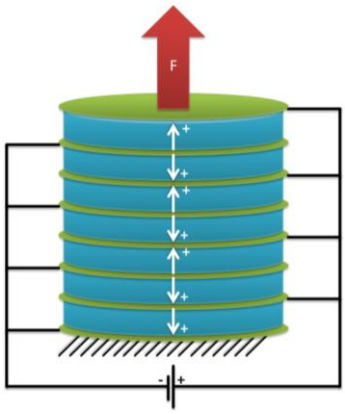

Figure 2.2: Stack actuator principle (Physik Instrumente GmbH & Co. KG, 2012)

One alternative is the piezo bending actuator, which is designed to produce a relatively large mechanical deflection. In a bending actuator two thin layers of piezoelectric ceramics are bonded together, usually with parallel polarisation direction, and are electrically connected in parallel. When a voltage is applied, one ceramic layer expands and the other contracts causing the actuator to flex. This deflection offers a large displacement but a limited force compared to a stack actuator. Anyhow for the control of piezo actuators, voltages in the range of several 100 V are required (APC International Ltd., 2011). This high voltage is for safety reasons often not allowed or at least undesired. In industrial applications 24 V is standard, so that these types of actuators need additionally current sources and safety precautions.

2.2.2 Magnetostriction

Magnetostriction was the first smart material to be recognised. As shown in Figure 2.3, as long as a material is not magnetised, the orientation of so-called domains in the inner of a ferromagnetic material is random. When a ferromagnetic crystal is magnetised the spontaneous magnetisation occurs and the domains become oriented with their axes roughly parallel to one another, causing a shape change. This phenomenon is called magnetostriction. When the magnetisation is taken away the orientation of the domains, as well as the shape, goes back to its original state (Bozorth, 1951). In the case of iron this length change can be of about 14 µm/m or 0.0014 % which is normally invisible. Nevertheless this effect can be recognised easily by the transformer "Hum" noise. Magnetostriction experienced a renaissance in the 1970s, when Terfenol-D was developed. This is an alloy with a "giant magnetostrictive effect" of about 1000-2000 µm/m and therefore is capable to produce shape changes of up to 0.2 % (Janocha, 2013). This material is named after the ingredients terbium, iron (Fe) and the place where it was developed, the Naval Ordnance Laboratory in USA (NOL), the 'D' comes from the addition of dysprosium (Jiles & Devine, 1994).

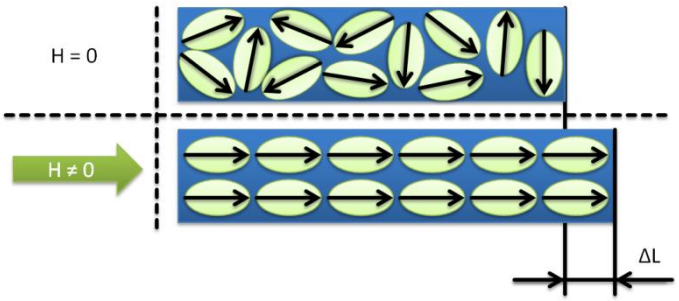

Figure 2.3: Magnetostriction

In 1865 Emilio Villari discovered the inverse magnetostrictive effect, also known as Villari effect. This effect is the change in magnetisation in dependence on stress and is based in the behaviour of magnetic domains. This has impact on magnet steels. Due to high cutting forces during the mechanical treatment the material can be braced mechanically and hinder an orientation during the magnetisation that finally leads to reduced permeability. On the other hand this effect is suitable for sensor applications. Such devices were researched for example for underwater acoustic sensors (Hunt, 1947) and are used as level sensors for turbines of gas and steam power plants.

In general, magnetostriction can be used for actuators (Nyce, 2003). Devices such as sonar transducer linear motor or electro-hydraulic actuators for example were researched (Olabi & Grunwald, 2007). The reachable elongation depends on the length of the main element besides on material properties in general. Although Terfenol-D offers a remarkable magnetostrictive effect, the obtainable strain value is still small for many applications. For example, for an application that needs 1 mm of elongation the Terfenol-D element needs to be 500 mm long, nearly three times longer than the commercially

available samples (Janocha, 2013). The magnetic characteristics of Terfenol-D (Linnemann, 2007) are relatively poor compared to iron, which makes it difficult to apply a sufficient magnetic field along a big Terfenol-D sample. Therefore this effect is suitable for applications with high forces in combination with small elongation. Otherwise a gear mechanism is needed, which leads, in combination with the necessary electromagnetic circuit, to a bulk device, which in turn makes magnetostriction rather unattractive for many actuation purposes.

2.2.3 Shape Memory Alloy

This section is based on the contents of Gümpel (2004), Smith (2005), Lagoudas (2008).

Shape Memory Alloys (SMA) are a group of metallic alloys that "remember" their original shape when they are exposed to a stimulus. This could be temperature or stress. This function is realised by the transformation between two phases or structures accompanied by a shape change, which is called shape memory effect (SME). In contrast to most metals, SMAs have two temperature-related phases in the solid state: the high temperature phase is called austenite and the low temperature phase is called martensite. As shown in Figure 2.4, the shape change between these two phases, that is induced by heat, is called thermal shape memory effect. Differently from the austenite, the martensite phase has two possible crystal structures, called variants. An applied mechanical stress can favour the presence of one or the other variant. Furthermore if the material shows magnetic anisotropic behaviour, this mechanical stress could also be induced by applying an external magnetic field. In this case, the shape change is called MSM effect. The two martensite structures are sometimes described as twinned and detwinned martensite (Liu & Xie, 2007). But in context of an actuator, it is rather precise to refer to the differently oriented crystallographic axis of the two martensite variants (the short and long axes of the martensite variants are depicted in Figure 2.4 as red and black arrows). The class of MSM alloys will be discussed in detail in Section 2.4.

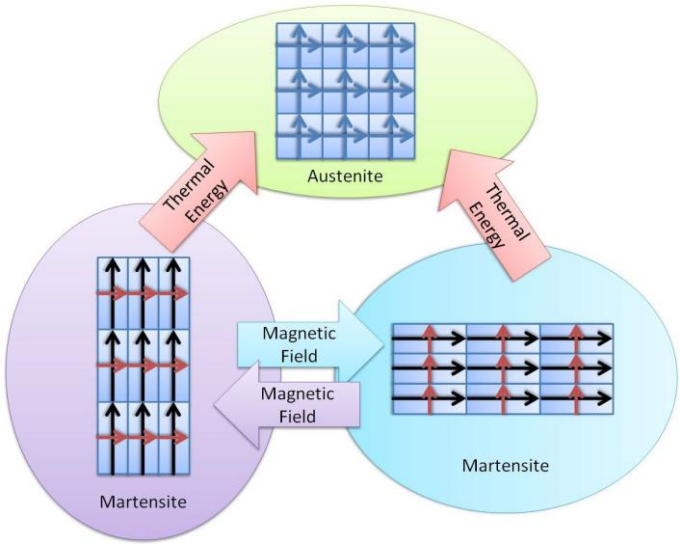

Figure 2.4: Illustration of the microscopic shape change effect

In thermal shape memory alloys, the shape change is based on the temperature dependent lattice and phase transformation between martensite and austenite. According to Otsuka and Wayman (1999), Arne Ölander discovered the pseudoelastic behaviour of the Au-Cd alloy in 1932. In 1963 the discovery of Nitinol (Buehler, Gilfrich, & Wiley, 1963) was a breakthrough for this class of material. The name Nitinol is an acronym for its composition of nickel, titanium and the name of the research institute (Naval Ordnance Laboratory). In contrast to pure titanium and nickel the composition shows

an ordered cubic crystal structure. This composition is able to perform a shape change of up to 8 % (Langbein & Czechowicz, 2013) and can be used up to 400°C (Janocha, 2013). Over the last seven decades several compositions have been researched by alloying elements to existing compositions with a variety of properties (Lagoudas, 2008).

The actuation of this kind of material can be divided into the one way and the two way effect. The one way effect can be observed when a specimen is deformed mechanically in the low temperature martensite phase and afterwards heated up above its phase transition temperature. The specimen will undergo a phase transition to the austenite and can "remember" its shape. Because of that it changes back to its original shape, the one before it was deformed. If the specimen is cool down to the martensite again, it will remain until it gets a new stimulus for deformation. The two-way shape memory effect appears any time when material undergoes, a phase transition between austenite and martensite; therefore it shows the shape memory effect during both, heating and cooling phases.

Thermal shape memory, from a commercial point of view, is a already successful smart material that is used for example in automotive applications in pneumatic valves for seat adjustment, camera autofocus or in minimally invasive endovascular medical applications. Here, Nitinol is used in particular as a self expanding stent induced by body temperature that has the ability to adapt to the shape of certain blood vessels. In particular this example the actuator device in its simplest form just consists of the SMA itself. In this case the heat source is the human body; therefore this device needs only one actuation over lifetime. In such passive systems the heat is caused by the environment, whereas in active systems some heat source is necessary. Usually SMA devices are heated electrically with an electrical current that produces Joule heating, while the cooling is typically obtained by free convective heat transfer to the environment. This makes this actuator quite small and low in weight. As a result of this actuation principle only the first shape change from martensite to austenite can be performed very fast. However, the cooling is relative slow because it cannot be controlled and is at present a drawback of this technology. As shown in Table 2.2 the transformation temperature from austenite to martensite (cooling) is minimum 15 K lower than the transformation temperature from martensite to austenite, i.e. in the heating phase. This makes the cooling by free convective heat transfer even more time-consuming. An improved heat transfer to the environment would lead on the one hand to a faster cooling, but would also reduce the heating performance as well as the overall efficiency of the actuator system. Another drawback of SMA is the amount of reachable switching cycles. As shown in Table 2.2 the NiTi alloys are capable to reach 100,000 switching cycles, which is a too small number for many actuation purposes. Furthermore, the maximum elongation can be obtained only with the one way effect, while with the two way effect it is reduced by more than 50%.

Alloy	NiTi	CuZnAl	CuAlNi	
One way effect	7	4	6	%
Two way effect	3.2	0.8	1	%
Permitted stress	100…130	40	70	N/mm²
Transformation range	-100 … +100	-200 … +110	-200 … +170	°C
Hysteresis	30	15	20	K
Peak temperature	400	150	300	°C
Heat conductivity	10 … 18	120	75	W/mK
Switching cycles	≥ 100,000	≥ 10,000	≥ 5,000	

Table 2.2: Properties of SMA (Janocha, 2013)

2.3 Magnetism

2.3.1 The Magnitude of Magnetism

This section is based on the contents of Kallenbach, et al. (2012), Feynman, Leighton, & Sands (2007) and Janocha (2013).

In order to be able to design electro-magnetic actuators, it is important to know the impact variables. The international system of units (abbreviated as SI from French: Le Système international d'unités) uses two different physical units to describe the value of a magnetic field, on the one hand the magnetic field strength *H* in Ampere per meter (A/m) and the magnetic flux density *B* (so-called "magnetic induction") with the unit Tesla (T), named after Nikola Tesla.

The magnetic field strength *H* describes a field, which is generated in the centre of a single circular coil with *n* turns and a diameter *d* carrying a current *I:*

$$H = \frac{I\,n}{d\,\pi}. \qquad \textbf{2-1}$$

Meanwhile the magnetic flux density is defined by its experimental measurable force on moving electric charges (Jiles, 1998). The magnetic flux is typically given by the Greek letter Phi, (Φ) in the units of Weber (Wb) after Wilhelm Eduard Weber. The amount of flux within a given unit area is the flux density. Since flux is measured in Wb and area (*A*) in metres squared (m^2), the flux density is therefore measured in Weber per meter^2 (Wb/m^2); since 1960 the flux density is denoted by *B* and its unit is called Tesla (T). The magnetic permeability (μ) determines the permeability of a matter to magnetic fields. In absence of magnetic material (vacuum), the flux density vector B_0 and the magnetic field strength vector *H* are depend proportionally via a constant factor, the permeability of the vacuum μ_0 ($4\,\pi\,10^{-7}\mathrm{N/A^2}$):

$$\overrightarrow{B_0} = \mu_0\,\overrightarrow{H}. \qquad \textbf{2-2}$$

Depending on the class of material, the relation between *B* and *H* can be linear or nonlinear. In the case of ferromagnetic materials, the relation involves their relative permeability μ_r, which can be constant but in general depends on *H*. In particular, the relative permeability plays an important role in this thesis, because the model of the magnetic behaviour of MSM alloys is described by μ_r:

$$\vec{B} = \mu_0\,\mu_r\,\vec{H}. \qquad \textbf{2-3}$$

Isotropy implies identical properties in all directions, whereas anisotropy implies direction-dependent properties. The physical characteristics of materials reflect the symmetry of the inner material structure. In many materials the anisotropy of the magnetic properties is small and a scalar permeability (as in Equation 2-3) is a sufficient description for magnetic behaviour of the material. In MSME the anisotropy is large and it has to be considered depending on the simulation model and usage in the actuator. The magnetic permeability of MSME is (like many physical properties of materials) actually a three-dimensional tensor of second order:

$$\vec{B} = \mu_0 \begin{bmatrix} \mu_{rx} & 0 & 0 \\ 0 & \mu_{ry} & 0 \\ 0 & 0 & \mu_{rz} \end{bmatrix} \overrightarrow{H}. \qquad \textbf{2-4}$$

Furthermore the overall magnetic flux density B can be divided into the flux in vacuum B_0 and the flux in magnetic material J at the same field strength. To calculate mechanical stress, which is caused by magnetism, it is important to consider which amount of magnetic field actually acts upon the MSME. Therefore the polarisation describes the material contribution to the total magnetic flux density B, and is also referred to as intrinsic magnetic flux density:

$$\vec{B} = \overrightarrow{B_0} + \vec{J}. \qquad \textbf{2-5}$$

As mentioned, depending on the material class the relation between field strength and flux density can be a constant factor or can have nonlinear behaviour.

2.3.2 Magnetisation and Polarisation Curve

The magnetic flux density and the magnetic field strength are related to the permeability. The relative permeability can be directional dependent and shows nonlinear behaviour in all ferromagnetic materials and therefore also in MSM. There are several known graphs that represent the permeability functions of such materials. In the area of electromagnetic actuators, two graphs are common. One is the so-called polarisation curve, which shows only the flux in the magnetic material (J) in dependence on the field strength; the other is the magnetisation curve that shows the flux density (B) in dependence on the field strength (thus, it additionally considers the contribution of B_0).When a ferromagnetic material is magnetised for the first time it shows a curve starting at the origin, with strong gradient at the beginning and subsequent reduction of the gradient, as sketched in Figure 2.5. It is called the initial magnetisation curve or virgin curve (blue). From the point where the gradient is constant the material is magnetically saturated. A polarisation curve only displays the material contribution and shows therefore an asymptotic behaviour. If the magnetic field is now reduced, the magnetisation follows a different curve. At zero field strength (when $H = 0$), the magnetisation is offset from the origin by an amount B_r, called the remanence. To bring the remaining flux density back to zero an external field in the opposite direction is necessary, which is called coercivity H_c. If an alternating (e.g., a sinus) magnetic field is applied to the material, its magnetisation will follow a "hysteresis" loop (red). The word hysteresis, derived from an ancient Greek word, was used in 1890 by Sir James Alfred Ewing to describe the behaviour of magnetic materials which relate to the existence of magnetic domains: if the material is not demagnetised by a coercive magnetic field or by a temperature above the Curie temperature, it will remain magnetised with a remanence indefinitely long (Tipler & Mosca, 2004) (Feynman, Leighton, & Sands, 2007). The process of decreasing or eliminating the remanence is called degaussing. Due to magnetic hysteresis it is generally not possible to reduce a magnetic field completely to zero, so degaussing typically induces a very small "known" field referred to as bias.

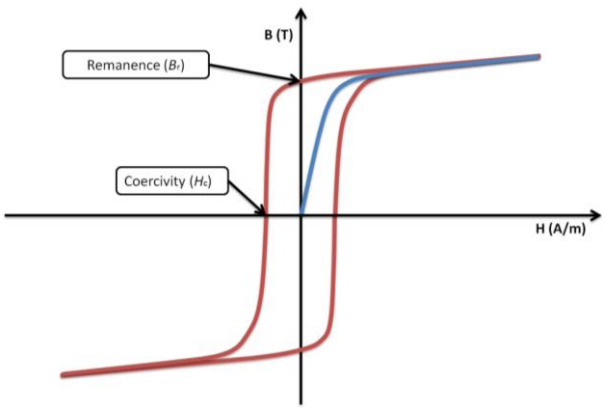

Figure 2.5: Schematic initial magnetisation curve (blue) hysteresis loop (red)

2.3.3 Classes of Magnetic Material

In order to perform magnetic simulations, it is important to consider the properties of the magnetic materials that are adopted in the actuator design. For example, components having a permeability of about μ_r=1 can be simply neglected. So to reduce the complexity of the simulations, it is necessary to estimate which components are neglectable. All common matter show magnetic effects, some materials more than others (Tipler & Mosca, 2004). A material with distinctive magnetic properties is iron and similar effects are observed in nickel or cobalt. Also aluminium is interacting with a magnetic field but this interaction is so negligible, that a human can hardly perceive it. The reason for the different magnetisation and permeability is based on interacting magnetic moments in the material. Each atom has, according to its structure from the electron shell and the core, a shell and a core moment (Feynman, Leighton, & Sands, 2007). The core moment has a much weaker contribution than the shell moment and can therefore be neglected (Mayer-Kuckuk, 1997). In some materials, there is no collective interaction of atomic magnetic moments, whereas in other material the interaction is very strong. One way to introduce the different types of magnetism is, to describe how materials respond to external magnetic fields and finally the value of relative magnetic permeability μ_r. The magnetic behaviour of materials can be classified into the following groups:

- Diamagnetism $\mu_r < 1$
- Paramagnetism $\mu_r > 1$
- Ferromagnetism $\mu_r >> 1$
    - Antiferromagnetism
    - Ferrimagnetism

Diamagnetism is a very weak form of magnetism where a material, when magnetised in an external magnetic field, reduces the magnetic field proportional in its interior. Gold, copper, and bismuth are examples of such known elements. These materials have a tendency to migrate out of an inhomogeneous magnetic field, so it shows a type of a repulsing effect. The diamagnetic magnetisation has a gradient lower than that of vacuum. In contrast, paramagnetic material (e.g. aluminium or platinum) shows slightly improved magnetisation compared to vacuum. When an external magnetic field is applied, the magnetic moments will tend to align themselves in the same direction as the applied field, thus reinforcing it and therefore paramagnetic materials have a tendency to be drawn into a magnetic field. Anyhow Diamagnetism as well as Paramagnetism shows a very weak kind of magnetic effect and are often not applicable in a device and so, are perceived as non-magnetic.

Ferromagnetism shows the strongest magnetic effects: when ferromagnetic materials are magnetised, the magnetic flux density in their interior is increased enormously by a relative permeability that can exceed several thousands in the non-saturated range, as shown in Figure 2.6 for the carbon steel (blue). In an inhomogeneous field, a ferromagnetic body as well as a paramagnetic one undergoes a force toward the location of the strongest magnetic field, generated in order to reach a low energy states as a consequence, mechanical work is performed. The amount of this work is the same that is necessary to remove the attracted body from the field. Ferromagnetic and paramagnetic materials are attracted to the magnetic pole of the external magnetic field, irrespective of the polarity. The ferromagnetism arises from elementary magnetic moments that have a parallel order, which persists through the interaction of the moments with each other, even without an external magnetic field. The direction of the parallel-aligned areas, so called domains or Weiss domains, within the ferromagnetic material rotates in order to align parallel to the external magnetic field (Bergmann, Schaefer, & Raith, 2006).These domains typically occur in sizes from 0.01 microns to 1 micron and are not uniformly oriented in the non-magnetised state of the material.

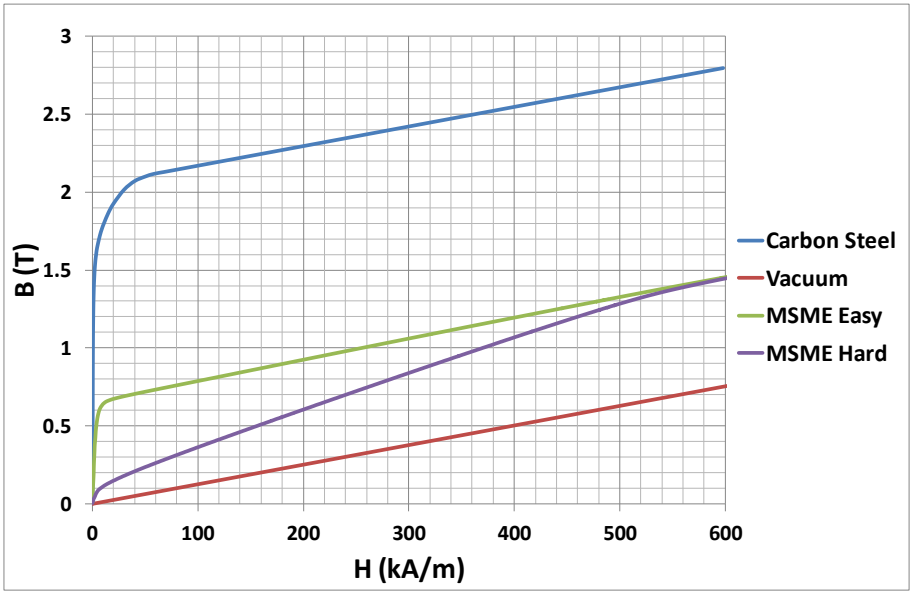

Figure 2.6: Magnetisation of materials

In the periodic table the chromium element is close to iron, nickel and cobalt. Therefore it might be expected that chromium shows the same magnetic behaviour, but the spin direction of each atom in chromium is alternating (spin up ↑ and spin down ↓). There is an interaction with the external magnetic field, but from a technological point of view this is of lower interest because there is no usable interaction with an external magnetic field. This behaviour is called antiferromagnetism. (Feynman, Leighton, & Sands, 2007). In contrast, in ferrimagnetism the orientation of the magnetic moments in either direction is stronger and they do not cancel each other completely (Kittel, 2006) but again the useful effect is low, compared to iron.

2.3.4 Temperature Dependence

Ferromagnetic behaviour is depending on temperature. So every ferromagnetic material has its own characteristic temperature, called the Curie temperature (T_c), or Curie point, (named after Pierre Curie) above which it loses its ferromagnetic properties. This critical temperature point can be considered or neglected, depending on the operational temperature. For example iron is often assumed to have constant magnetic properties at about room temperature, because room temperature is far away from its Curie point (768°C). At room temperature only three elements are known to show ferromagnetic behaviour (iron, nickel and cobalt), while at lower temperatures only some lanthanides. A special class of ferromagnetic alloys are the so-called Heusler alloys, which exhibit characteristics, that mostly would not be expected from the combination of the alloying elements. For example, the first discovered Heusler alloy consists of the non-ferromagnetic elements copper, manganese, and aluminium (Cu_2MnAl), but the alloy shows ferromagnetic behaviour even at room temperature (Heusler, 1903). The MSM alloy is such a Heusler alloy. It shows ferromagnetic behaviour at room temperature, but in contrast to iron MSM has a lower Curie point of 100°C. Therefore, either the particular temperature dependence of MSM alloys needs to be taken into account, or it must be ensured that all measurements are performed far away from the Curie point, or at the same temperature.

2.4 Magnetic Shape Memory (MSM)

The MSM alloys, also ferromagnetic shape memory alloys (FSMA), are smart materials that show effects at the low temperature martensite phase. In 1977 early results were shown in which a plastic

deformation occurred by an applied mechanical stress as well as magnetic field at cryogenic temperatures of 4.2 K in Dysprosium (Liebermann & Graham Jr., 1977). MSM received growing interest since the discovery in 1996, when strains of nearly 0.2 % have been induced in a Ni_2MnGa alloy by a magnetic field ten times lower than in previous works, at 265 K (Ullakko, Huang, Kantner, & O'Handley, 1996). Up to now, Ni_2MnGa is the most studied alloy and shows strain up to 12 % (Sozinov, Lanska, Soroka, & Zou, 2013) and temperature stability up to 353 K (Pagounis, Chulist, Szczerba, & Laufenberg, 2014). In these materials the transformation between two martensite variants can be performed easily by applying a mechanical stress. For application in actuators several shapes can be cut out of the casted crystal. A typical bulk sample has a tetragonal shape and each edge is several mm long and is often called Magnetic Shape Memory "stick" or Magnetic Shape Memory "element" (MSME). Because of their magnetic properties this stress can be induced by an applied external magnetic field. This is advantageous because the magnetic field can be switched fast compared to thermal shape memory alloy. However, the reachable stress in MSM is lower because the phase transformation of the thermal shape effect shows higher stress.

MSM also undergoes a temperature induced phase transition from martensite to austenite by heating and thus shows also thermal shape memory behaviour. Therefore it could be thinkable to use both effects, for example in a circuit breaker. In the case of sudden power overload, they could be activated by applying a magnetic field or, if a continuous load leads to a creeping thermal overload, it could be activated by the resulting heat (Claeys & Vogel, 2006). Anyhow for typical applications where only the MSM effect should be used the temperatures have to be kept below the austenite temperature.

To receive the MSM effect, a combination of material characteristics is required:

- Martensitic crystal structure
- Magnetic anisotropy
- Low twinning stress

2.4.1 Crystal Structures

The atoms in crystals are packed in a periodic pattern, known as the atomic lattice. A crystal consists of so-called unit cells. These unit cells are stacked next to each other in every direction and give the structure of the crystal. The unit cell is defined by the lattice constants, which are the lengths of the cell edges (a, b and c) and the angles between them (α, β and γ) (Kopitzki & Herzog, 2007).

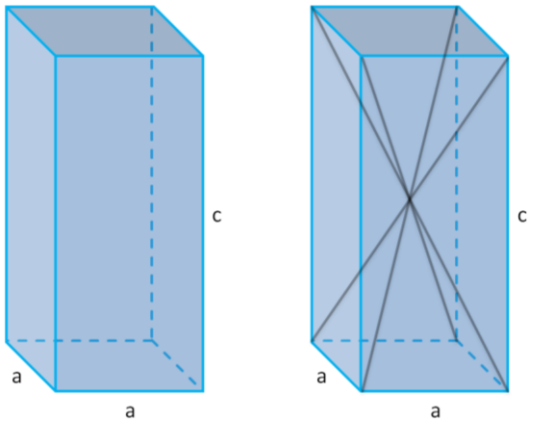

Figure 2.7: Example of a Tetragonal Bravais lattice

For actuation purposes, the ideal MSME completely consists of the same crystal structure which is called a single crystal. Also polycrystalline material could be used, but in this case the macroscopic

effect of the shape change is reduced, so that finally lower elongation of the sample can be expected. The most common composition is an off-stoichiometric Ni_2MnGa alloy that shows a tetragonal Bravais lattice in the low temperature martensite phase. The phase transition temperature from martensite to austenite is today up to about 60°C (ETO Group, 2013) and for improved materials as MAGNETOSHAPE® up to 80°C (Pagounis, Chulist, Szczerba, & Laufenberg, 2014). While cooling down from the austenite phase with a cubic lattice, the crystal typically transforms to a tetragonal lattice as shown in Figure 2.7. The cubic lattice of austenite has obviously a higher symmetry than the tetragonal lattice of the martensite. Consequently, there are multiple configurations of the martensite lattice possible, which are called variants.

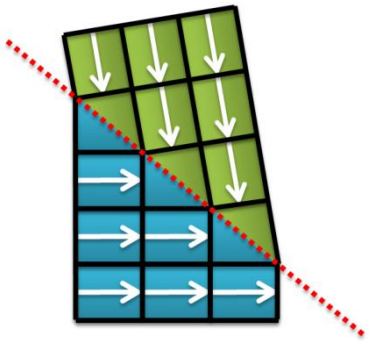

Figure 2.8: Schematic twin variants (white arrow indicates orientation of c axis) and twin boarder

As shown in Figure 2.8, a twinning is formed when two variants (green and blue area) of the martensite phase with different orientation of the c axis (white arrow) coexist. The symmetry axis (red dotted line) between two adjacent variants is called twin boundary. Macroscopically the twins appear as parallel bands (Figure 2.9) alternately containing a different variant. In the case of MSM those twin boundaries, i.e. the borders of such twins, can move when the martensitic variants are oriented by applying a mechanical stress. This microscopic orientation leads finally to a macroscopic shape change and the c/a-ratio of the lattice constants is maximum possible shape change of a complete single crystal MSME. This ratio depends on the modulation of the unit cell.

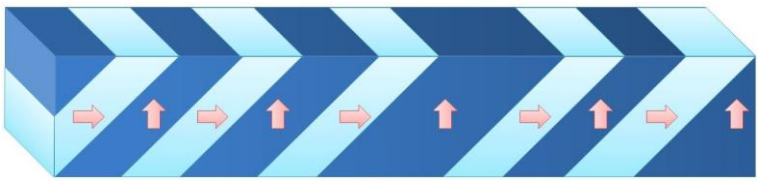

Figure 2.9: Illustration of MSM Sick with martensitic variants and easy axis (red arrows)

During the crystal growth the Ni_2MnGa is cooled down from the high-temperature austenite phase to the martensite phase, where the atomic lattice is transferred from a cubic to the tetragonal form. And because of the different edge length a shift in the lattice will appear as shown in Figure 2.10 on the right. In the simplified schematic view a pattern is recognisable, which is called modulation and is understood as the arrangement or the stacking sequence of a unit cell. The most common modulation is the 10M which is also described as $(\bar{3}\ 2)_2$ (Otsuka, Ohba, Tokonami, & Wayman, 1994) and enables an elongation of the MSME of 6 %. The 10M structure is also referred to as 5M structure. As shown in Figure 2.10 the planes shift three times to the right, two times to the left and the unit cell structure is periodic after these five planes (5M). However, after 10 planes not only the structure, but also the chemical sequence is repeated, so that the structure is called 10M. Additionally, in the scientific area

the 14M structure is known, which should enable a shape change of 10 % and furthermore the so-called nonmodulated structures are supposed to enable an elongation of 20 % (Chmielus, 2010).

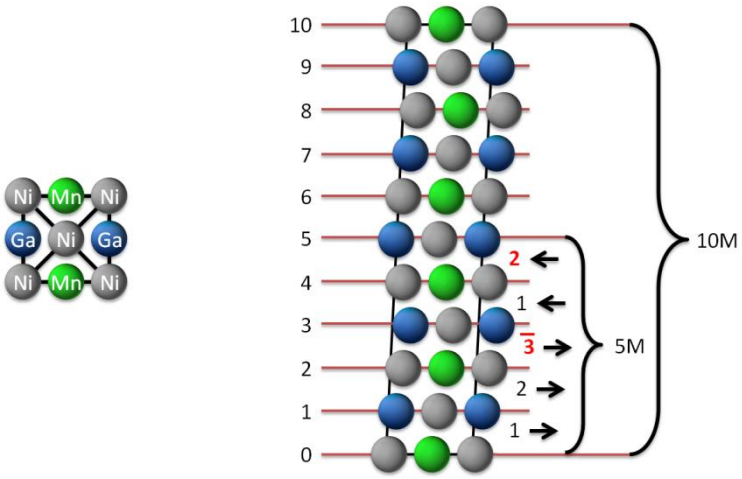

Figure 2.10: Cubic unit cell in the austenite phase (left) and the10M modulation of unit cell in the martensite phase (right) according to Schöppner, 2011

2.4.2 Magnetic Anisotropy

The anisotropy of MSM enables the possibility to have a magnetically-induced stress in the material, which allows the variants reorientation and thus the shape change of the material. This anisotropy is based in the magnetic behaviour of the unit cells, for which the permeability along the short edge, is better than the one along the long edge. This has also effects to the behaviour of a complete sample. When a macroscopic single crystal consists only of a single variant, the magnetisation curve of the complete sample should show the characteristic similar to the unit cell. In Figure 2.11 two polarisation curves of a complete sample are shown. This sample was compressed in a near single variant state: the blue curve represents the hard axis and the red curve represents the easy axis, i.e. the axis with low and high permeability, respectively. This behaviour enables a torque, that is acting upon the crystal structure, when a magnetic field is applied. So the easy axis of each martensitic variant tends to orientate in the direction of the external magnetic field to reach a lower energy state in the magnetic circuit. This torque related to the difference in the magnetisation of the hard and easy axis.

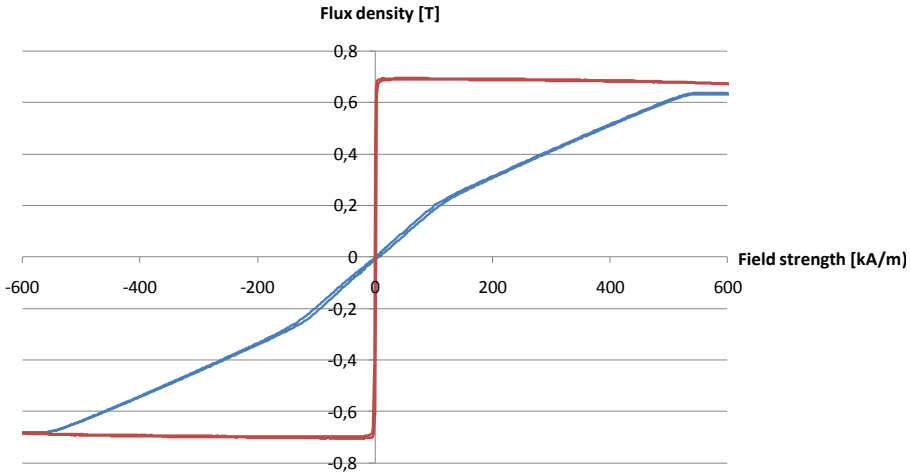

Figure 2.11: Magnetisation curves of a Ni-Mn-Ga element measured along the magnetic easy (red) and hard axis (blue)

2.4.3 Low Twinning Stress

Even a small MSM sample of 1 mm^3 consists of several trillions unit cells, so it is also easy to imagine that several imperfections could affect the sample. These imperfections are called defects. Whereas in standard materials like carbon steel they are common or even wanted, in MSM they are undesired because they prevent the reorientation of the martensitic variants and therefore reduce the amount of the MSM effect. These defects can have several sources. One could be the crystal growth process, where imperfections in the crystal grid could be caused by the phase change from austenite to martensite; because of the asymmetric crystal structure of the martensite. After the production of an MSME a specific mechanical treatment, the so-called "training", can break up some of those defects in the MSME or reduce their amount. This treatment could considerably improve the mobility of the microstructure. But finally imperfections in the crystal are unpreventable. Another source of defects could be inhomogeneity, which can be reduced by an additional thermal treatment. Any of these imperfections will cause lower mobility of the martensitic variants. This is comparable to a bearing without lube or, even worse, to corrosion where the required amount of energy will rise so high that it will be finally immoveable. In a final MSME a minimum amount of stress is needed to induce this reorientation, which is called Twinning stress (σ_T).

2.5 MSMA in Actuators

Most electromagnetic actuators are based on the reluctance principle. Magnetic reluctance is also called magnetic resistance. This magnetic resistance is analogous to the electrical resistance, but rather than dissipating electric energy it stores magnetic energy. Similar to the electric field that causes an electric current to flow across a resistance, a magnetic field generates a magnetic flux over a magnetic reluctance. In a magnetic circuit many magnetic resistances are switched in serial or in parallel. As shown in Figure 2.12, an "air-gap" is a local increase of this magnetic resistance and, as such it tends to store more energy. It is a physical principle that every system tries to get into the lowest energy state and also the magnetic circuits will do. Moveable ferromagnetic parts, like the armature tend to change their position to reduce gaps (the so-called reluctance principle); for the movement forces are generated, called Maxwell forces. MSM actuator obeys to the same principles: the motion of the variants under magnetic the field in MSM actuators occurs because the actuator tries to reach a low-energy state. Anyhow there is a second contemporary effect that can have impact to the actuator behaviour. The reluctance principle will also try to reduce the air gap between the MSME and the magnetic core and will generate Maxwell forces, which rotate the sample within the actuator.

Furthermore it needs to be considered, that in contrast to electricity, air has not the function of isolation. Air is mere a worse magnetic conductor than iron. A part of the magnetic flux does not take the path of the magnetic circuit but possibly flows into air. This flux that gets "lost" in the air is called leakage flux.

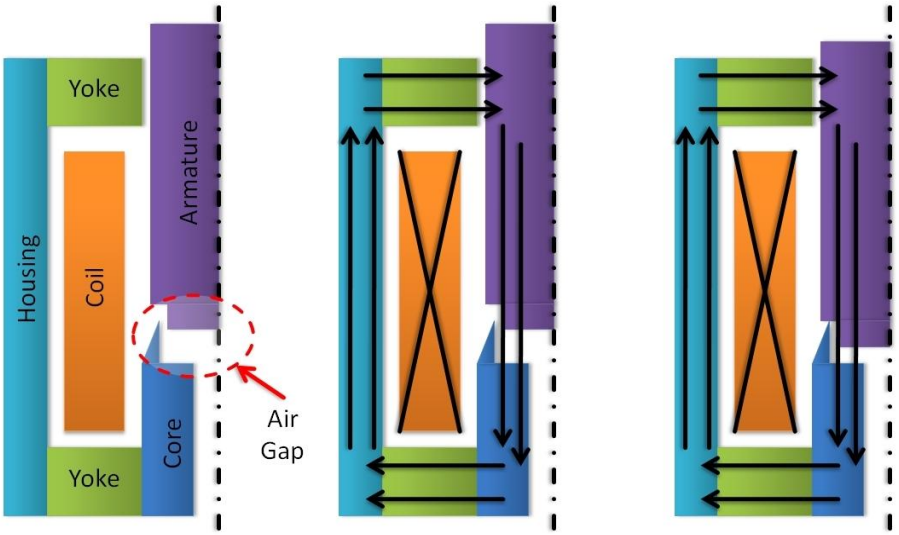

Figure 2.12: Sectional view of a solenoid and schematic magnetic field

To design an MSM based actuator that enables a usable MSM effect the working principle has to be considered. As shown in Figure 2.12, in a solenoid the external usable Maxwell force is acting upon the armature when the magnetic field flows directly from the armature across the air gap into the core. The effective direction of the force is the same as the direction of the magnetic vector field and also equivalent to the direction of motion. As shown in Figure 2.13, in an MSME the external usable expansion force is perpendicular to this vector field. This change of the effective direction has an influence on the design of the actuator itself (Suorsa, 2005). Since the volume remains constant the MSME shrinks in the direction of the vector field. This is caused in the permeability of actual available MSM that is compared to pure iron relative low, but of course much better than air. Finally this leads to a relative thin and long MSME to realize an efficient design with relative small contraction in the direction of the vector field and comparative big elongation along the long side.

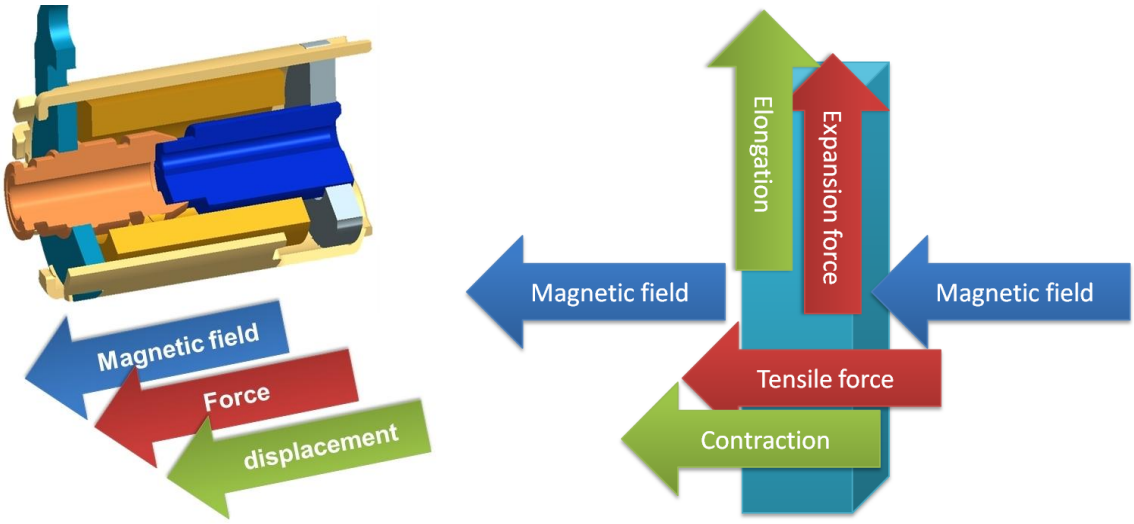

Figure 2.13: Actuator principles in comparison (Left: Solenoid; Right: MSME)

In any reluctance actuator the resistance of the magnetic circuit decreases with increasing stroke (i.e. shrinking air gap) and the resulting force increases accordingly. In contrast, in the MSM actuator (where the air gap is small at the beginning and will grow with the stroke) the force is maximum in the beginning and reduces continuously during elongation. In both cases the force delivery is based on the

principle of the lowest energy state. In the MSM actuator this state is not reached when the air gap is the smallest, but it is reached when the easy axis is aligned to the external magnetic field. The configuration of the anisotropy in the MSME is arranged in a way that the easy axis is along the short edge, and therefore when the MSME is oriented in that way the maximum air gap will appear. This circumstance needs a different kind of thinking while designing an MSM actuator. This shape change has several impacts for the simulation procedure. It influences the magnetic resistance and inductance of the magnetic circuit. As shown in Figure 2.14, with increasing stroke the surface of the MSME (in blue) pervaded by the magnetic field grows and causes a reduction of the magnetic resistance. Simultaneously the air gap between the MSME and the cores (in green) grow, which causes an increase of the magnetic resistance.

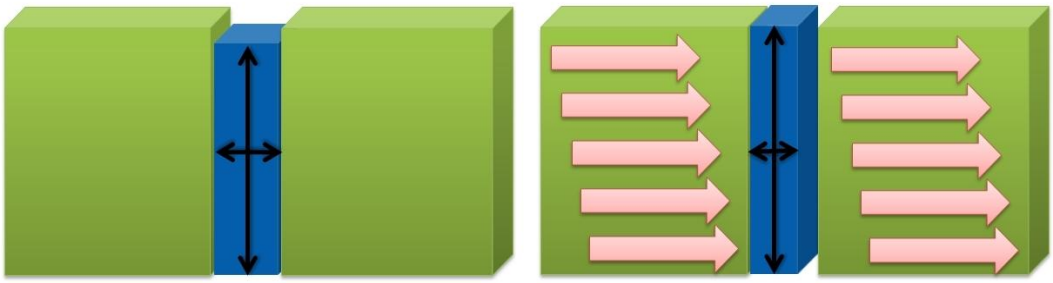

Figure 2.14: Impact of magnetic field-induced shape change of MSM element on magnetic circuit

2.6 Simulation Techniques Related to MSM

Simulation is an approach to analyse dynamic and complex systems. Irrelevant or negligible things can be hidden by simplifications and boundary conditions to gain a deeper insight into the real system (Bungartz, Zimmer, Buchholz, & Pflüger, 2009) (Atherton & Borne, 1991). Although MSM is a very small component, there are several effects in different areas and on different geometrical levels that are worth to research with simulation tools to get a deeper understanding of the nature of MSM.

2.6.1 Phase Field Simulation

The phase field method is a numerical simulation which is mainly focused on the simulation of solidifications including phase transformations (Boettinger, Warren, Beckermann, & Karma, 2002), (Koyama, 2008). This method is qualified for simulations of solidification of dendrites of metals. Therefore, multiple diffusion equations can be coupled and finally allow to solve eutectic solidifications of alloys. These type of simulation is intended on order to determine problems as crystal growth, crystal size or growth direction regarding thermodynamic laws. It also has been extended and utilised across many fields of material science and for types of complex microstructure changes, like in MSMA (Mennerich, Wendler, Jainta, & Nestler, 2011). Nevertheless, this type of simulation is adequate for researching microstructure and to understand the deeper nature of the MSM effect, but not useful to simulate and evaluate the interaction between electromagnetic actuator and the MSME.

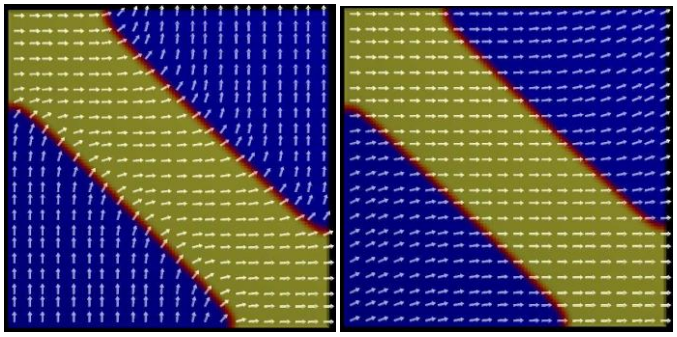

Figure 2.15: Phase field simulation (Mennerich, Wendler, Jainta, & Nestler, 2011)

2.6.2 Ab-initio Simulation

Ab-initio simulations are used to simulate molecule dynamics. This type of simulation calculates the interaction between atoms and molecules for a short period. Because of the huge computing requirement, it is possible to do such simulations for medium-size systems only (Gruner, Entel, Opahle, & Richter, 2008) meaning that these systems are still on a molecular level. So it is suitable to research new compositions and to predict their properties but not for actuator simulation.

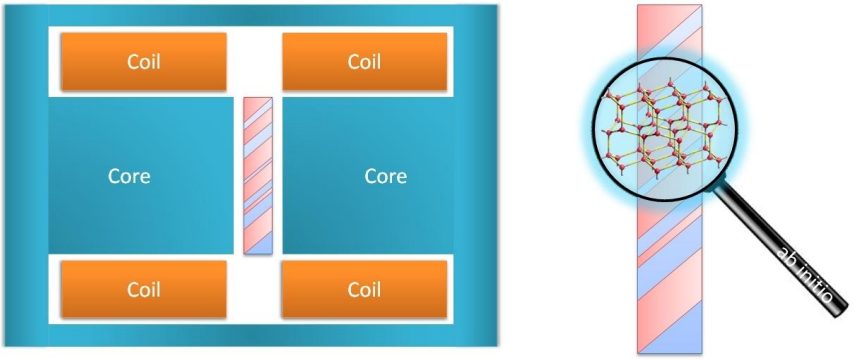

Figure 2.16: Complete actuator (left) vs. schematic Ab-initio (right)

2.6.3 Magnetic Field Simulation

The calculation of the magnetic field plays a central role in the simulation of MSM because the magnetic stimulus induces the shape change in this material. In the area of electromagnetic actuators several simulation methods are well known and used. Thereby the geometric complexity of the problem and the research targets has to be considered (Schneider, 2000). The two most commonly used are the Magnetic Network Method (MNM), also known as 1D and the Finite Element Method (FEM), also called Finite Element Analysis (FEA). The MNM calculates the magnetic flux Φ in a defined magnetic circuit extremely fast. But the time spent on modeling increases with the accuracy requirements and the demand on the engineer is particularly high when the model needs simplifications. FEM is an effective instrument for solving the Maxwell equations for a geometrically based model (Kallenbach, et al., 2012). FEM is fast but compared to the MNM it is a time-consuming method. Both methods are widespread and often used in the scientific and product-engineering areas. Both methods can be extended by multi-domain physics simulations and for instance be coupled to thermodynamics, fluid dynamics and structural analysis. This so called multi-physic simulation enables to emulate the magneto mechanical behaviour of MSM in the simulation. These advantages could be the reason that a lot of work in the area of MSM has been done with this method. There are several measurements and findings that describe and explain the reaction of a MSM as a response to a magnetic field as well as external stress (James & Wuttig, 1998), (Tickle, James, Shield, Wuttig, &

Kokorin, 1999), (Likhachev & Ullakko, 2000), which can be used for building simulation models. One of the first of these models was presented by Suorsa in 2005 where a MNM approach is proposed for a particular actuator (Suorsa, 2005). Ziske proposed also a MNM, with a Tellinen hysteresis model (Tellinen, 1998) based on look-up tables (Ziske, Ehle, Neubert, Price, & Lienig, 2014). Also this model suits to one particular actuator. A drawback of the MNM is that the calculation preciseness of leakage flux is limited (Kallenbach, et al., 2012). To receive precise results it is necessary to adjust the leakage either by a real prototype or a FEM simulation, otherwise, depending on the actuator design, a deviation of more than 10 % is possible (Roos, 2015). So it can be said that MNM is more suited for the analysis of existing actuators and less for the design of new ones.

The main focus of this research is the modelling of MSMA in a magnetic circuit for industrial applications. As mentioned, FEMs are often used for new actuator concepts because of the precision they offer for simulations, and such early-stage precision is indispensable for a successful engineering processes. In industry, simulations with FEMs having deviations from reality below 5 % are quite common. This is due to the possibility to estimate the magnetic flux as well as the leakage flux of an electromagnetic device in a very precise manner. Nevertheless, the unusual behaviour of MSM, compared to any standard magnetic material, can cause difficulties for the simulation with commercially-available simulation software. A critical issue is that MSM alloys change their magnetic characteristic curve (B-H curve) and thus their magnetic properties during elongation. While nonlinear behaviour of magnetic materials and the presence of moving parts, such as a magnetic armature, are standard and solved problems for simulation software, the presence of strong anisotropies (e.g., the magnetic anisotropy of MSM alloys) and the interconnection with the shape change are not. In the field of MSM, standard simulation approaches have often been used for designing actuators mainly devoted to laboratory testing and research. The objective was to obtain an electromagnetic device, that is able to correctly excite a MSMEs (Stephan, Pagounis, Laufenberg, Paul, & Ruther, 2011), while no issues about optimisation were taken into account (Gauthier, Hubert, Abadie, Lexcellent, & Chaillet, 2006), (Krevet, 2010), (Niskanen & Laitinen, 2012). Nowadays, the possibility of a precise FEM calculation of a MSME in an actuator still needs an approach which embeds the peculiar properties of MSM in such simulation environment; for the time being, commercial FEM software does not offer the required features. For instance, an important one would be the description of the changes induced in the magnetic circuit during deformation of the MSM alloy (Schiepp, Laufenberg, Pagounis, & Maier, 2011). For example, the compression of the MSME in the direction of the magnetic field and the elongation perpendicular to the field shown in Figure 2.14 lead to a change of the magnetic resistance and inductance of the magnetic circuit. With increasing elongation the surface of the MSME pervaded by the magnetic field grows, and the permeability of the element in the field direction also improves, causing a reduction of the magnetic resistance of the element. At the same time the air gap between the MSME and the cores (in green) shrinks, which causes an increase of the magnetic resistance, i.e. a degradation of the magnetic circuit. In general FEM software is not able to capture such interconnected variations in standard solutions. To conclude, to design actuators for commercial applications it is desired and necessary to develop a FEM simulation model that allows considering the peculiar characteristics of MSM alloys, and that offers to the actuator/product-designer enough precision and adequate calculation time. This thesis discusses and investigates a simulation approach, which gives to the user such a FEM model of MSM-based actuators.

2.7 Problem Discussion

To gain commercial success with this kind of technology, it is indispensable to consign a possibility for product designers to estimate the behaviour of such a MSM actuator. So he can design an efficient device that suits to customer requirements and is competitive to existing solutions in the market.

Therefore a simulation approach is needed that can simulate the actuator with good precision, low computation burden and in a possible easy-to-learn way.

FEM simulation is an established solution for engineers to design products in several areas. Because this tool is particular suitable for non linear problems where geometrical behaviour is relevant and deeper insight is desired. Although several researchers were working in this field, there is no commercial software available that offers the calculation of MSM based actuators. This is due to the fact that MSM, up to now is not that commercial important like reluctance actuators for instance.

Anyhow such a simulation model has to consider the function principle of MSM, the magnetic anisotropy and the calculation of stress. It is possible to induce mechanical stress by an applied external magnetic field and lead to a fast actuation in both directions. To predict the behaviour of a MSM, that is pervaded by an external magnetic field, several physics are to consider. While electricity is transformed in magnetism which is transferred in the MSME into a mechanical stress it has to be considered if the shape will change or not is also depending on several stresses for example. Because MSM is a ferromagnetic material and has also a solid austenite phase, this class of materiel additionally shows a magnetostriction as well as a thermal shape memory effect.

The combination all effects into a simulation model is only restricted possible and often not necessary. While engineers are accustomed to work with FEM software it is not easy to transfer all these considerations into existing standard simulation software. The thermal shape memory effect as well as magnetostriction is neglected in the frame of this thesis because it is assumed that in the device the temperatures are kept below the austenite temperature and the magnetostriction effects are that low that they can be neglected.

2.8 Conclusion

Actuators are controllable work producing devices. There are several types of actuators existing. Many of them are electromagnetic actuators that are working after the reluctance principle. Particular these actuators are drawing their energy from electricity but others also can be from chemical or mechanical sources for example. These devices differ in their characteristics like stroke (elongation), force and capable switching cycles among others (Zupan, Ashby, & Fleck, 2002). The so-called smart materials are a class of materials that provide interesting properties and therefore can be used as such actuators. They already can and certainly will solve more and more problems in several devices. Since 1996 MSM received growing interest and current state of research makes this class of smart material interesting for actuation purposes.

Several researchers were working on modelling of MSM in several fields. The main focus was on the research of the characterisation and improvement of the MSM alloy. Therefore Ab-initio simulation is an attempt to improve the composition of the MSM alloy and the phase field simulation is a method to optimise the production process like crystal growth. Some attempts also involve the modelling of MSM as response of external stimuli, like magnetism. Nevertheless the interaction between an electromagnetic device and the MSM, for engineering purposes was not on focus. In order to perform magnetic simulations, it is important to consider the properties of the magnetic materials that are adopted in the actuator design. Therefore the magnetic properties of MSM, as well as all magnetic material in the circuit, need to be considered. For the engineer it is desired to be also able to estimate the actuator behaviour of complete new designs so that he can design an efficient actuator that suits to customer requirements and is competitive to existing solutions in the market.

3 Research Method

3.1 Data Collection and Presentation Method

MSM is young and the availability of data is limited to scientific publications. These however are from materials of the ongoing research. Therefore they show variation in the composition as well as production procedure and finally they have variation in the material characteristics. At the moment there is no standard material with defined characteristics available. To be able to validate the simulation approaches, it is necessary to have the characteristics that sufficiently describe the material behaviour. ETO is capable to produce MSM material and is able to characterise standard magnetic material. In this thesis some already existing measurement devices are modified, to enable the characterisation of MSME sufficiently. Therefore these primary data are quantitative and are measured to validate the simulation approaches. Some of these data confirm measurements from the scientific publications and some are totally new. Furthermore these measurement techniques will be used for further studies.

3.1.1 Magnetisation Curves

For any magnetic simulation purpose, magnetisation curves are required, in particular initial magnetisation curves. Usually simulation software possesses a standard database with useful magnetic materials, but at present, there is no data about MSM magnetisation curves. Therefore measurements are necessary. The PERMAGRAPH® is a standard in academia and industry for measuring magnetisation behaviour of "hard" magnetic material. While "soft" magnetic material (for example pure iron) can be magnetised but does not tend to stay magnetised, "hard" magnetic material (for example NdFeB35) in contrast exhibits a high remanence B_r. To measure the coercive field strength H_C the sample needs to be demagnetised in the measurement device. In contrast to iron some permanent magnets have such a high energy density that a magnetic field strength H bigger than 1000 kA/m is necessary. The change form "hard" to "soft" magnetic materials is fluent and the MSMA itself is no "hard" magnetic material in the usual understanding, but its behaviour requires a huge measurement range up to 600 kA/m as shown in Figure 3.1.

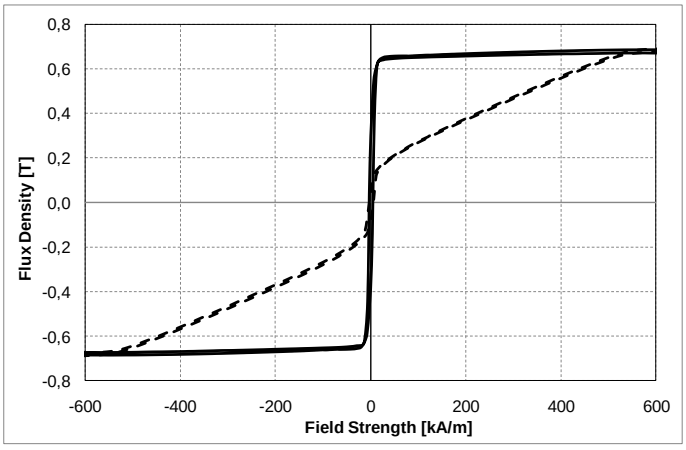

Figure 3.1: Polarisation curves of a MSMA sample measured in the elongated (solid line) and the compressed state (dashed)

The PERMAGGRAPH® is designed to measure remanence, coercivity, maximum energy product and magnetisation curves of permanent magnets up to a field strength of 1800 kA/m. It can handle small specimens with diameter of less than 3 mm up to 60 mm and minimum height of 1 mm which makes this device suitable for MSME measurements and meets the requirements of DIN EN 60404-4:2009-

08. As shown in the schematic view in Figure 3.2, the core can be adjusted by a crank so that the specimen can be placed with the measurement coil in the inner of the device and higher magnetic fields can be reached during measurement by reducing the air gap.

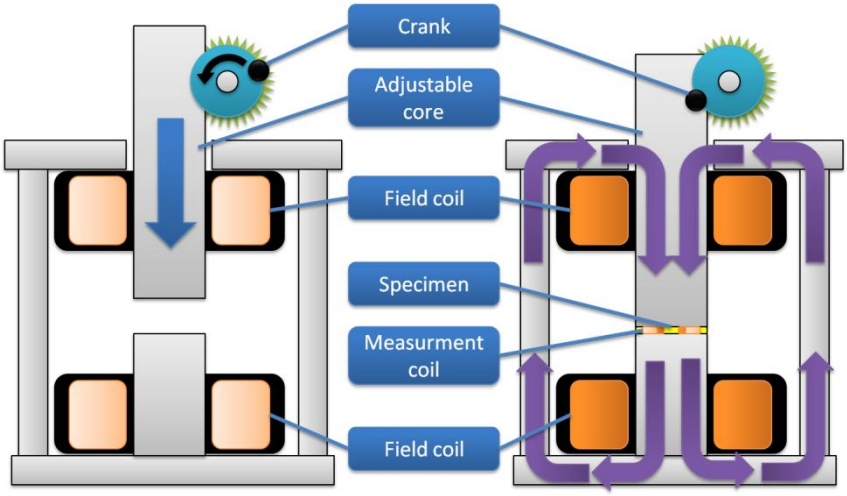

Figure 3.2: Schematic view of PERMAGRAPH® left without and right with sample

When the field coils are energised, the specimen is magnetised and the resulting magnetic field in the specimen can be calculated. The measurement of the magnetisation curve with the PERMAGRAPH® (Steingroever & Ross, 2009) is an indirect measurement method. This means, that conclusions are drawn on the magnetic field in the specimen for selected conditions. As shown in Figure 3.3, the measurement device (yellow on the right) has two coils (left). During the measurement all three areas (green, light blue and dark blue) are pervaded by the magnetic field, generated by the field coils. The dark blue area is the specimen measurement zone, which is partially filled with the specimen (green). The light blue area is the reference zone of the surrounding coil, which measures the magnetic field in the air near the specimen. Therefore, the magnetic flux density *B*, as well as the magnetic field strength *H* that surrounds the measurement zone is known. Finally this makes it possible to calculate the magnetic polarisation *J* of the sample because the surface ratio of the specimen and the measurement zone are known. (Steingroever & Ross, 2009)

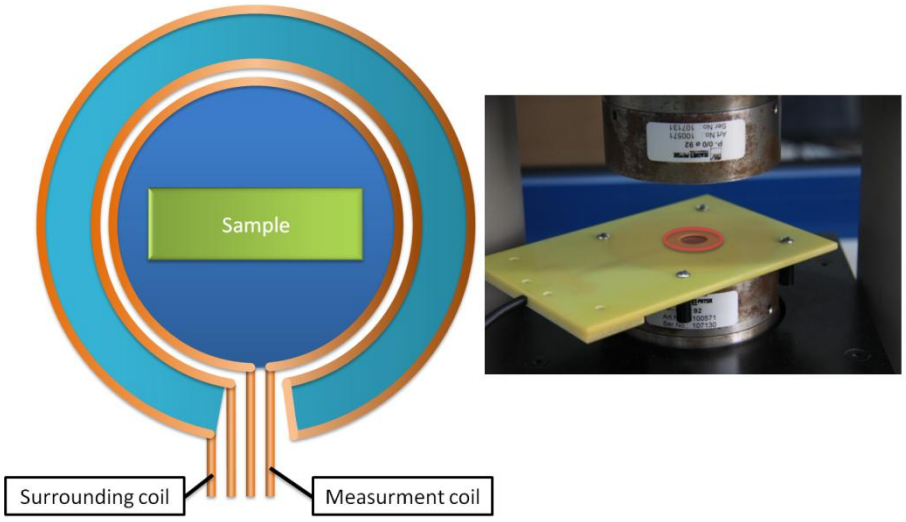

Figure 3.3: Measurement arrangement in the PERMAGRAPH®

3.1.2 Stress-Elongation Curves of a MSME

A force-strain curve describes the quasi-static (i.e., dynamics is neglected) characteristic of force output over strain of a MSME with a particular size at a specific magnetic field. The measurement set-up to obtain such a characteristic entails three devices: the magnetic field generator, the MSMA and the force measurement device. As shown in Figure 3.4, a dipole electromagnet Type 5403 from GMW Electromagnet Coils is used. This device can generate magnetic fields up to 2 T in the measurement zone. An additional temperature unit can cool or heat the MSMA from -30°C to 100°C.

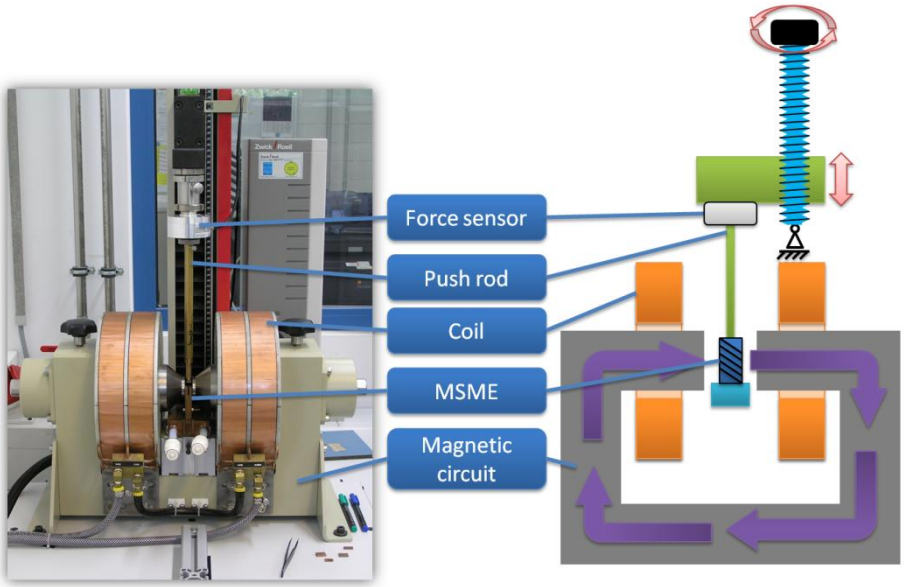

Figure 3.4: Stress elongation measurement device, schematic (right) and photo (left)

For the measurement a device is necessary that can follow a specified position trajectory with an adequate resolution and continuously records the force. Normally this device is used for mechanical testing in tensile and compression mode and is intended for quasi-static loading with continuous, static, pulsating or alternating load sequences and can be controlled by an external computer. A measurement sequence can be programmed and repeated several times, if necessary. The single column Zwicki Line testing machine type 2.5 can operate with a positioning repetition accuracy of +/- 2 µm and drive a system with travel resolution of 0.0828 µm, and is combined with a KAF-TC force sensor which can measure up to 200 N with a resolution of 0.005 N.

In Figure 3.5 typical measurements at room temperature are shown. The upper branch ($H \neq 0$) shows the generated force over strain, when a magnetic field, sufficient to elongation, pervades the MSME. The lower curve ($H=0$) shows the needed amount of force, that is necessary to recompress the MSME into its initial state. The illustrated measurement was made with a particular sample, having dimensions of 2 x 3 x 15 mm³.

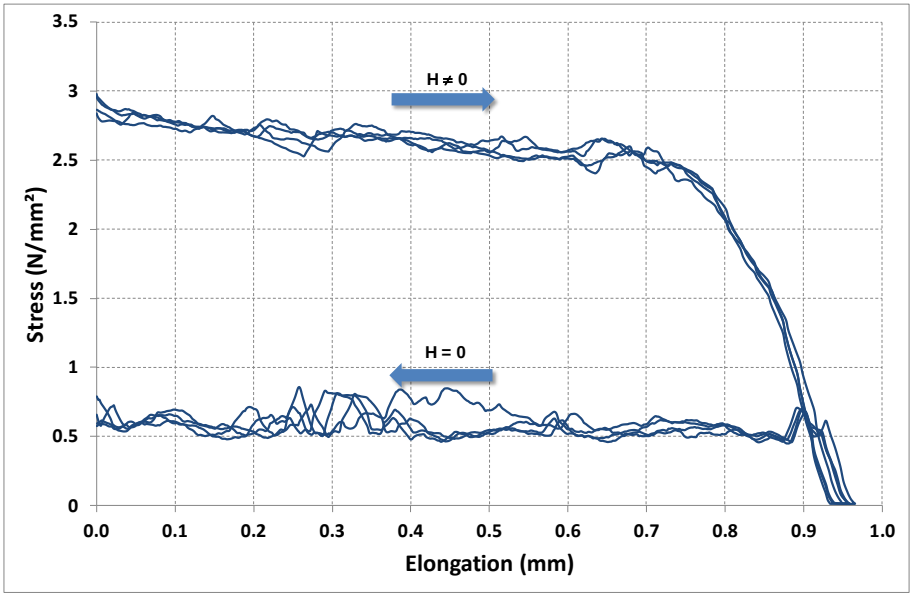

Figure 3.5: Stress-elongation behaviour of an MSME measured in the test setup

3.1.3 Stress-Displacement Curves of a MSM Actuator

This measurement is similar to the one described in Section 3.1.2 with the difference that here a complete MSM actuator is characterised and the resulting force of the complete MSM actuator is measured. The force will be typically lower than measured in the GMW because the actuator, having smaller coils than the GMW, will likely generate a lower magnetic field. As shown in Figure 3.6, the GMW is replaced by the MSM actuator. It is possible to control the current profile with an external circuit through an interface. This is necessary because the measurement current has to be applied to receive the elongation and has to be switched off during compression to measure the restoring force.

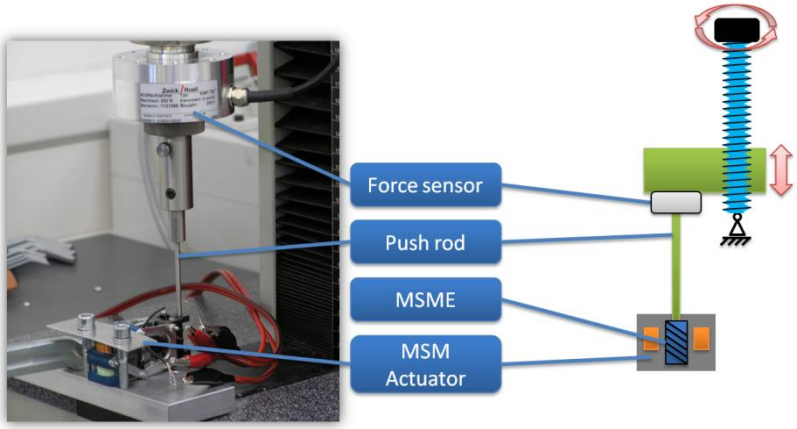

Figure 3.6: Measurement setup with mounted MSM actuator

3.1.4 Current-Displacement Curves of a MSM Actuator

The electrical current flowing through a conductor generates a magnetic field. If the coil, the magnetic circuit and the MSME are arranged in an ideal configuration a low current is necessary to induce a shape change in the MSME. In this measurement the shape change in relation to the needed amount of current is shown. To measure the strain as shown in Figure 3.7, a triangulation laser from Micro-Epsilon optoNCDT 1630-10 is mounted. This laser can measure a range of 10 mm with a resolution of

0.5 µm and a linearity of +/-20 µm. The MSM actuator with a MSME with typically 15 mm length can elongate of about 0.9 mm so that the strain can be measured in approximately 1800 steps.

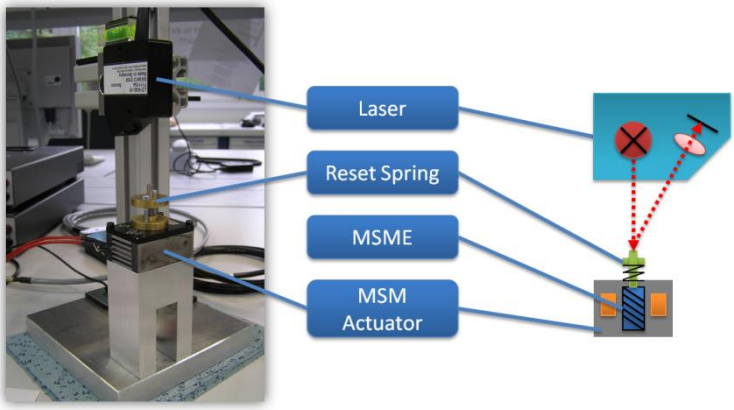

Figure 3.7: MSM actuator and triangulation laser

3.1.5 Elongation-Field Curves (Butterfly Curves)

The so-called "butterfly curves" characterise the reachable elongation of a MSME under a defined load (pre-stress) and over the applied field strength (Karaman & Lagoudas, 2006). These curves are particularly useful to design MSM actuators with external load. The pre-stress is related to the cross-section of the specimen, but the cross-section will decrease during elongation and increase during compression because of the shape change. Therefore this measurement is challenging because ideally the pre-stress should remain constant all along the measurement. In this measurement procedure the magnetic field will increase continuously from zero to maximum and decrease back to zero. The measurement of the magnetic field is, in this case, also challenging, because it is only possible to measure the magnetic field beside the MSMA in an air gap of the magnetic circuit. The location of the sensor has to be considered carefully to draw correct conclusions because of inhomogeneity of the magnetic field between the poles.

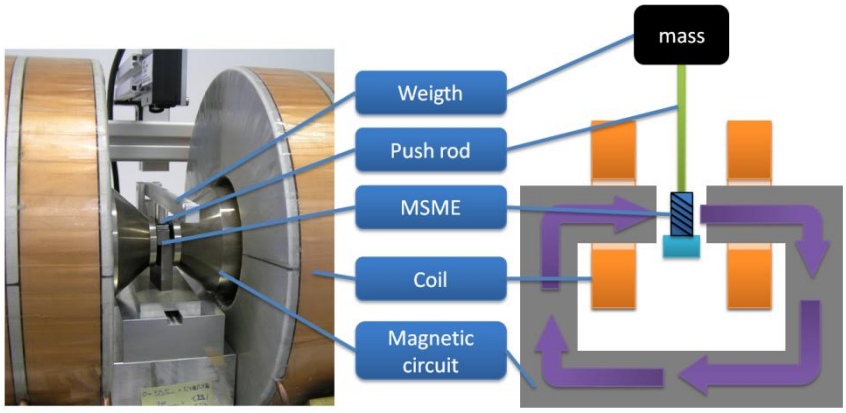

Figure 3.8: Measurement setup for elongation field curves

The black curve in Figure 3.9 shows the behaviour with nearly zero pre-stress, where maximum displacement at lowest external magnetic field can be achieved. The blue curve shows the behaviour under a load (pre-stress) of 0.5 N/mm². The required magnetic field strength increases to receive maximum stroke but after the magnetic field is switched off the MSME almost comes back to its initial state. The red curve shows a complete elongation and a complete return to the initial state as well. So it can be seen that the pre-stress should be slightly higher than for the blue one, because this

allows full stroke at a minimum magnetic field strength. Furthermore the orange curve at a pre-stress of 3.0 N/mm² shows elongation of 1.5 % at higher fields. It can be seen that it would be possible to receive a small elongation at very high pre-stress, or full stroke at lower pre-stress, so that a design trade-off must be met. The value of pre-stress which does not allow the elongation of the MSME is called blocking stress.

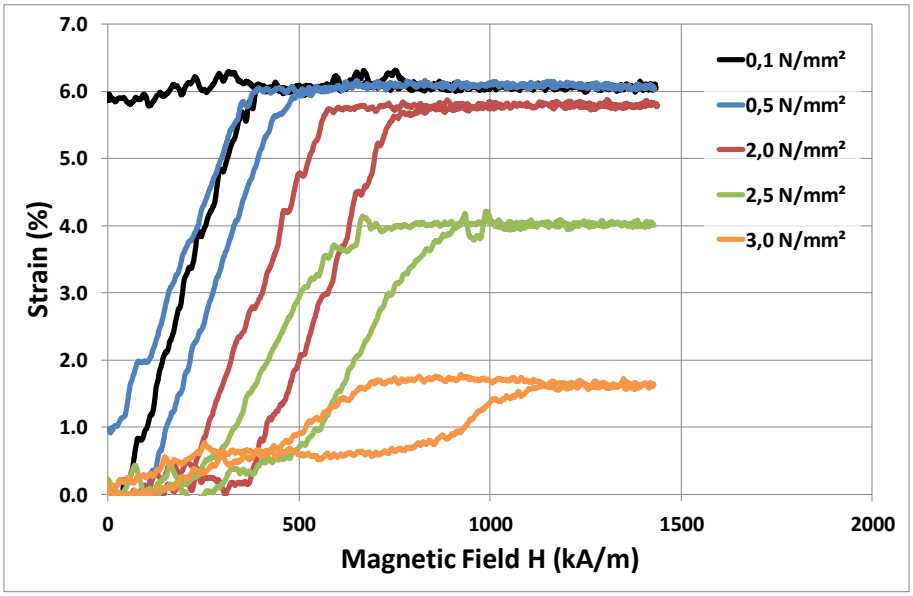

Figure 3.9: Butterfly curve at several pre-stress levels (ETO Group, 2013)

3.1.6 Field-Stress Curves

To estimate the magnetically induced force of an MSME it is necessary to measure the force development in relation to the magnetic field. For this measurement again the GMW dipole electromagnet in combination with the Zwicki testing line machine is used. The sample is in the initial state and blocked by the Zwicki line testing machine, so that the force generated by the applied magnetic field can be measured. As previously mentioned for the strain-field curves it has to be considered that the measured field strength is between MSME and magnetic core and obviously not within the MSME.

3.1.7 Simulation Software

As already discussed for this thesis FEM software is used to simulate the behaviour of MSM. Depending on the simulation approach Software is needed that can handle anisotropic behaviour of MSM and it is also necessary that it is possible to access the simulation procedure to implement changes in the sequence. The 2-D open source software FEMM (Meeker, Finite Element Method Magnetics, 2012) is able to calculate magnetic fields and resulting Maxwell forces in a given geometry, under defined boundary conditions, in a precise and efficient way. FEMM is not able to solve mechanical problems and cannot include magneto-mechanical stress or transient behaviour. Therefore a second software tool is needed which generates the MSME geometry, evaluates the simulation results and restarts the simulation with new geometries, if necessary. FEMM has also the ability to be used in a slave mode via an ActiveX interface, in which an external program can use FEMM only for solving the magnetostatic problem. For instance, this can be realised with Microsoft Visual Studio Express or Visual Basic embedded in Microsoft Excel. Excel is effective because the amount of data which has to be processed in both directions is huge and Excel is suitable to do the mechanical calculations.

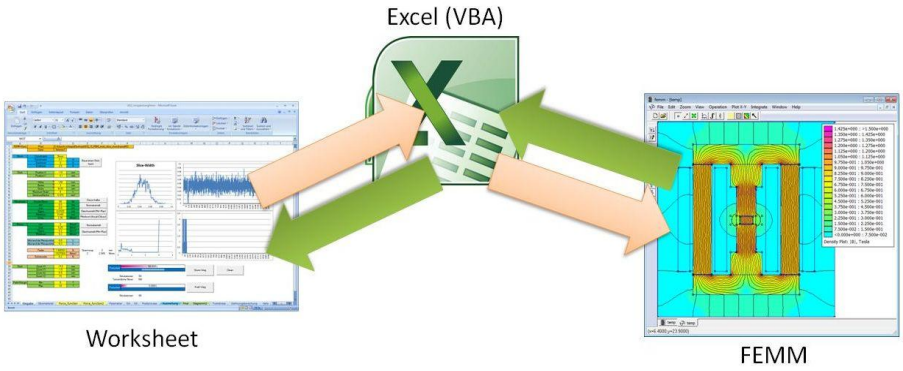

Figure 3.10: Principle of interaction between Excel and FEMM

FEMM is not able to directly magnetic handle anisotropy (Meeker, Finite Element Method Magnetics, 2012), but it is possible to take into account a lamination of magnetic material in any direction. This feature can be used to treat anisotropic behaviour (Mohammed, Demerdash, & Nehl, 1983). Lamination means that sheets of material are stacked. Between the sheets is a small gap filled with non-magnetic material. This gap reduces the magnetic conductance in the out-of-plane direction. This effect is frequently used for reducing eddy current effects in transformers. Anyhow, it can be a solution to consider an easy and a hard magnetic direction.

3.1.8 Pressure and Stress Measurement

The Fuji Film Prescale is a foil that allows measuring maximum applied stresses locally. Prepared foils can be placed between two components and the contact pressure can be measured between them with a lateral resolution lower than 0.1 mm. In the case of stress lower than 50 MPa a two sheet solution is used. The foil thickness of the two sheet solution is about 110 ± 5 µm. As shown in Figure 3.11, one sheet is coated with differently sized microcapsules that are filled with a colour forming material and the other one with a colour developing material. In the case that the applied pressure bursts the capsules the released liquid reacts with, the sensitive colour-developing layer of the second sheet and causes a pressure dependent red colour (FUJIFILM Europe GmbH, 2007).

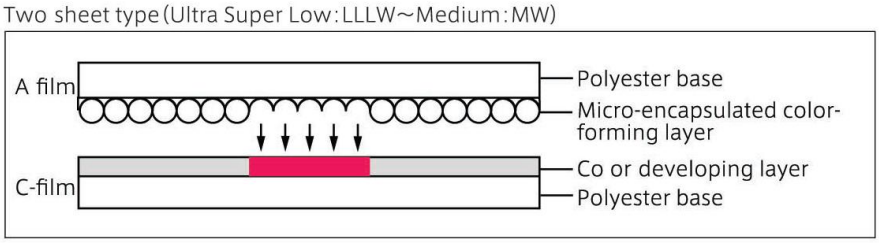

Figure 3.11: Two sheet types of Fuji Film Prescale

The functionality range and preciseness is restricted but depending on the terms of influence it is a smart and adequate solution.

- typical accuracy ± 10% or better
- recommended temperature range from 20°C to 35°C
- recommended humidity range from 35% RH to 80% RH

3.2 Data Analysis and Validation Method

To validate a simulation model, a comparison between simulation results and measurements on a prototype is necessary. The current-elongation curve is for the end user a meaningful graph that allows estimating the performance of the MSM actuator. From the simulation point of view, it is challenging to estimate this behaviour because several modelling steps, such as the various energy transformations that occurs (starting from the input electrical energy to a output mechanical work), are quite hard to describe. In distinction to Section 3.1.5, the current-elongation curves are measured with the complete actuator and depend on the complete design. For comparison, the elongation calculated from the simulation will be compared to the elongation measured from the actuator.

To judge whether a simulation method is good or not, a validation method is needed to quantify the error/deviation between the measurements and simulation results. In Figure 3.12 two simulated (red and blue) and one measured butterfly curve (purple) is shown. Visually it can be estimated that the red suits slightly better to the measured behaviour. Anyhow to evaluate which simulation method is the most precise it is necessary to use a quantitative approach.

The correlation analysis serves to determine the direction and strength of a relationship between two or more variables. The correlation handles both variables equally and it cannot prove a causal relationship, or explain a relationship, in terms of cause and effect. But it can estimate the linear association of continuous variables, which is determined by a correlation coefficient *R*. *R* is also known as the product moment correlation (Bravais, 1846), or Pearson correlation (Pearson, 1901).

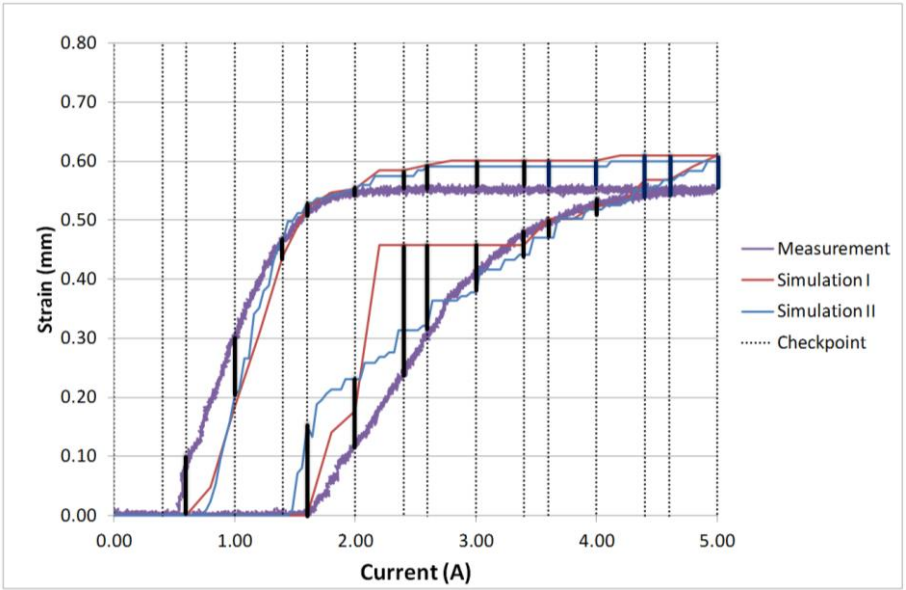

Figure 3.12: Current strain curve, simulated (blue and red) and measured curve (purple)

The range of values of the correlation coefficient lies in the interval [-1, 1] with:

- $R = 0$: there is no linear relationship.
- $R = -1$: there is a perfect negative linear correlation, the larger X, the smaller is Y and vice versa.
- $R = 1$: there is a perfect positive linear relationship, the larger X, the larger will be Y, and vice versa.

The coefficient of determination (R^2) is the square of the correlation coefficient *R*. It can be interpreted as the percentage of the spread of a variable, that can be explained by the other variable (and vice

versa). It is the ratio of explained variance to the total variance. Because *R* is squared it is not possible to recognise if the correlation is negative or not. But especially in this case a negative correlation can be neglected because a negative elongation or better a compression of the MSME by an applied magnetic field is not possible. The coefficient of determination is used to judge the preciseness of the simulation runs.

3.3 Summary

To develop a simulation method that can predict the behaviour of an electromagnetic actuator with MSMA, several input parameters are necessary. The methods used are, as expected, commonly used in the area of electromagnetic actuators. Nevertheless, most of the required measurements have to be modified because of the unusual behaviour of MSM material. The simulation software has to be FEM software, because this allows observing the interaction between the electromagnetic circuit and the MSMA, if an adequate MSMA model can be found. It also can be expected, that the simulation software has to be modified because the shape change and reorientation of magnetisation is unusual for this type of simulation. For the validation of the simulation quality, a direct comparison between simulated model and prototype will show if the simulation approach is appropriate.

4 Proposition of New MSMA Simulation Methods

4.1 Introduction

To predict the behaviour of MSME in electromagnetic actuators, in this Chapter, three new methods will be proposed, designed and developed, with the goal of reaching precise and computationally efficient models:

- Stress based simulation (SBS)
- Dynamic magnetisation curve (DMC)
- Stress dependent magnetisation curve (SDM)

These simulation methods are varying in the complexity of modelling of the MSME and the data preparation. All models were designed, to suit into a magnetic FEM simulation that calculates the elongation behaviour under the defined external stress, in relation to an applied current. It was decided to choose 2D instead of a 3D FEM environment, because the simulation model can run faster and the MSM material researched in this thesis exhibit an almost bidimensional magneto mechanical behaviour. Each method takes into account the interaction between the electromagnetic source, the magnetic circuit, and the behaviour of the MSME. Particularly the consideration of the MSME behaviour in FEM software is a contribution of this thesis. The behaviour of this interaction will be described for all models in the following order for the comparative analysis of the simulation models.

- MSME geometry behaviour
- Magnetic behaviour
- Switching behaviour
- Simulation architecture

4.2 New Stress Based Simulation (SBS)

The concept of the Stress Based Simulation method (SBS) presented in this section was published in the proceedings of COMPUMAG2013 (Schiepp, Maier, Pagounis, Schlüter, & Laufenberg, 2013) and in (Schiepp, Maier, Pagounis, Schlüter, & Laufenberg, 2014). The idea of this method is to emulate the structure of martensite variants on a macroscopic level (Straka, 2007). This model is, compared with the conventional FEM simulation, an unusual and complex attempt to get as close as reasonable with this kind of simulation type. As shown in Figure 4.1, the MSME will be divided into different slices and the magneto mechanical stress will be calculated in each of these slices individually.

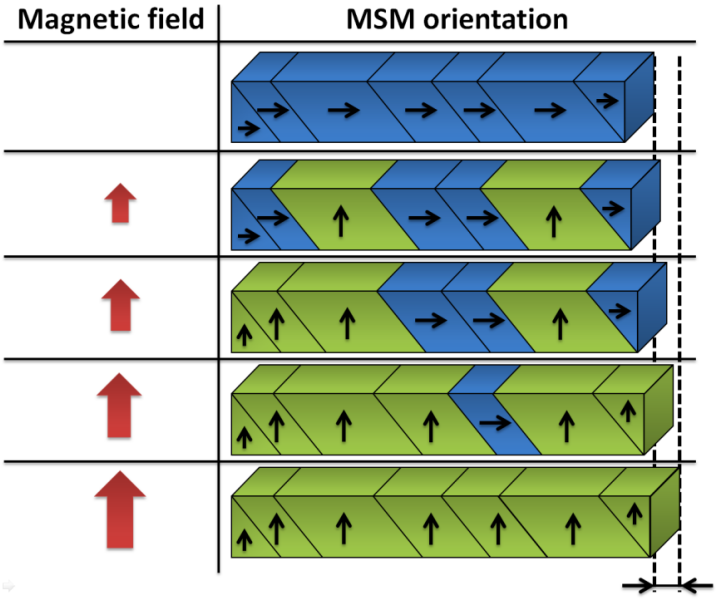

Figure 4.1: Switching behaviour in the SBS model

4.2.1 MSME Geometry Behaviour

In an actual MSME the twin boundaries, i.e. the boundaries between slices with differently oriented martensitic variants, are tilted by 45° with respect to the sample edges (Figure 4.2). As shown in Figure 4.3, this structure is represented in FEMM by slices. This is an attempt to imitate the MSME geometry as close as reasonable and a unique property of the SBS and the fundamental difference to other simulation models available in literature. The size, width and twinning stress of each slice are defined and generated in Excel. This can be determined either by measurement data of an individual MSME or average values of standard material. For a complete simulation run, this particular MSME geometry remains unchanged until a shape change, for example an elongation induced by a magnetic field. Only the reorienting slices produce strain and the MSME itself elongates with the amount of shape change caused by these slices. All other slices remain in their state. Although the strain of each individual slice is taken into account, a possible tilt was neglected otherwise an overlap with the magnetic circuit could not be avoided.

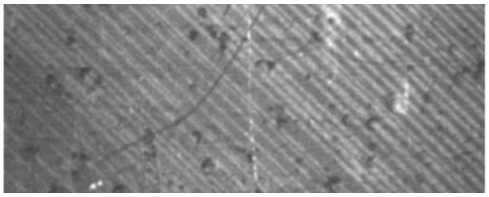

Figure 4.2: Microscopy of a MSME (Source: www.magneticshape.de)

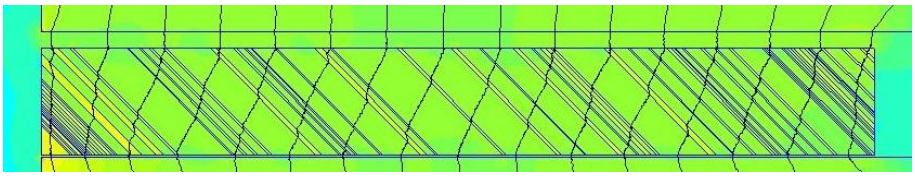

Figure 4.3: MSME in FEM simulation (FEMM)

4.2.2 Magnetic Behaviour

In the SBS method the slices are provided with an anisotropic magnetisation curve as shown in Figure 4.5. The hard axis is oriented in each twin area, depending on the current state of external field and stress (Figure 4.1). In the tetragonal lattice the hard axis is always along the longer crystallographic a-axis and the easy axis is the shorter c-axis. Therefore, in this type of model two magnetisation curves exist (Figure 4.5) and the orientation of the area affects the direction of the hard and easy axis. The magnetic axis and the geometry are directly linked to each other in every individual slice. The orientation of the slices depends on the current state of the MSME. This orientation affects the electromagnetic behaviour of the whole MSME and thus the actuator.

FEMM cannot be used directly to handle anisotropic curves, i.e. a separate magnetisation curve for each direction. But it is still possible to take into account the anisotropic behaviour. Many magnetic devices are built of thin laminations in order to reduce eddy current effects. One unusual and, from computational point of view, time consuming way is to model these materials by designing the laminations and the insulation in several sheets which finally requires a 3D simulation and leads to a complex mesh and very high computational efforts. An alternative is to treat the laminated material (Figure 4.4) as a continuum and derive bulk properties that yield essentially the same results, while requiring a much less elaborate finite element mesh (Mohammed, Demerdash, & Nehl, 1983).

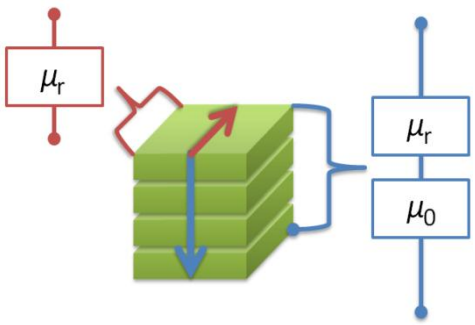

Figure 4.4: Equivalent magnetic circuit for flux in the hard (blue) and easy (red) direction

A disadvantage of this treatment is that in FEMM over the entire range of the magnetisation curve the anisotropy can only be described with a constant factor (i.e. the lamination fill factor), which is insufficient. Since in the case of MSM the permeability difference between hard and easy axis is depending on the field strength, as shown in Figure 4.5 where after saturation the inclination of the hard magnetisation curve (blue) is better than in the easy axis, the magnetic permeability for the hard axis improves until it reaches the level of the easy axis. Therefore this lamination factor needs to be modified in every simulation step, depending on actual field strength in each individual slice. Anyhow, this approach of simulation is stepwise and the current and the magnetic field will be increased constantly, under the premise that the current steps are finely graded and the enfoldment of the magnetic field is slow. Thus, the fill factor can be adapted by the magnetic field continuously in every slice depending on the applied magnetic field of the previous simulation runs.

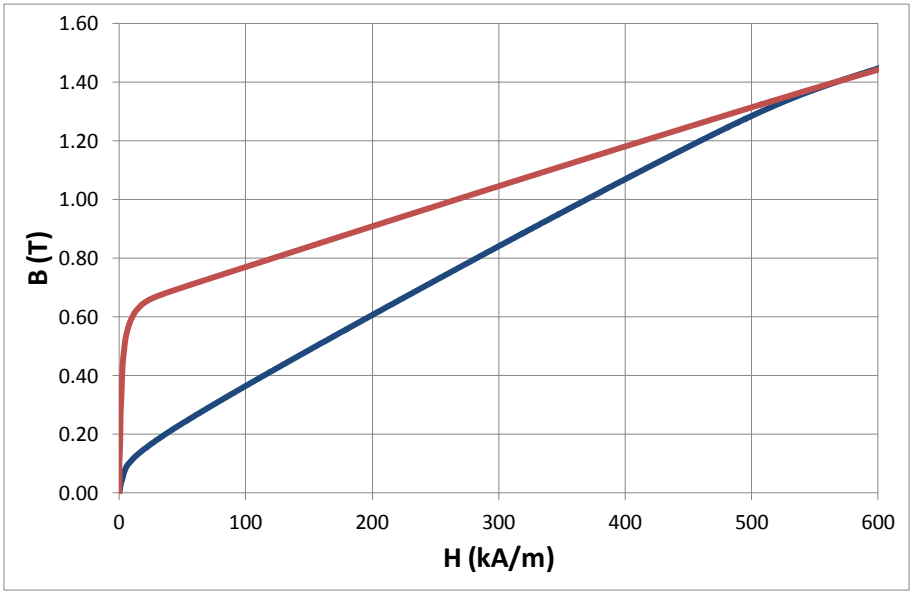

Figure 4.5: Magnetisation curves of hard (blue) and easy (red) axis

4.2.3 Switching Behaviour

Inside an actuator the MSME can be affected by several types of stress (Figure 4.6) which can be divided into internal and external stresses (Straka, 2007). The internal stresses can be subdivided into magneto stress and twinning stress σ_t. In the SBS method the magneto-, twinning and restoring stress as well as Maxwell forces are calculated individually for each slice, depending on direction and amount of magnetic field. Finally the orientation of each slice can be predicted, as explained in detail in the following.

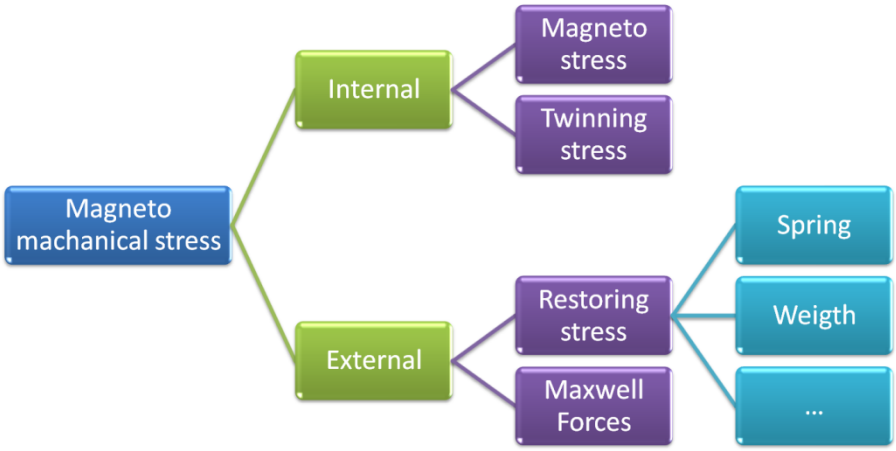

Figure 4.6: Stress types that act in or upon the MSME

Internal: Magneto Stress

The maximum magneto stress σ_{max}^{mag} is caused by an external magnetic field and depends on the magnetic anisotropy constant K_1 and the maximum strain ε_0 of the material, which is determined directly from the ratio of the lattice constants of the tetragonal lattice (Straka, 2007).

$$\sigma_{max}^{mag} = K_1/\varepsilon_0 \qquad \textbf{4-1}$$

In this model the generated magneto stress will be calculated in dependence on the magnetic field that pervades the individual MSME slice, and will be evaluated with the measured force-field behaviour shown in Section 5.4.

Internal: Twinning Stress

The twinning stress hinders the reorientation of the martensitic twins and is the minimum amount of energy that has to be overcome by the magneto stress, to enable twin variant reorientation in the MSME. Once they are reoriented the same amount of energy is necessary to get back to initial orientation, which leads to the typical hysteresis of the MSM. It must be considered that a measured curve does not reveal the position of the particular switched twins in the MSME.

External Stress

The external stresses $\sigma_{x,y}^{ext}$ in x- and y-direction can be caused by a spring, a pneumatic pressure or due to friction effects that all can act on the MSME. Depending on its direction, they favour or hinder a reorientation of twins and therefore the macroscopic strain of the MSME. Especially the friction and magneto-mechanical stress based on Maxwell forces, can be considered in an Excel tool and easily be calculated by the FEM simulation tool.

Magneto-Mechanical Stress

Finally all internal and external influences are summarised. During simulation the current and thus the magnetic field H is increased stepwise. Using equation 4-2 (graphically explained by Figure 4.7), where $\sigma_{x,y}^{mag}$ are the magneto-stresses in x- and y-direction, respectively, it can be determined in every simulation step and for each individual slice, whether this slice will reorient or not.

$$\sigma_x^{mag}\left(\sigma_{max}^{mag}, H\right) + \sigma_x^{ext} > \sigma_t + \sigma_y^{ext} + \sigma_y^{mag}\left(\sigma_{max}^{mag}, H\right) \qquad \textbf{4-2}$$

For example the reorientation of any individual slice, having the easy axis oriented in y-direction, occurs when the overall stress in x-direction is larger than the stress in y-direction. It must be noted that the reorientation of each slice, corresponding to a change of geometry, is simulated as an instant process: as soon as the stress condition is met, the slice instantly deforms up to the maximum (e.g., 6% for commercial MSM).

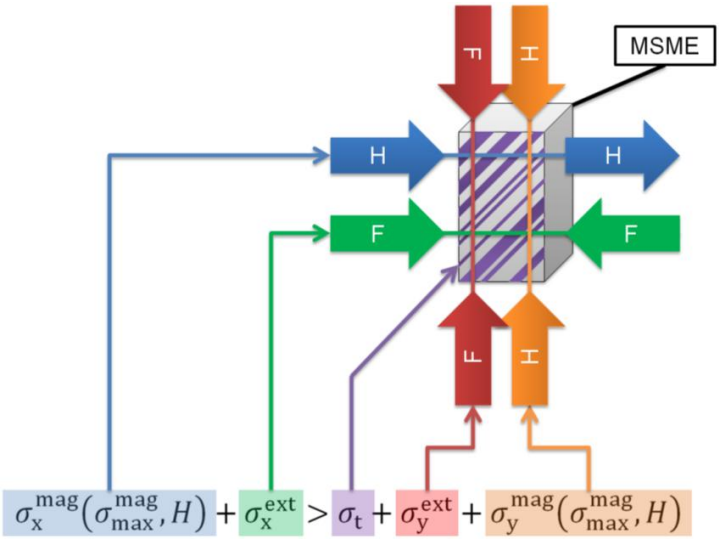

Figure 4.7: Magneto mechanical stress equation

The maximum magneto-stress $\sigma_{\max}^{\mathrm{mag}}$, which is a constant value for a specific alloy, is obtained using measured field-force curves of MSM material. This parameter allows determining the magneto stress $\sigma^{\mathrm{mag}}(H)$ in x as well as in y direction as a function of the external magnetic field H. The highest positive stress value of all slices, which has not yet reoriented, is multiplied by the MSM element cross-section in order to calculate the resulting force. After each simulation step the FEM representation of the MSM element is rebuilt, based on the same slice pattern, but with slices that have undergone a switching. These slices are strained by 6% and their magnetic easy and hard axes are rotated by 90°.

4.2.4 Simulation Process (Flow Chart)

To calculate the current-stroke behaviour, the current needs to be increased and decreased step by step. The complete simulation sequence is shown in Figure 4.8. Before a simulation can be started the boundaries and properties, that describe the used MSME as well as the actuator geometry, have to be entered. This method is based on fundamental considerations and therefore only a low amount of measurement data is necessary. However, to be able to predict the behaviour of a standard MSM, material statistical data of this MSM type must be available. Furthermore, the average width or distribution of the slices (twins) and twinning stress as well as the magneto-stress behaviour is needed. At present, these statistical data are not known and therefore individual measurements for each used sample were used. In summary the following input data are required:

- Actuator geometry
- MSME size
- MSME type (modulation: 10M, 14M or NM)
- Minimum and maximum current and current step width
- Twin width (average, distribution or directly measured data)
- Twinning stress (average, distribution or directly measured data)
- Magneto stress behaviour
- Magnetisation curves (hard and easy axis)

Once these parameters are set, the simulation procedure starts with the definition of the MSME structure and setting a start current. Next, a connection between Excel and FEMM will be initiated and the geometry data as well as magnetisation curves (easy and hard) will be transferred to FEMM to build the MSME geometry with all slices, within a predefined magnetic circuit. Afterwards the first calculation step can be executed.

After the magnetic field is calculated in FEMM, information, such as field strength and magnetic flux of each slice, is transferred to Excel and the connection to FEMM is cut off. In the next step the magneto-mechanical stress has to be calculated in each slice individually. In the case that the magneto stress in a slice is large enough, the single slice elongates and the magnetisation curves will change. The deformation of one slice influences the overall deformation of the MSM bar, which is updated. After the data is stored, the next simulation step is performed by increasing the current with a predefined current step and using the MSME geometry, updated from the previous simulation step. This procedure will be repeated until the maximum current is reached. Afterwards the current is decreased again step by step, so that the restoring behaviour can be calculated. As soon as the current reaches the starting current again, the simulation is finished and the current stroke curve can be displayed.

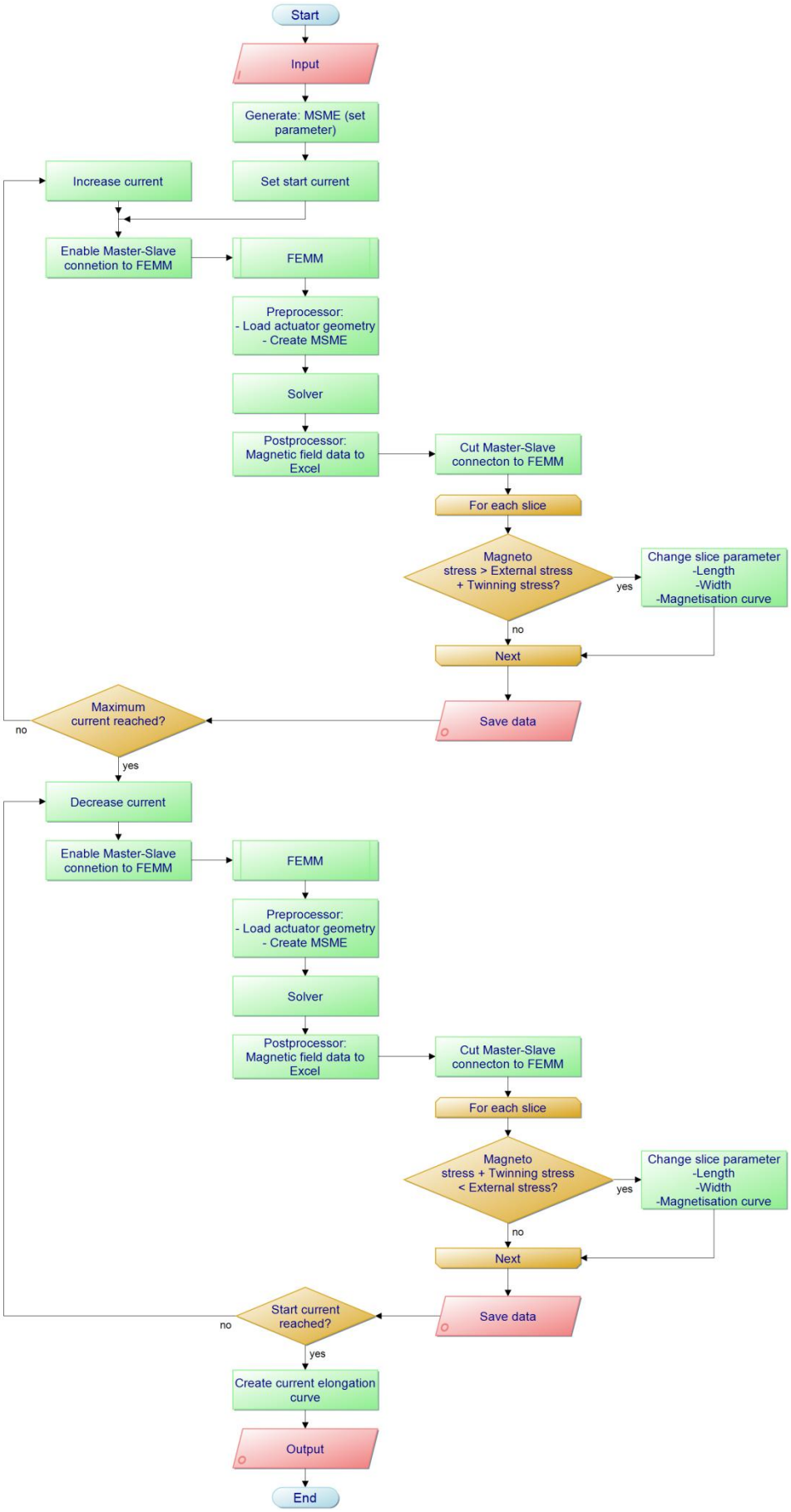

Figure 4.8: Flow chart of the stress based method

4.3 New Dynamic Magnetisation Curve (DMC) Method

The concept of the dynamic magnetisation curve method (DMC), presented in this section, was published in the proceedings of (Schiepp, Laufenberg, Pagounis, & Maier, 2011). The magnetisation curve of MSM depends on strain and anisotropic behaviour. In an intermediate state each variant has one of the magnetisation curves shown in Figure 4.5 but the whole sample shows an average magnetisation curve as in the measurements of Figure 4.9. This magnetisation curve will improve with increasing strain, while the average magnetisation curve in the perpendicular direction will simultaneously degrade. In the following this is called "dynamic anisotropic behaviour" (Schiepp, Laufenberg, Pagounis, & Maier, 2011). This is caused by the strain of the MSME, where more and more areas adjust their easy axis along the magnetic field and the average magnetisation curve of the sample will improve continuously. The idea of this approach, is to treat the MSME as a "black box" in contrast to the SBS approach presented in Section 4.2, where the twin structure of the element was explicitly taken into account. The DMC is less complex than the SBS, although it may require more measurement effort.

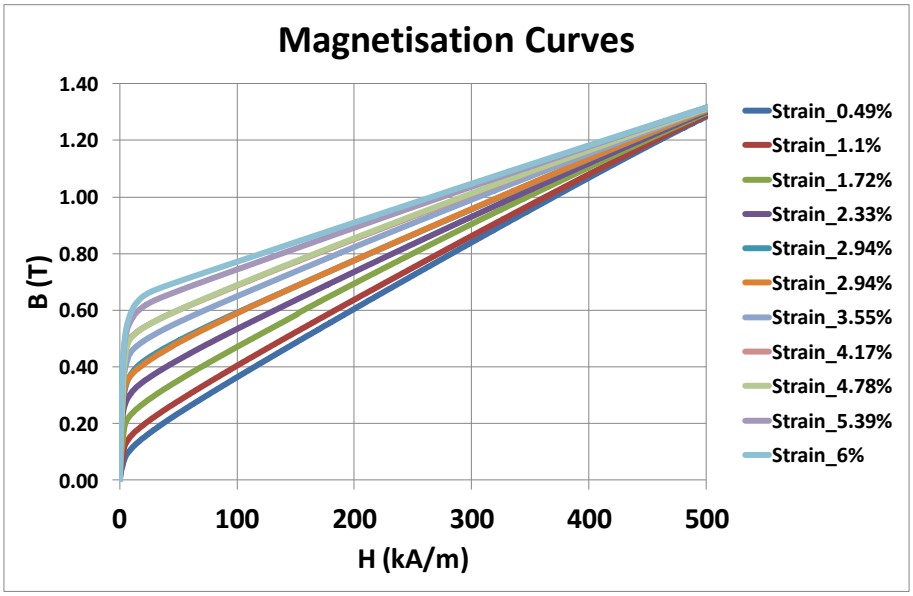

Figure 4.9: Dynamic anisotropic behaviour of a MSME elongated in y direction

4.3.1 MSME Geometry Behaviour

The MSME is represented geometrically by a rectangle. As mentioned before, the internal structure of the alloy is not considered explicitly in the DMC, whereas only average macroscopic magnetisation behaviour is taken into account. In case of a shape change, both side lengths will be changed accordingly, so that the effect of shape change is adequately represented in this type of simulation method.

4.3.2 Magnetic Behaviour

As already said the average magnetisation curve of a complete sample is varying in dependence on strain. Therefore, in each simulation step, a magnetisation curve is implemented for the MSME, depending on the current strain level. In this work 100 magnetisation curves, corresponding to 100 strain levels have been used.

4.3.3 Switching Behaviour

The stress calculation is similar to the SBS method, with the important difference that the magneto stress is calculated for the complete sample and not for an individual slice. This reduces computing time significantly because less data has to be transferred between FEMM and Excel, the mesh of the FEM has fewer nodes and finally the calculation of the elongation is faster.

The material is not treated as anisotropic in the DMC. In other words, the MSM "rectangle" has isotropic magnetisation properties, based on the average strain-dependent magnetisation curves. Since the MSME is treated as a "black box" and local effects between differently oriented areas / twins are neglected, any field through the material is not expected to leave the original direction, so that a uni-axial description of the material becomes possible. As shown in equation 4-3, the uni-axial assumption also reduces the complexity of the stress calculation as only the magnetic field in one direction has to be computed.

$$\sigma^{\mathrm{mag}}\left(\sigma_{\mathrm{max}}^{\mathrm{mag}}, H\right) + \sigma_{\mathrm{x}}^{\mathrm{ext}} > \sigma_{\mathrm{t}} + \sigma_{\mathrm{y}}^{\mathrm{ext}} \qquad \textbf{4-3}$$

In the DMC method the geometry change is also depending on stress. As soon as the combined external stresses and the magnetic stress are higher than the twinning stress, the shape of the MSME will change. In the next step length and width of the MSME will be updated, based on the calculated strain level. Even though the twins are not represented in the FEM model, the size and the twinning stress distribution are considered in Excel, where a twinning stress is assigned to the slices and the magneto stress that is calculated in the FEM can be used to determine if it has switched or not. The accuracy of the simulated strain depends finally on the precision of these parameters in the simulation model.

4.3.4 Simulation Process (Flow Chart)

Similarly to Section 4.2 the minimum required data, such as actuator geometry, MSME size, and type of lattice modulation as well as minimum current step are necessary. In the case that these data are not available, additionally the twin width and stress information as well as magnetisation and magneto stress are indispensible.

While in the SBS model two magnetisation curves were sufficient to describe the MSME in all its elongation states, in this case many (e.g. 100) strain dependent magnetisation curves are necessary. This indicates an increased amount of measurements or data processing for the preparation of a DMC simulation.

When the input data are defined, a connection between Excel and FEMM will be initiated and the geometry data (the MSME "black box") as well as the initial magnetisation curve will be transferred to FEMM. Afterwards the first calculation can be performed, which starts in accordance with the lowest current. Then the magnetic field of the MSME, calculated in FEMM, is transferred to Excel to determine the stress in the MSME sample and the connection to FEMM is cut off. In the DMC method this magnetic field information is only a single value in contrast to the SBS where the magnetic field is evaluated in every slice.

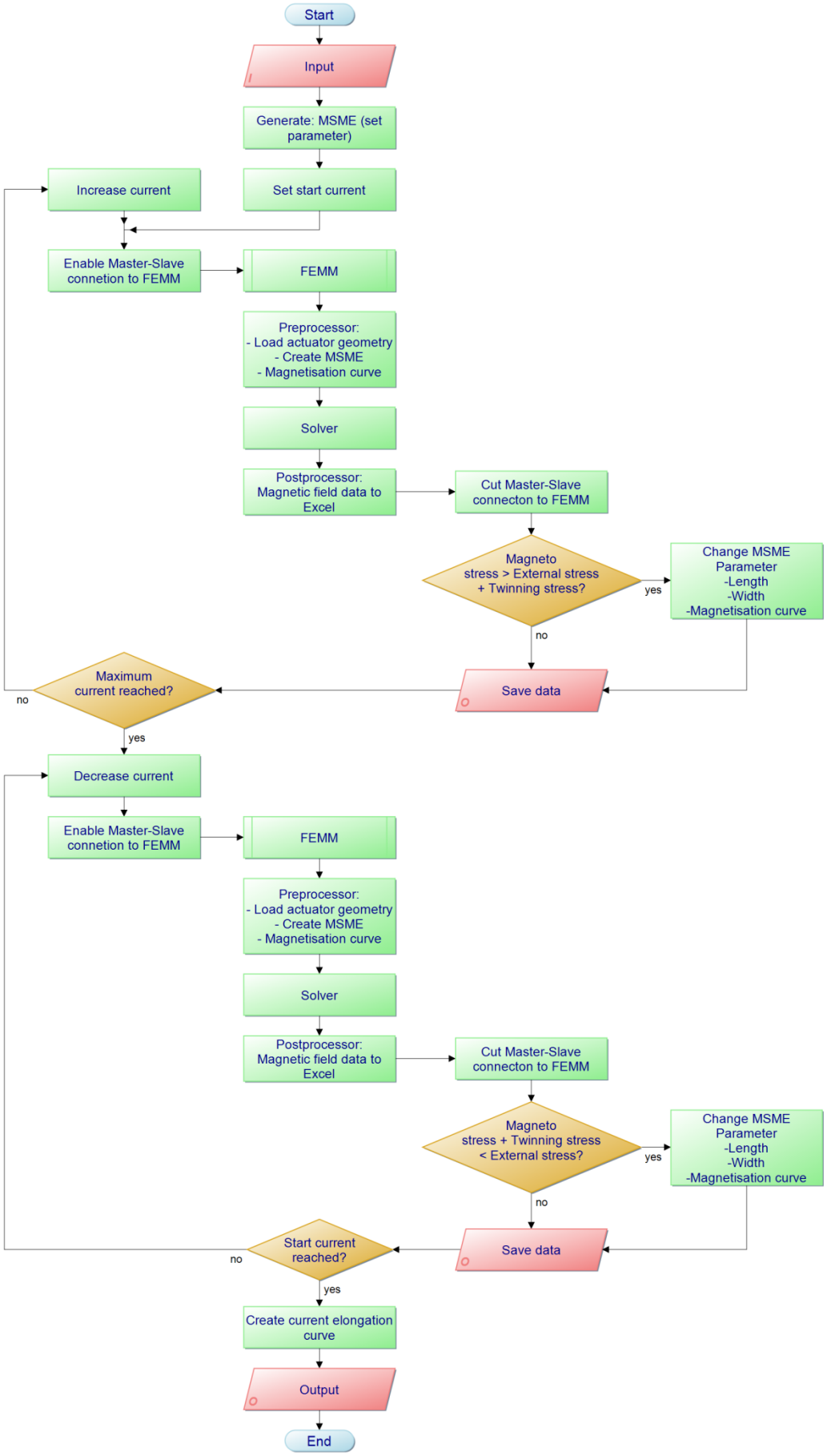

Figure 4.10: Flow chart of the dynamic magnetisation curve method

Nevertheless, also the size, width and twinning stress of the twins is set here, so that the switching behaviour can be considered in the next step. Each twin for which the calculated magneto stress exceeds the sum of twinning and external stress, leads to elongation of the MSME and accordingly to an improved magnetisation curve. The shape of the MSME and the magnetisation curve are adjusted in dependence on the strain. Afterwards the current is increased continuously and the elongation is calculated, as described, until the maximum current is reached. Subsequently the current is decreased again stepwise until the start current is reached.

4.4 New Stress Dependent Magnetisation Curve (SDM) Method

In the stress dependent magnetisation curve method (SDM) the computational and modelling complexity is further reduced. Therefore a deeper understanding of the magnetic behaviour and a modified measurement method for magnetisation curves of the MSME is necessary. The main idea of the SDM is, to transfer a part of the magneto-mechanical calculation into the input data. In particular in the SDM it is assumed, that a magnetisation curve, corresponding to a defined stress scenario, is available. This leads to the advantage that the stress calculation during simulation becomes unnecessary. In the SBS and the DMC it is necessary to simulate iteratively, to estimate the elongation behaviour and to determine if the full stroke is achievable within a particular actuator design. The SDM instantly allows the estimation if the maximum current is sufficient for full stroke. This possibility leads to new opportunities, like the implementation of optimisation algorithms (Rechenberg, 1994), which helps to improve the actuator. The drawback of this approach is that a specific magnetisation curve must be found for a specific stress scenario.

4.4.1 MSME Geometry Behaviour

In the SBM the MSME will be a simple rectangle like in the DMC. However, here the shape change is neglected because it is included in the magnetisation change. Due to the twinning stress the MSME shows a hysteresis that leads to a different magnetisation curve for the elongation and the compression. Finally, for this method only two magnetisation curves are necessary for the complete simulation procedure and it is not necessary to perform a shape change, which reduces computing time.

4.4.2 Magnetisation Curve Behaviour

The magnetisation curve has to fulfil several functions in the SDM. Since the strain has a significant impact on the magnetisation behaviour of the MSME, the idea is to measure the magnetisation curve of the MSME during elongation and compression under defined pre-stress. This pre-stress is working antagonistically as soon as the magneto stress exceeds the sum of external stress and the twinning stress, the MSME will change its shape and the magnetic permeability as well.

The large hysteresis of MSM has to be considered by individual magnetisation curves for an increasing and for a decreasing magnetic field. In the case that an MSME does not reach full elongation, a magnetisation curve is necessary to represent the current state of elongation. Finally for this approach a lot of measurement data is necessary to simulate a MSME under any conditions. Furthermore the simulation may be very alloy specific.

4.4.3 Mechanical Switching Behaviour

In the SBS and DMC methods a stepwise simulation is mandatory. The advantage of the SDM method is that the magneto mechanical behaviour of MSME is implemented in the magnetisation curve. This allows determining in a single simulation run, if an actuator is efficient or not. Additionally the amount of elongation can be calculated from the magnetic field, in the inner of the MSME.

4.4.4 Simulation Process (Flow Chart)

The emphasis in this method is on a complex magnetisation curve. This makes this method on the one hand attractive for simulation purposes and on the other time-consuming for the required measurements.

The simulation process starts with the input data and a selected magnetisation curve that corresponds to the external stress profile of the final actuator. To estimate if this actuator is efficient only one simulation step is necessary, but in order to compare the simulation methods, it is necessary to calculate the current-elongation behaviour. Therefore the current will be increased stepwise, as shown in Figure 4.11. The elongation state can be estimated by the actual magnetic field in the inner of the MSME. Therefore a stress calculation is not necessary. After the maximum current level is achieved, a different magnetisation curve for the decreasing current is used. This curve has to suit to the elongation state that is achieved with the increasing current. Then the current is decreased again.

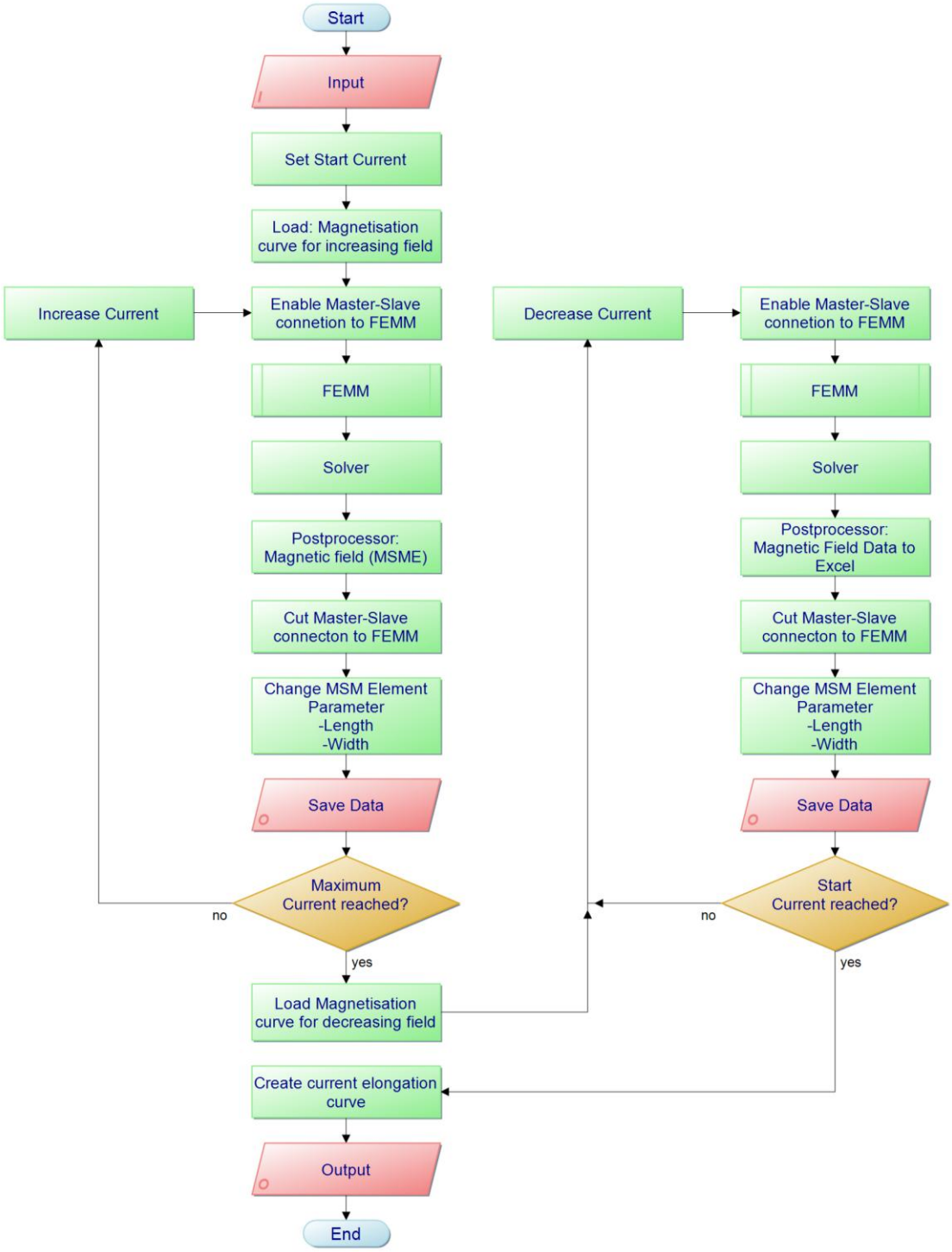

Figure 4.11: Flow chart of the stress dependent magnetisation curve method

4.5 Conclusion

Each simulation model has its individual advantages and drawbacks. The SBS tries to get as close as reasonable to the real phenomena within the MSME. So the geometrical simulation of the MSME is complex and the stress calculation is based on fundamental considerations. The DMC is an attempt to reduce the complexity of the FEM model, at the cost of a larger measurement effort. The SDM is a "black box" approach that handles the MSME as any other ferromagnetic material without any shape change, but an unconventional magnetisation curve in such a magnetic FEM simulation. Therefore a deep understanding of the model behaviour as well as further improvements and modification of measurement devices is necessary. In the SDM the complete stress calculation is implemented in the magnetisation curve of this element and therefore the magnetisation curve has to correspond to the external stress profile. This leads finally to a large amount of measurements.

5 Modification of Measurement Methods

5.1 Introduction

The simulation methods proposed in Chapter 4 are useful for FEM simulation purposes. The framework of magnetic FEM simulation typically uses the magnetisation curves. In the case of MSM this is even more important because the magnetisation of the material is the basis for the variant reorientation and thus the mechanical strain. At the moment there are no commercially available devices that are suitable to measure the characteristics of MSM. Therefore existing measurement methods have to be modified, to be able to collect the necessary data for the simulation of MSM materials.

5.2 Magnetisation Curve

To measure the magnetisation curve or the relative permeability of a material, several devices are available. Normally they are optimised for a particular measurement demand. The company Magnet-Physik distributes two devices for hard and soft magnetic materials. The main difference between those two measurement devices is the sample size as well as the measurement range. The PERMAGRAPH® (Figure 5.1) is designed for permanent magnets and therefore for hard magnetic materials (Physik Instrumente GmbH & Co. KG, 2012). Anyhow if MSME is rather soft or hard, magnetic material plays a minor role in this case. For MSM alloys it is of interest that the device is able to measure at least up to a magnetic field strength of 600 kA/m (Heczko, 2005) and that it can handle an ETO typical MSME of 2 x 3 x 15 mm³. The aforementioned PERMAGRAPH® is an adequate device for those requirements.

Figure 5.1: PERMAGRAPH® L Type EP2 (Source: MAGNET-PHYSIK)

5.3 Static Magnetisation Curves

5.3.1 Measurement of the Magnetisation along the Hard and Easy Axes

The anisotropic behaviour of the MSMA can be appreciated from the magnetisation curves along the hard and easy axes as shown in Figure 3.1 and Figure 6.1. These curves are the core of the SBS method, because the material slices are described as magnetically anisotropic areas. For measuring the magnetisation curve, the specimen is placed in the PERMAGRAPH device, as shown in Figure 3.2, and the coils are excited by a current to generate a magnetic field through the element. However, it must be noted that to measure the magnetisation along the easy axis the MSME should stay completely elongated; similarly, to measure the magnetisation along the hard axis the MSME should stay completely contracted during the measurement. This is a main issue. For example, if the specimen

would be free to elongate during the application of the field, its magnetic permeability will change along with the variants reorientation and the measured magnetisation curve will be something in between the hard and the easy magnetisation curves. Another issue is, that the elongation of the alloy in one direction (perpendicular to the field) produces a contraction in the direction of the field, increasing the air gap between the PERMAGRAPH coils and the MSME. This introduces some undesired error in the magnetisation measurements. Both issues can be solved by mechanically constraining the MSME to the contracted state when measuring the magnetisation along the hard axis, and to the elongated state when measuring the magnetisation along the easy axis. To this aim some block-discs (Figure 5.2) were designed out of aluminium. The inner shape of the discs suits to the MSME and prevent the elongation mechanically.

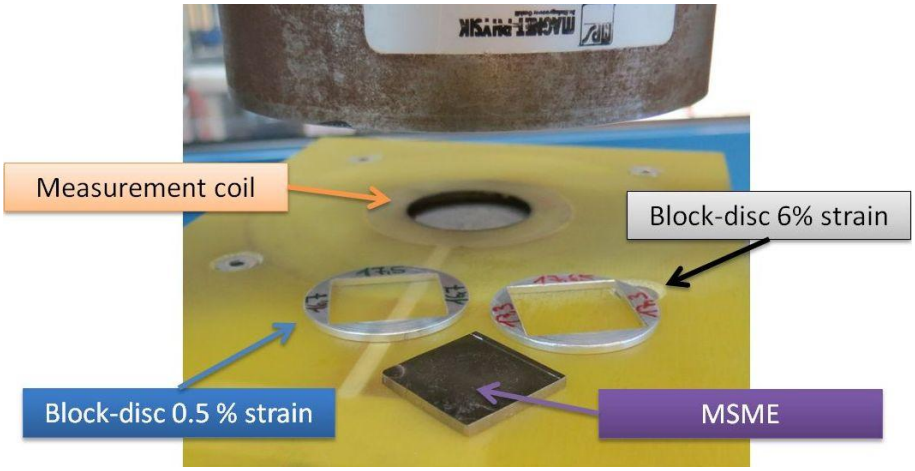

Figure 5.2: Block-discs for hard (left) and easy axis (right) with MSME (middle) in PERMAGRAPH®

5.3.2 Magnetisation Curves at Intermediate Strain Stages

When a MSME is half elongated, it consists of only two differently oriented martensitic variants and a measurement of the magnetisation of the complete specimen will yield an averaged curve, that is ideally in the middle of the hard and easy axis. This magnetisation curve depends on the actual elongation stage as shown in Section 6.2.2. In the DMC, in every simulation step the whole MSME sample is treated as a homogenous area with only one magnetisation curve which is bound to the actual elongation value. Consequently for the DMC magnetisation curves are needed that correspond appropriately to ideally any strain stage. Additional block-discs (Figure 5.3) were produced, to constrain the deformation of the MSME to intermediate magnetisation states, similarly to what was done for the measurement of the hard and easy axis magnetisations. For these measurements bigger samples were used to reduce measurement failure.

Figure 5.3: Bloc-discs to measure magnetisation at several strain stages

5.3.3 Stress Dependent Magnetisation Curves

For the SDM a magnetisation curve is needed that corresponds to the MSME behaviour under a certain stress profile. In this case elongation only takes place, when the magneto stress exceeds twinning and external stress. Also, the magnetisation improves with the elongation and exemplary measurement results are shown in Section 6.2.3. Therefore a device is needed, that allows applying an adjustable stress on the MSME and suits into the measurement coil of the PERMAGRAPH®. To receive best results pre-stress value as well as profile should correspond to the typical stress that will appear in the final actuator. This is only partial possible because the available space around the sample is limited by the surrounding measurement coil (Figure 5.4). On the one hand a bigger surrounding coil could provide more space, but on the other hand a greater measurement error is expected, because of a poor ratio between surrounding coil and specimen surface. Therefore a device was designed that suits into the measurement coil with the diameter of 26 mm and MSME samples size of 2 x 3 x 15 mm³.

The device shown in Figure 5.4 consists of two brackets (blue) that are combined with two return springs (black) which are mounted around threaded bolts (orange). The MSME (red) is placed between these two brackets. The pre-stress on the element can be adjusted by the screws. The device is made of non ferromagnetic material, so that the influence on the measurement device should be negligible. The ratio of sample to surface of the surrounding coil is round about 8.5 % and 9 %, depending on the elongation state. Therefore a higher measurement error is expected from these curves.

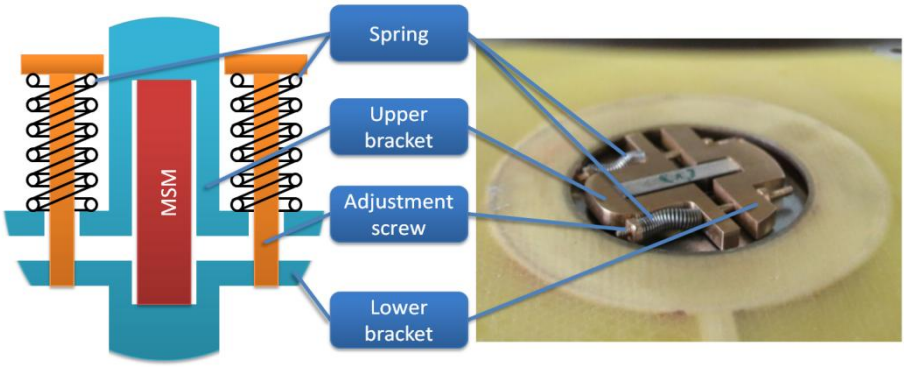

Figure 5.4: Measurement device Schematic view (left) in Permagraph® (right)

Furthermore it has to be considered that Maxwell forces appear while measuring. These forces cause an additional mechanical stress in the MSME and additionally they increase the friction force between the MSME and the core pieces. This effect was confirmed to be most severe, where the relative motion between the MSME and the adjacent magnetic cores is maximum, which is typically the case at the upper end of the MSME (Schiepp, Detkov, Maier, Pagounis, & Laufenberg, 2013). It is worth mentioning that this Maxwell forces also appear in the MSME actuators, although they can be partially neglected.

5.3.4 Measurement Preciseness

To ensure that the PERMAGRAPH® is an adequate device for MSME, it is necessary to estimate reachable preciseness. It is recommended that the sample surface should be at least about 50 % to 70 % of the measurement coil surface (Steingroever & Ross, 2009). The standard MSME sample geometry at ETO is 2 x 3 x 15 mm³, while the available standard coil has a diameter of 26 mm. In this configuration the ratio between surrounding coil and specimen surface is about 8.5 %, which is quite low. To estimate the error of a comparatively low ratio of coil and specimen surface, a MSM sample of 2 x 17 x 17 mm³ was prepared, which roughly corresponds to a surface ratio of 55 %. The

magnetisation of this sample was compared to the magnetisation of a standard small sample (surface ratio of 9%) in order to appreciate the deviations in the measurements. Both MSMEs were cut from the same crystal, so they have the same composition as well as the same casting parameters and therefore they should have the same magnetisation curve.

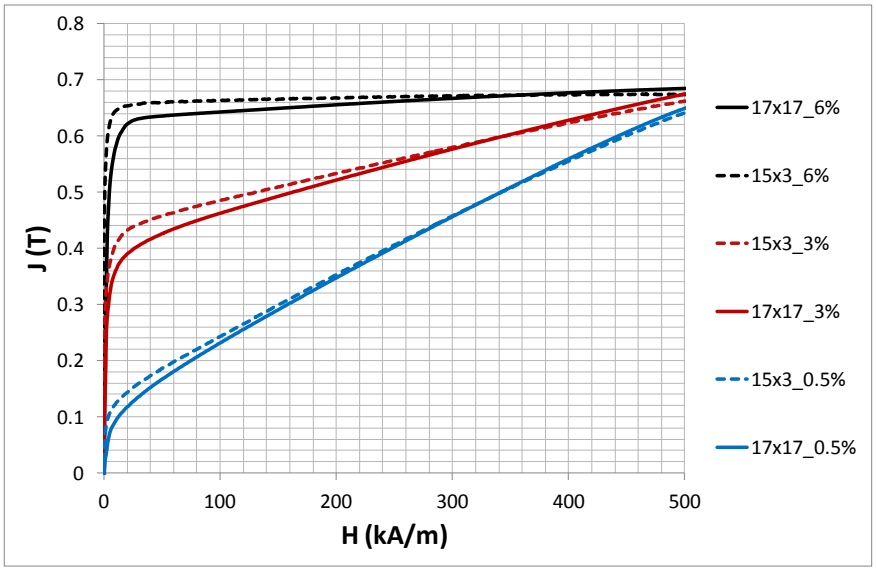

Figure 5.5: Polarisation at 3 strain levels of two different sized MSME

As shown in Figure 5.5 the small specimen (dashed lines) with the small surface ratio tends to higher saturation than the huge sample (continuous line) with a surface ratio of 55%. This kind of error would artificially and erroneously overestimate the magnetisation properties of the sample. This, in turn, would affect the simulation of a complete actuator, leading to higher calculated magnetic fields. Finally the needed amount of current in the real built actuator would be higher than the proposed and the actuator would not be in an optimised configuration. Although this measurement method is well-established, it is not designed to measure MSME specifically and therefore reduced preciseness is unavoidable.

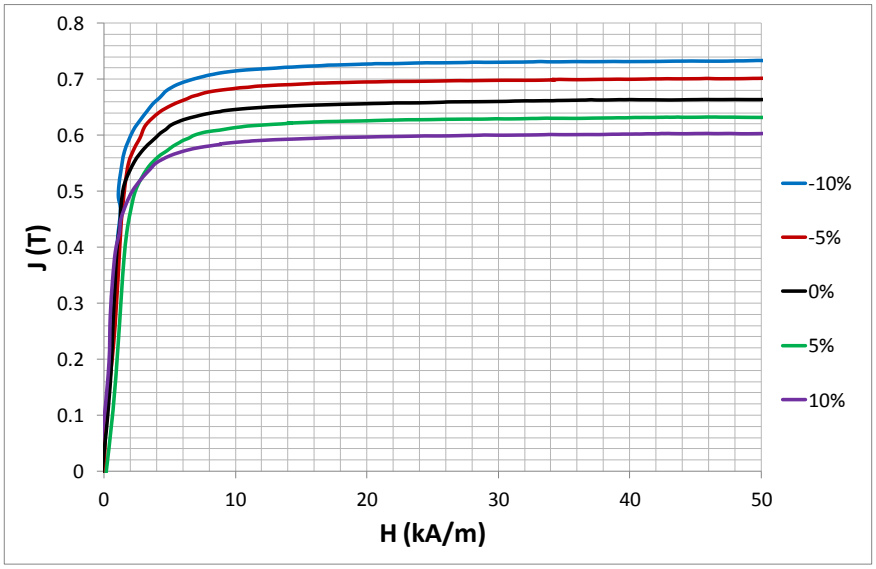

Figure 5.6: Polarisation of one MSME sample with deviated input data of the surface area in percent

Concluding, the measurement preciseness depends essentially on the surface ratio. It is also interesting to know if the variation of the surface itself leads to deviations. To research the impact of a sample surface variation on the measurement of the magnetisation curve, a MSME sample of 2 x 3 x 15 mm³ was used and the size was varied of ± 10 %. The result is shown in Figure 5.6. It is shown that the measured magnetic saturation tends to be higher if the flooded surface is corrected downwards and vice versa. A deviation of 5-10 % of the surface leads also to about 5-10 % failure in the measured magnetisation, especially at saturation. Anyhow in all cases the surface of the specimen plays a role in the measurement of the magnetisation curve.

5.4 Force Field Behaviour

The force field curve of MSME is necessary for the SBS and DMC approaches. This curve describes how much force is generated by the MSME, when a field is applied in perpendicular direction. The approach followed here is experimental and two ideas are presented to measure this curve. Results are shown in Section 6.4.

The first idea is to measure additionally the force during the measurements of the magnetisation curves in the PERMAGRAPH®. But the issue of restricted measurement space still exists and an impact of the high magnetic field on a force measurement device cannot be excluded completely. The second idea is to use the device shown in Section 3.1.2. This is advantageous because the force sensor is far away from the influence of the magnetic field and furthermore there is space around the specimen that can be used for magnetic field measurement. Also in this case it is not possible to measure directly the magnetic field within the material. One possibility is to measure the magnetic field near the MSME with a Hall sensor. The second idea is more feasible than the first.

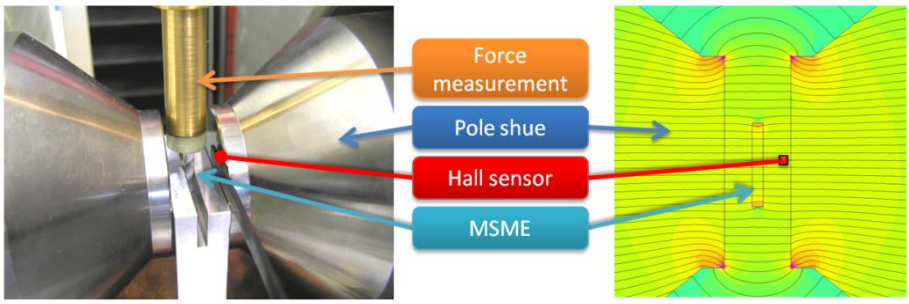

Figure 5.7: Measurement (left) and simulation (right) of force field behaviour

As shown in Figure 5.7 on the left, a MSME sample is placed in the measurement device between the pole shoes. The pushrod compresses the MSME to the start state. Then a magnetic field is applied, that pervades the MSME homogeneously. A sample with very low twinning stress (less than 0.1 MPa) enables the possibility to read off the magneto stress directly.

To receive the value of the magnetic field in the inner of the MSME, in relation to the applied current, simulations of the GMW dipole magnet are performed (Figure 5.7, right). During the measurements the MSME is in the start state and therefore in the simulations the MSME is defined by the magnetisation curve of the hard axis.

5.4.1 Initial State and Start State

It is important to make a distinction between the start and initial state. The initial state is the state when all areas are oriented in the same direction. This state is a theoretical state because defects in the atomic lattice or inhomogeneity make it statistically unlikely that the complete MSME is orientated in

one direction. This situation is in the following defined as the starting state. This could be the initial state or even in an actuator any other quasi static situation which is shown in Figure 5.8 as S_1.

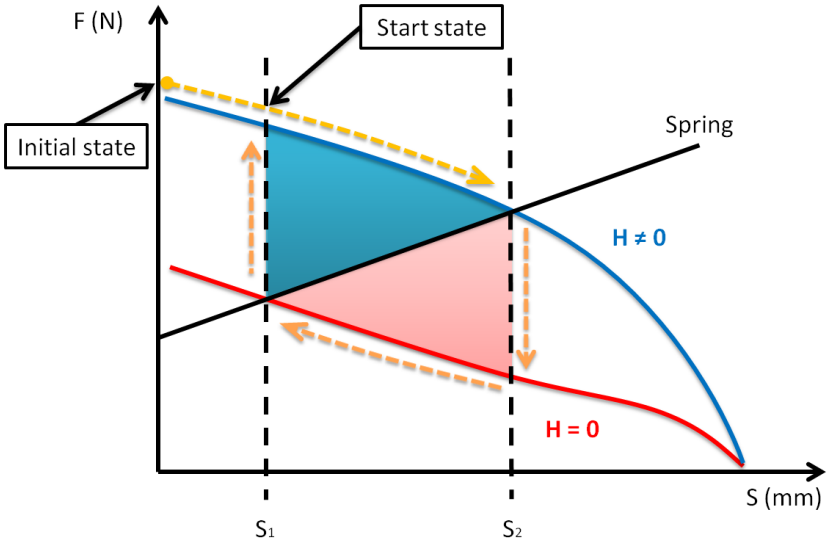

Figure 5.8: Schematic force elongation curve

Particularly in this case it is necessary to emphasize the fact, that the measurement procedure itself can have an impact on the specimen and finally could influence the measurement results. Figure 5.8 shows an exaggerated force elongation curve. that demonstrates an effect that has to be considered with MSME in actuators. The blue curve represents the theoretical force of an MSME, while it is pervaded by a sufficient magnetic field. The red curve represents the needed amount of force to reset the MSME to its initial state. The black line represents a counteracting spring and it can be seen that after first activation (orange path) this actuator will switch between stroke position S_1 and S_2. For a final application this amount of elongation could be sufficient but for the analysis of the measurements it is necessary to consider that, after very first usage, the working point of the device could be shifted and any following measurements will be based on this state. This could affect the elongation and force measurements as well as the magnetisation curves. For the measurements it must be ensured that the starting conditions are defined, or even that the MSME is in the initial state. In other words, the measurements must be done carefully to minimise the error yield by a wrong or changing start state.

5.5 Conclusions

MSM is a relative young technology, which is also commercially hardly acquirable. Therefore it is obvious that there are no tailored measurement devices for MSME available. Nevertheless it is necessary to characterise the properties of MSME for commercialisation as well as simulation purposes. Therefore existing measurement methods have been modified.

For the magnetisation curves the PERMAGRAPH® is used. This device is a good compromise between high flux density (saturation of MSMA at round about 600 kA/m) and reachable preciseness with small samples. With several modifications it is possible to receive the desired magnetisation curves for the simulation purposes. Reduced preciseness is expected in the case of inaccurate geometry as well as poor ratio of the surface of specimen and measurement coil.

The force field behaviour can be estimated by the combination of the force measurement and static simulation. In a first step the force can be measured in relation to the magnetic field in air near to the MSME and in a second step the persisting magnetic field in the MSME can be calculated by using the simulation tool.

6 Measurement Results

6.1 Introduction

To verify the effectiveness of the simulation methods, eight MSME samples out of three different single crystals were chosen with the target to compare simulation and measurement of an MSM actuator. Therefore the MSME were characterised with the modified measurement methods described in Chapter 5. The results shown here are the input data for the simulation methods. Additionally the current-elongation curves of all samples are measured in a prototype actuator to compare the simulation accuracy of the simulation methods with each other.

6.2 Magnetisation Curves

6.2.1 Hard and Easy Axis

The measurement of the easy axis, shown here, confirms earlier results (Sozinov, Likhachev, & Ullakko, 2002), (Heczko, 2004), (Suorsa & Pagounis, 2004). Figure 6.1 shows in blue the magnetisation curve obtained with the MSME blocked at 0.5 % strain. The mounting gap in the blocking disc is slightly bigger than the MSME in the initial state. This gap is necessary to mount the MSME in the disc without any damage. The red magnetisation curve is measured without a block-disc and shows the permeability change, which is caused by the reorientation of the martensitic variants. Furthermore it shows that the permeability until 70 kA/m is lower than for the 0.5 % strain curve (blue). Finally it is possible to estimate the 0 % strain curve (green dotted). The preciseness of these magnetisation curves is of high importance for the prediction quality of the SBS method. In particular a wrong 0 % strain magnetisation curve causes an error in the calculation of the force field behaviour. This error may be compensated by the circumstance that the force field behaviour is calculated on the basis of the magnetisation curve, but such undiscovered deviations could lead to wrong conclusions in further work. Anyhow to improve the quality of this measurement it is necessary to completely compress the MSME to bring it to the initial state. This can be an issue because of inhomogeneity or small defects in the MSME that hinder martensite areas from reorientation. Therefore it cannot be always ensured that the whole sample is totally compressed or slightly elongated.

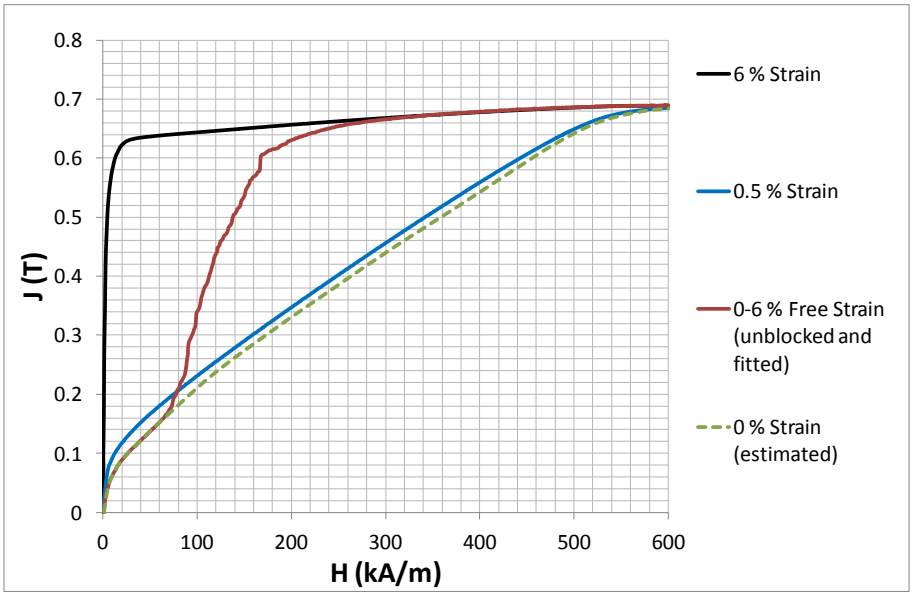

Figure 6.1: Polarisation curve of hard axis (blue), easy axis (black) and strained (red)

6.2.2 Magnetisation Curves at Intermediate Strain Stages

In a next step the blocking discs with intermediate gaps were used to measure the permeability of the MSME at different elongation stages. The results of these measurements are shown in Figure 6.2. It can be seen that the permeability at low fields continuously improves with the strain. Therefore the average saturation of the MSME depends on the elongation state and vice versa.

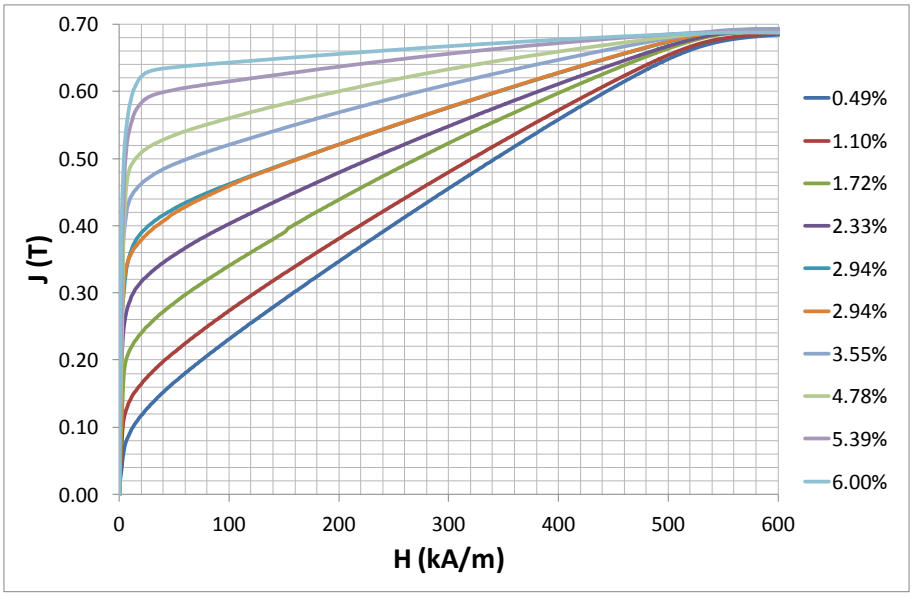

Figure 6.2: Measured strain dependent polarisation curves

Figure 6.2 shows measured polarisation curves at nine different strain stages. So they are strain dependent and represent the polarisation of MSM in an intermediate state while reorientation. The dark blue is measured along the hard axis and represents nearly zero strain and the light blue nearly full strain is along the easy axis, all others are in between. However, the curves at intermediate strain values can be obtained by interpolation of the measured curves. Finally 100 magnetisation curves are calculated that represent strain steps of 0.06 % of the MSME length. It can be observed that above 600 kA/m the polarisation of the MSME at all strain stages reaches the same maximum value of about 0.68 T. Once, at this magnetisation value, it can be assumed that a further increase of magnetic field will not increase the magneto stress and, as a result, a further elongation is impossible.

6.2.3 Stress Dependent Magnetisation Curve

It has to be ensured that the magnetisation curve of the start state is measured. Figure 6.3 shows a measurement of the polarisation. The red curve represents the first measurement, that begins in a compressed state and ends with the elongated MSME. The blue curve shows the directly following measurement during compression. The initial permeability of the blue curve is higher because some martensite variants of the MSME were reoriented by the field during the measurement of the red curve.

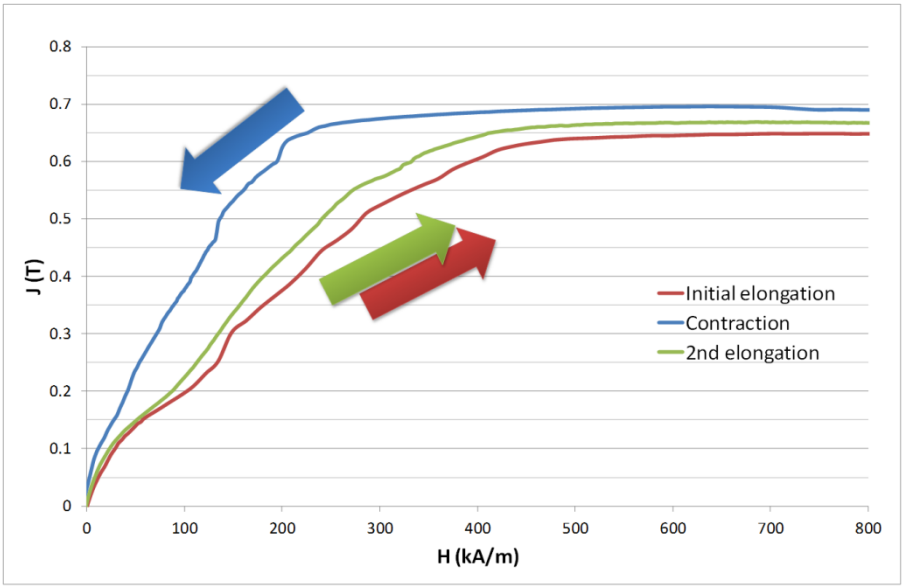

Figure 6.3: Polarisation curve of 1 MPa pre-stressed MSME

As already said, the twinning stress must be overcome by the magnetically induced stress so that a new orientation is possible. As long as in these variants the magnetic stress and the twinning stress are lower than the external stress, they remain along the applied field and are therefore not reset to the initial state. This causes a hysteresis in the force as well as in the polarisation. The green curve shows the behaviour when the return spring is not able to reset the MSME completely and some regions remain oriented in the direction of the measurement field, also after the magnetic field is reduced to zero.

The permeability, as well as the specimen surface, pervaded by the magnetic field increases during the measurement but the measurements of the magnetisation curve in the PERMAGRAPH® somehow assumes that the geometry of the specimen, to be characterised, is known and constant. However, the change of geometry, as in the case of MSME, has an impact on the estimation of the magnetisation curve (Steingroever & Ross, 2009). Figure 6.4 shows polarisation curves that demonstrate the impact on the shape change during the measurement. All three measurements (blue, red, and green) are taken from the same MSME sample: the blue curve corresponds to the compressed MSME, the red curve to the intermediate state at 3 % strain and finally the green curve to full elongation. The black, dashed curve shows the estimated polarisation that represents a real polarisation. This curve overlaps for low magnetic fields with the blue one which is correct only at lower field strength. The sudden increase of the polarisation at about 60 kA/m is caused by the reorientation and the resulting shape change. Between 60 and 100 kA/m the polarisation increases suddenly (red curve) because it represents the intermediate shape while elongation. Above the 100 kA/m the shape change is nearly completed and the green curve represents the polarisation curve of a complete elongated sample.

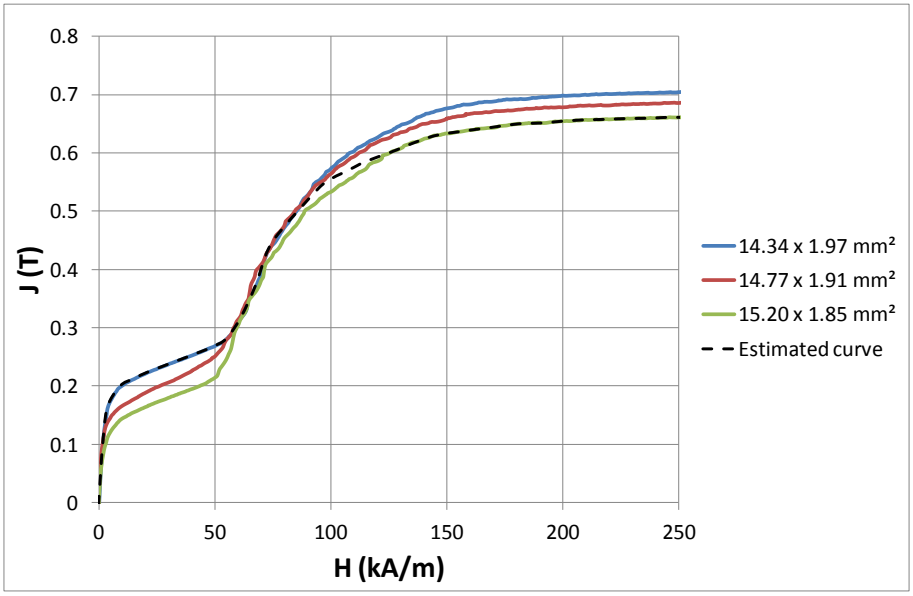

Figure 6.4: Free strain polarisation of one sample with varied surface data

6.3 Stress and Force Measurements

6.3.1 Twinning Stress

The twinning stress is a measure of the mobility of the twin boundaries of the MSM sample. Defects in the atomic lattice could increase this value. In the case that these defects occur with certain regularity, it would be possible to determine a deviation of this twinning stress behaviour. Since this value is equal to required minimum energy, that is needed to initiate reorientation of the martensitic variants, it is a necessary value for the SBS as well as the DMC method.

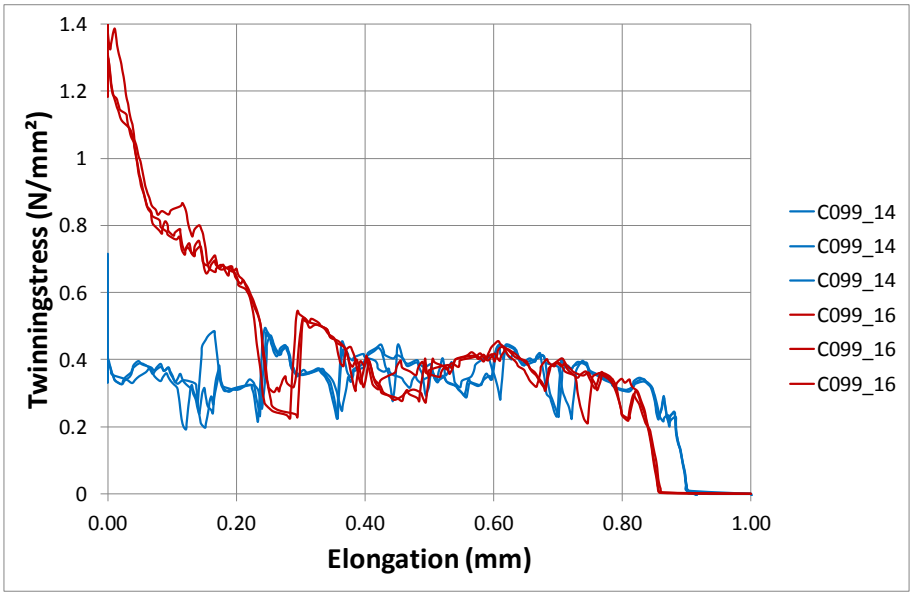

Figure 6.5: Measurement of twinning stress of the samples C99_14 and C99_16 with three repetitions

The twinning stress can be measured by using the method described in Section 3.1.2, in which the samples are pushed back from the elongated to the compressed state. The force over the sample surface that is necessary to contract the sample is the twinning stress. And, as shown, this is varying

along the sample elongation. The twinning stress is measured with the target to identify a statistical distribution, which is representative for any samples cut from an identical crystal. Furthermore the samples of C99 are cut from one slice of the same crystal. It is expected that the slices are homogenous and all samples have nearly the same properties. Nevertheless, despite the expected homogeneity, local displacements in the lattice could occur and small changes in the mobility of twin boundaries can have impact on final behaviour in the actuator. As shown in Figure 6.5, the twinning stress of MSME C99_14 (blue) is low and nearly constant, while the MSME C99_16 (red) shows slightly increased twinning stress up to more than 1.2 MPa for small elongation. Additionally it can be seen that the repeatability of the measurements is good and uniform. This deviation between the twinning stresses can be an indication of defects in the atomic lattice of these samples. Finally this difference of the twinning stress has a huge impact on the functionality of an actuator and on the simulation results as well. The measurements of all MSME used in this thesis are shown in Figure 6.6.

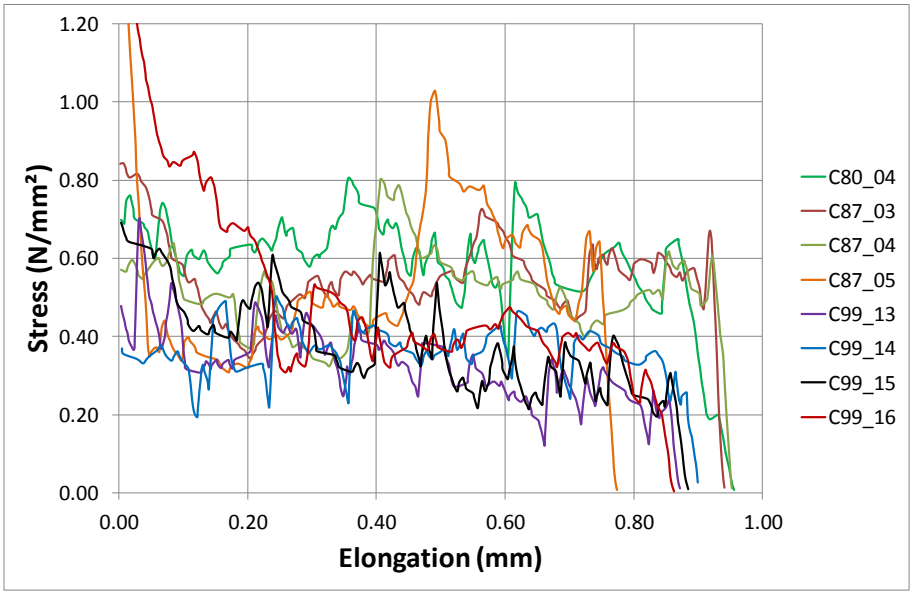

Figure 6.6: Measurement of twinning stress

6.3.2 Twinning Stress, Size Distribution and Training Effects

One objective of all simulation methods here proposed is, to be able to predict the performance of an actuator in exciting the MSM alloy adequately. Therefore the simulation model should represent MSME samples with reasonable tolerances. The idea is thus to estimate some twinning stress distribution and twin width for a given MSM material type, so that the behaviour can be estimated for all samples made from this material type. In Figure 6.5 and Figure 6.7 the stress over strain of two samples is measured three times. However the behaviour of the two samples is however different. While the distribution of stress shows similarities in the distribution peak, the maximum stresses are differing, in particular between 0.5 MPa and 1.4 MPa.

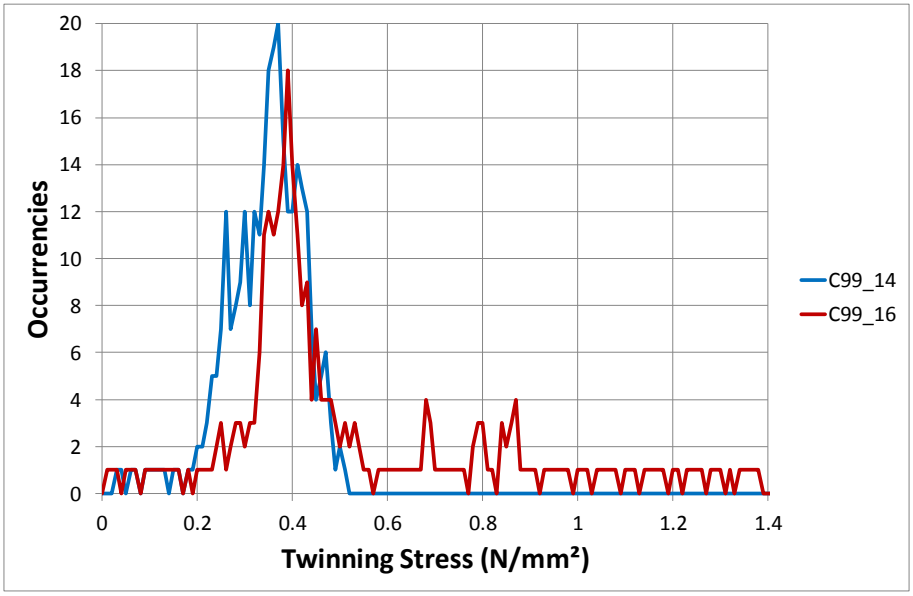

Figure 6.7: Stress distribution of C99_14 and C99_16

As shown in Figure 6.6, the twinning stress seems to be different in any MSME. C99_14 has the lowest twinning stress of all samples. The maximum stress of C99_16 is the highest of all samples, although all samples are cut from the same crystal. This makes it difficult to make a statement about the distribution of the twinning stress. Furthermore it is known, that the structure of the martensitic variants improves after many switching cycles (Aaltio, Soroka, Ge, Söderberg, & Hannula, 2010). This refinement has an effect on the twin size as well as on the mobility and therefore the twinning stress is lower and more homogenous. It can be said that the amount of measurements and samples is not enough to define a generalised stress distribution that describes a material in a general way and under various conditions. In this thesis all measurements were carried out in a timely manner, so that it can be assumed, that such refinements, as well as aging effects, are negligible. On the other hand it plays a subordinate role to determine the quality of the simulation method, because every sample can be individually tested. Therefore in each simulation run the individually measured data, such as twinning stress, as well as twin size, is used directly. Particularly in the SBS method the data of each individually measured sample is randomly assigned to the slices of the MSME in the simulation.

6.4 Force-field Behaviour

As discussed in Section 5.4, direct measurement of the magnetic field in the inner of the MSME is not possible, but can be accessed indirectly. The resulting force-field behaviour is shown in Figure 6.8. It can be seen, that the force, as well as the maximum value, differ from sample to sample. This can be caused by differences in the twinning stress or by individual defects in the atomic lattice of each MSME. This variation will also have an impact on the current elongation curve of the prototype actuator. The force-field behaviour shows an asymptotic behaviour that can be explained by the polarisation results in Section 6.2.2, when above a certain magnetic field no anisotropy is visible.

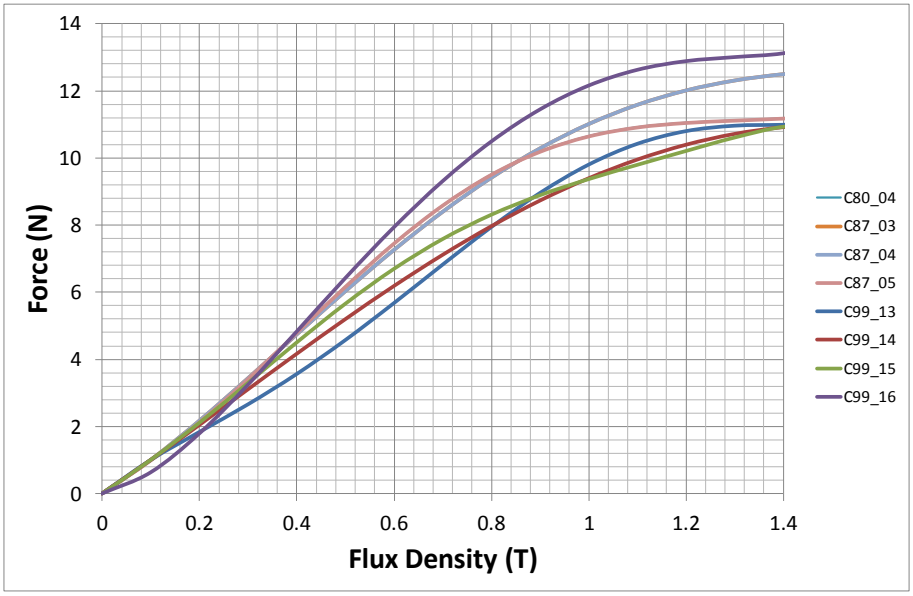

Figure 6.8: Force-field behaviour of MSME samples

6.5 Geometrical Measurements of MSME

Although all samples are produced in the same dimensions (2 x 3 x 15 mm³) it can be seen that in reality every sample shows deviations from these dimensions (Table 6.1). This is due to the manufacturing process of the elements, in particular the cutting of the crystals. When the MSM crystals are casted as martensitic single crystals, the arrangement of the atomic lattice is measured. Subsequently they are cut out by EDM and the obtained orientation of hard and easy axis is unknown. That means that all areas are either in one or another state. Finally the dimensions of the samples can vary by 6%. The elongation was measured without any stress and shows, that some samples reach higher elongation than others.

	Sample number	Cutting date	Xmin (mm)	Ymin (mm)	Zmin (mm)	Zmax (mm)	Elongation (mm)
1	C80_04	2012-09-14	2	2,98	14,71	15,5	0,79
2	C87_03	2012-11-09	1,87	3,04	14,68	15,61	0,93
3	C87_04	2012-11-09	1,86	3,01	14,66	15,57	0,91
4	C87_05	2012-11-09	1,85	2,97	14,63	15,49	0,86
5	C99_13	2013-05-24	1,88	2,99	14,33	15,19	0,86
6	C99_14	2013-05-24	1,87	2,97	14,32	15,18	0,86
7	C99_15	2013-05-24	1,86	2,98	14,36	15,2	0,84
8	C99_16	2013-05-24	1,86	3,01	14,39	15,2	0,81

Table 6.1: Geometrical measurements of MSME samples

6.6 Current Elongation Curve of MSM Samples in an Actuator

To be able to validate the simulation, measurements with actuator prototypes are necessary. Therefore an MSM standard actuator (Figure 6.9) from ETO MAGNETIC was used. This actuator is designed to achieve large strokes, combined with fast frequency response. The MSME sample is placed in the centre of the actuator, beneath a return spring. This counter acting spring is used to return the MSME to its start state after elongation through the magnetic field. The spring's initial tension can be adjusted and was measured by a force sensor beneath the MSME sample. The elongation over current was measured with a triangulation laser and recorded with an oscilloscope. In general, this actuator is able to demonstrate a stroke of almost 0.9 mm at frequencies up to 400 Hz, with a response time of about 1.6 ms. To ensure that the simulation approach is able to consider the external load adequately, the

spring pre-stress was increased so that full elongation is never possible, also for MSMEs that have very low twinning stress. The pre-stress ensures that any element remains in an intermediate state of deformation. A good simulation method should be able to predict the reachable elongation of an MSME under such conditions. The measurements were performed with all samples and are shown in Figure 6.10.

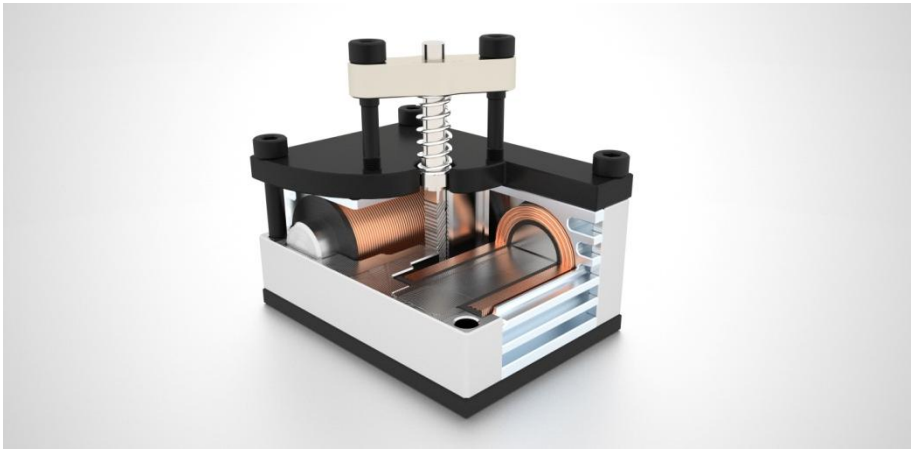

Figure 6.9: MSM prototype actuator (rendered sectional image)

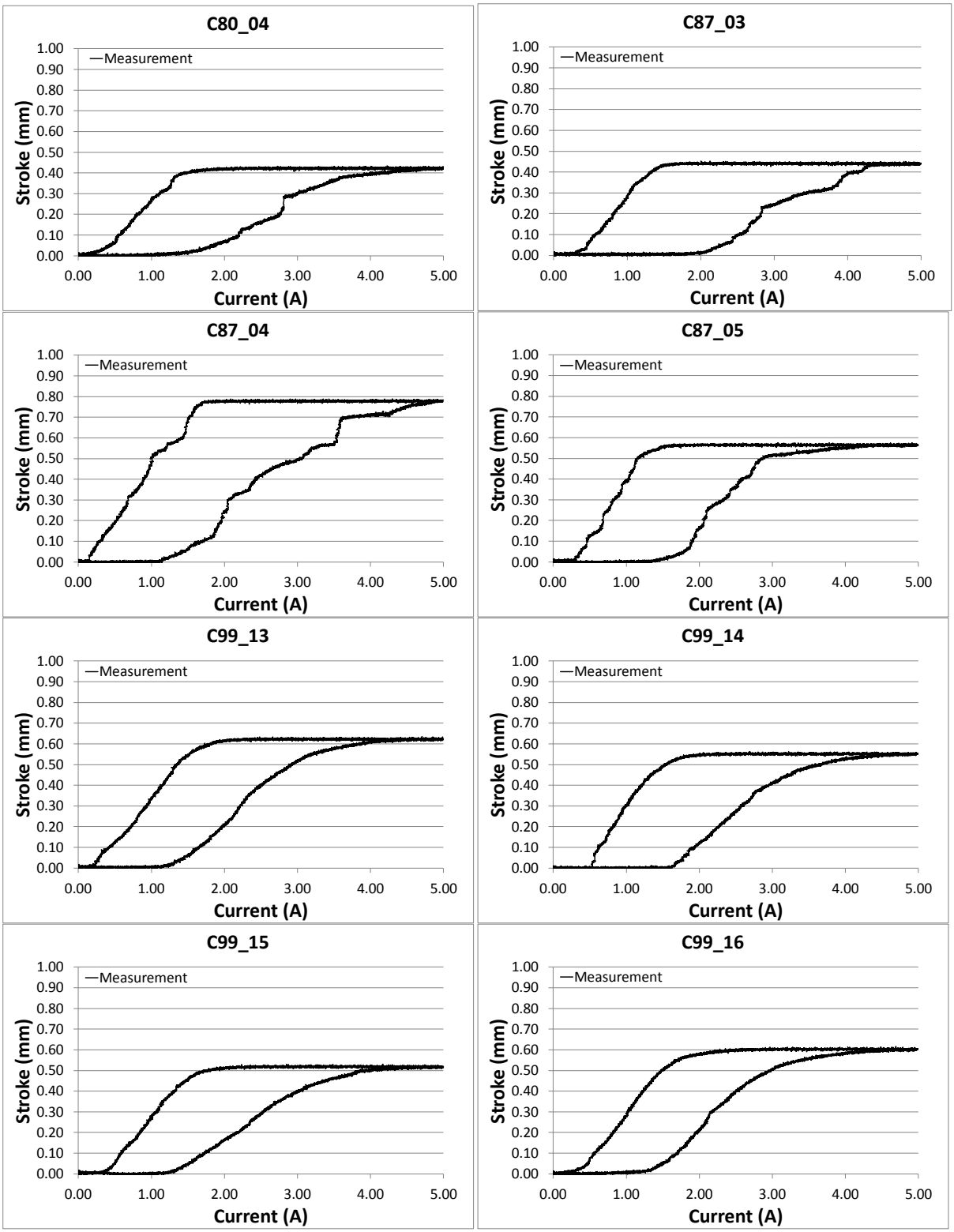

Figure 6.10: Measurement of current-displacement curves

6.7 Conclusion

In preparation of the simulation procedures the characterisation of all MSME samples was done and the performance of 8 samples was measured in an MSME prototype actuator. The sample preparation is of high importance for precise results and therefore high attention is set on this procedure.

The geometrical measurements of the MSME, as well as elongation under pre-stress in the prototype actuator, are measured with standard measurement devices. The measurements of the magnetisation curves needed modified ad-hoc methods. The precision of these modified methods, in particular with the Permagraph, is limited by several practical aspects, which are depending on the measurement procedure. However there is enough room for improvements.

The width and twinning stress of each material slice, which are elementary parts of the material that is used in the simulation methods, cannot be determined precisely from measurements. As shown, the samples characterised here have random tendencies and nearly unpredictable behaviour. This suggests that also some additional interaction in the slices could have an effect on the twinning stress. Such effects could be reduced by a cyclic usage, which is also known as training effects. It was not possible to estimate a distribution that is suitable to describe the behaviour of a complete MSMA cast. To the aim a deeper understanding of aging effect and of the stabilising of twinning types is necessary. Anyhow, to prove the quality of the simulation methods in this work, we perform our experimental results and tests on some MSME and avoid generalisation to a complete cast.

7 Analysis and Evaluation of Simulation Results

7.1 Introduction

In this Chapter the simulation results are presented and discussed, to evaluate the quality of the simulation methods proposed in this thesis, as well as their computing time. Therefore each approach is rated in terms of the following parameters:

- Computing time
- Precision

The computing time aims at comparing the complexity of the simulation methods in a qualitative way. To make the results consistent, all models were calculated on the same computer so that the influence of the hardware is approximately negligible. The quality of each model also plays a role for the computing time, in the sense that some models need less simulation steps to reach an acceptable precision. Anyhow, the main focus is on the quality of the simulation methods, intended as the precision of predicting real actuator behaviour in the simulations. The characterisation data of the MSME, obtained with the measurements techniques described in the previous chapters, were used as input to each simulation model, to estimate and predict the elongation of the MSME in the prototype actuator under design. Afterwards the accuracy of each simulation, compared to the measurement, is evaluated by means of a correlation analysis.

7.2 Stress Based Simulation (SBS)

The SBS method is the most complex of these three simulation approaches. Depending on the current step width and the amount of twins/slices, a simulation run needs several hours. Furthermore, solving the Maxwell equations is time consuming, especially when two connected MSM areas are differently oriented. Particularly critical is the high anisotropy of the MSME itself, which is difficult to handle also for commercial FEM programs.

7.2.1 Precision

The measurements shown in Figure 7.1 demonstrate the measured current-elongation behaviour of the particular MSME sample in the prototype actuator (black) and the predicted behaviour using the SBS method (blue). It can be observed that the maximum achievable elongation in many cases can be predicted quite precisely. Nevertheless, in the early phase, when current rises all simulations show strong increase of elongation. As shown in Figure 7.2, the results are with an average coefficient of determination of 0.89 and an average deviation of 10.1 % in general in good agreement with the experiments, though the shape of the elongation does not coincide with the predicted profile. It is noticeable that when the current is decreasing, the compression of the MSME is very abrupt in all simulations. Particularly the sample C99_15 shows the lowest coefficient of determination of 0.78 and maximum average deviation of 16.3 %. It is visible that the hysteresis, especially in this case seems to be narrower in the calculation than in the measurement.

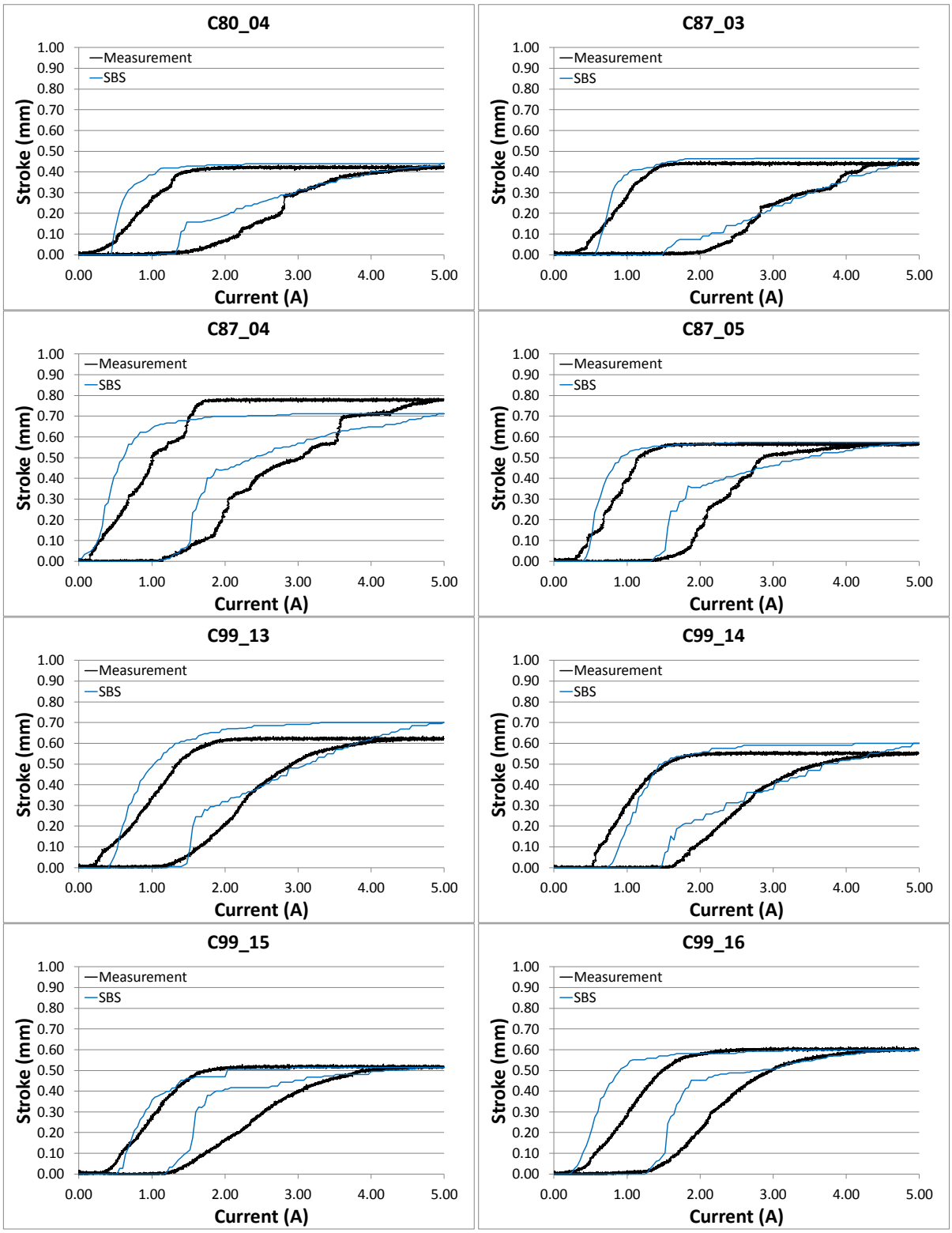

Figure 7.1: Measurement (black) and SBS simulation (blue) of current-displacement curves

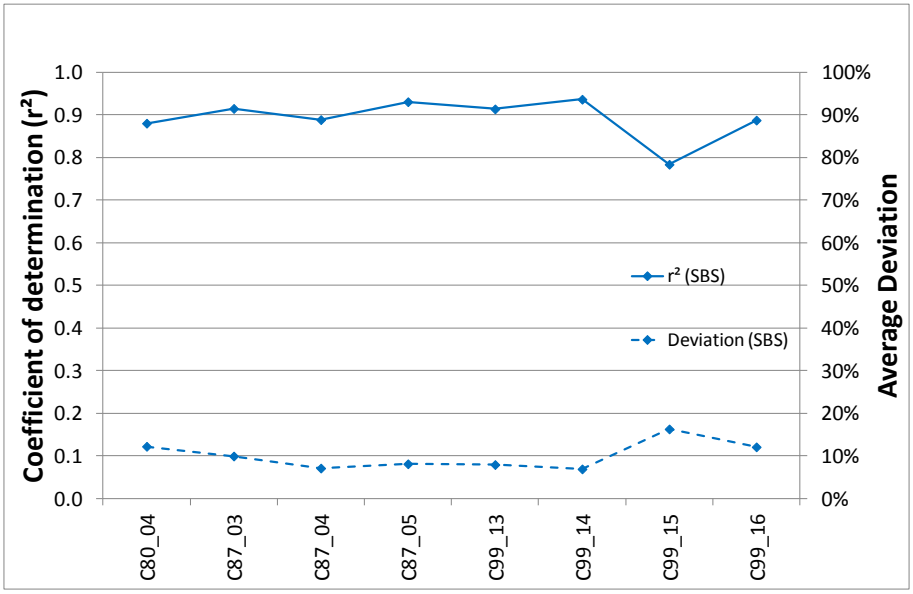

Figure 7.2: Coefficient of determination and average deviation of all SBS simulation runs

	SBS	
Sample	r^2	Deviation
C80_04	0,88	12,2%
C87_03	0,91	9,9%
C87_04	0,89	7,1%
C87_05	0,93	8,1%
C99_13	0,91	7,9%
C99_14	0,94	6,9%
C99_15	0,78	16,3%
C99_16	0,89	12,1%
Average	0,89	10,1%

Table 7.1: Coefficient of determination and average deviation of all SBS simulation runs

7.2.2 Computing Time

Because of the complexity the SBS approach is a time consuming method. Simulation times between 4 and 8 hours were experienced. The necessary computing time for predicting the deformation at one current value varies between one or two minutes, and the simulation methods performs this calculation for each current value between the chosen minimum and maximum currents. Furthermore it can be seen (Table 7.2) that the calculation time is largely determined by two factors. The first is the number of "slices" of the MSME and the necessary interaction between FEMM and Excel to calculate the stress in every individual slice at all current values. Obviously the calculation can be shortened by choosing a reduced number of slices. Nevertheless a minimum number of slices are needed to predict the elongation with good agreement with experiments. The second factor is that the simulation for each current value needs one or two minutes and therefore the current-step width has an impact on the overall computing time of a simulation run. Since each simulation step always starts from the states calculated at the previous step, the quality of the simulation prediction depends on the current-step width and therefore a relatively small width is necessary.

Sample	Slices	Step size (A)	Time	Time (per step)
C80_04	201	0.02	477 min	114 sec
C87_03	201	0.02	527 min	126 sec
C87_04	162	0.02	511 min	123 sec
C87_05	177	0.02	440 min	106 sec
C99_13	176	0.02	440 min	106 sec
C99_14	96	0.02	232 min	56 sec
C99_15	108	0.02	266 min	64 sec
C99_16	158	0.02	393 min	94 sec
		Average	411 min	99 sec

Table 7.2: Computing time of SBS approach of all samples

7.2.3 Evaluation

This approach shows an adequate precision and allows a deeper understanding of the material behaviour in combination with a complete magnetic circuit. The actuator design can strongly benefit from this detailed knowledge and simulation result.

7.2.4 Further Improvements

The biggest drawback of this approach is the huge computing time. This could be reduced by several means. A lower amount of slices could reduce the computing time. It can be very roughly assumed, that the calculation of one slice over all currents takes about 2 minutes so that a reduction of slices would have a large effect. This has to be treated carefully, because the reduction of slices would also reduce the elongation resolution and could lead to wrong results. Anyhow, the calculation of the sample C87_03 with 201 slices needs two times longer than C99_14 with 96 slices and comparable precision.

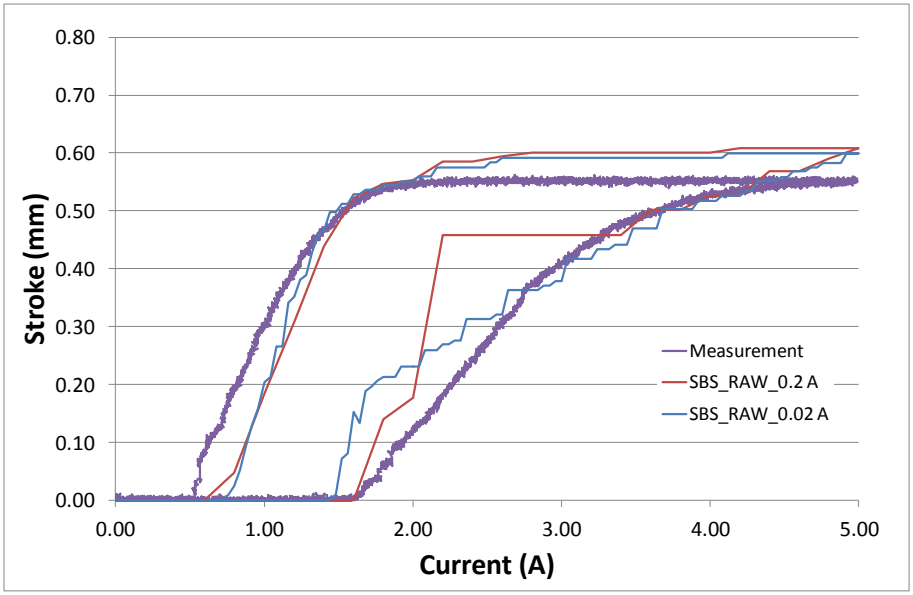

Figure 7.3: SBS with 0.2 A steps (red) and 0.02 A steps (blue)

Moreover the width of the current-step could be reduced. In Figure 7.3 two simulation results of the same MSME are shown. The red curve shows the predicted elongation with a current-step width of 0.2 A and the blue with a current-step width of 0.02 A. The other simulation parameters, such as the

size, the position and twinning stress of every individual slice, are identical. It can be seen that the red curve shows a sudden elongation at 2 A. Because of the comparatively large current-steps of the red curve, several twins switch together with the suddenly increased current. While the blue one shows small intermediate switching states that lead to a different elongation process, which in turn results in a different variation of strain and thus permeability of the electromagnetic circuit. In other words, since each simulation step influences the consequent step, a finer current grid is recommended to obtain meaningful results.

7.3 Dynamic Magnetisation Curve (DMC)

The DMC method is less complex than the SBS, from a computing point of view. The computing time for one simulation is always about 1 hour. The geometrical complexity of the simulation model is reduced and the permeability is taken into consideration by a set of strain dependent magnetisation curves. This is an advantage, because the entire sample in every simulation step needs only one particular magnetisation curve that suits to the strain situation and reduces the complexity of solving the Maxwell equations in the MSME.

7.3.1 Precision

The average coefficient of determination is 0.73 and the deviation 20.8 % (Table 7.3). Figure 7.4 shows the behaviour of the MSME samples, predicted by the simulation in red and the measurements in black. It is striking that all simulation runs reach the full elongation, in contrast to the real measured samples, and the DMC method is thus not able to predict the intermediate state properly. In fact, the average permeability of the MSME corresponds to the actual strain and therefore, as the strain increases, the magnetic resistance of the alloy decreases and the magnetisation of the alloy improve, leading to higher fields and higher forces produced by the alloy. A higher force would produce a higher strain at the next simulation step: as a consequence, the strain of the MSM alloy increases continuously during the simulation. This problem is due to the fact that in real alloys the maximum magneto-stress is not a constant, but decreases with the strain.

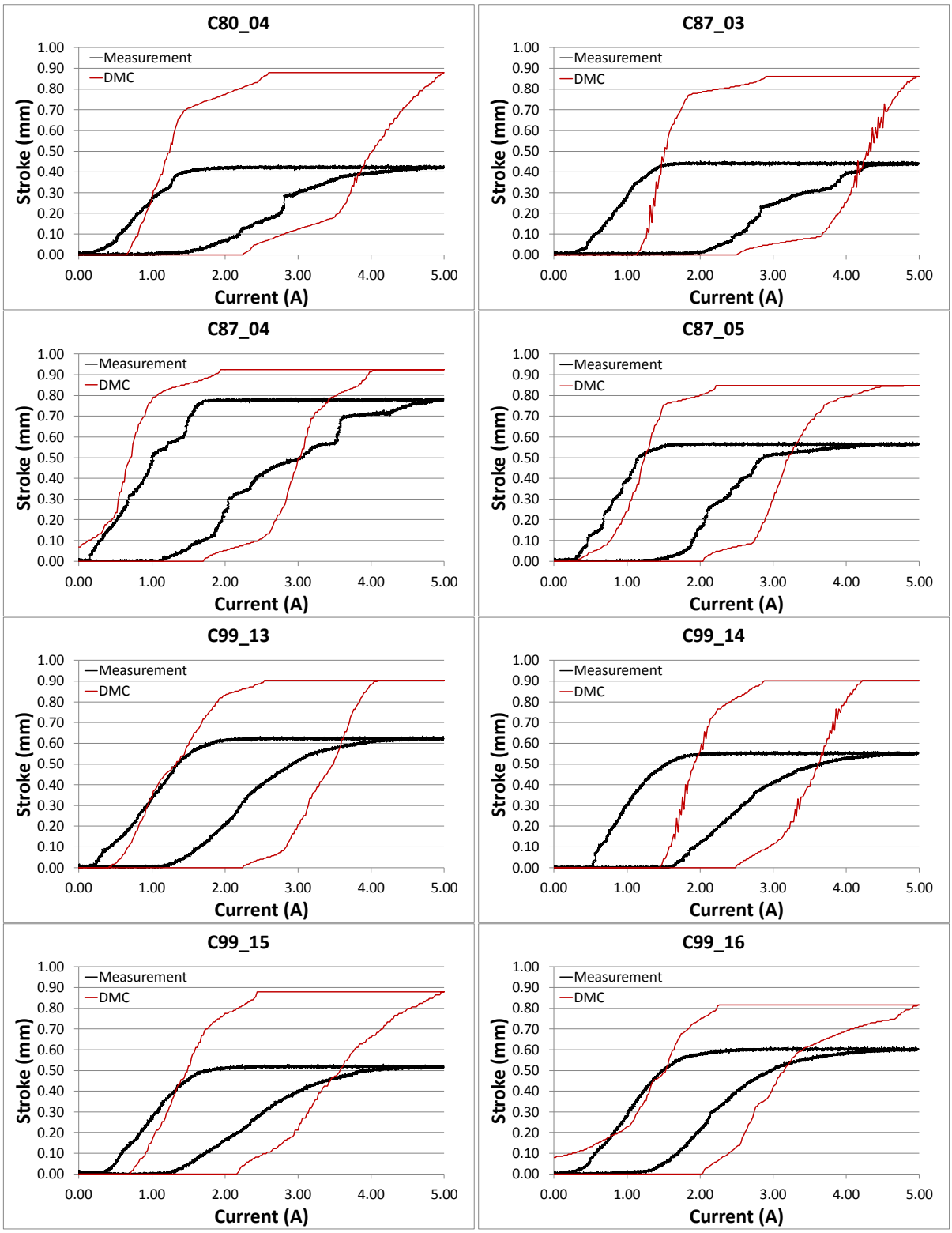

Figure 7.4: Measurement (black) and DMC simulation (red) of current-displacement curves

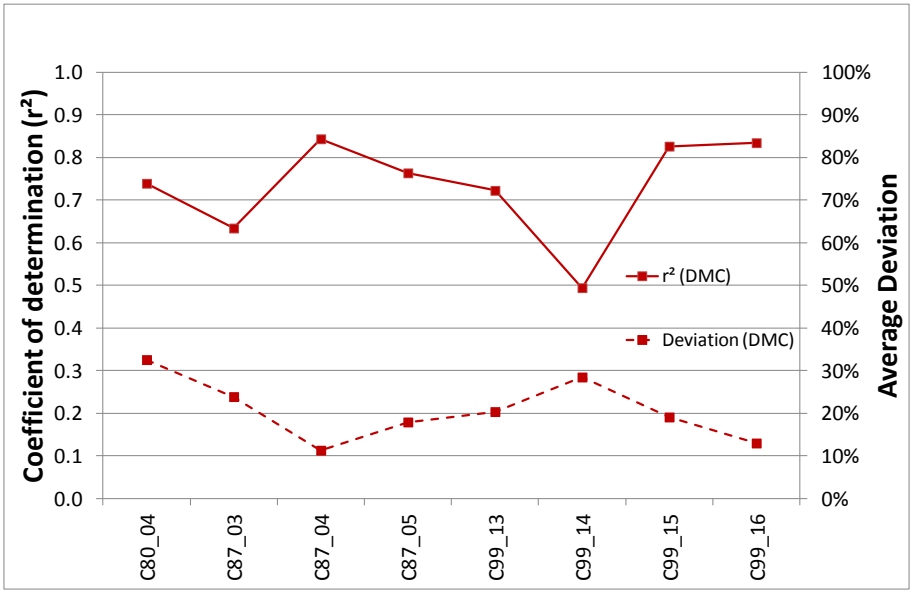

Figure 7.5: Coefficient of determination and average deviation of all SBS simulation runs

	DMC	
Sample	r^2	Deviation
C80_04	0.74	32.6%
C87_03	0.63	23.9%
C87_04	0.84	11.3%
C87_05	0.76	17.9%
C99_13	0.72	20.3%
C99_14	0.49	28.5%
C99_15	0.83	19.1%
C99_16	0.83	13.0%
Average	0.73	20.8%

Table 7.3: Coefficient of determination and average deviation of all SBS simulation runs

7.3.2 Computing Time

As expected, the DMC approach is about seven times faster than the SBS, because of lower complexity in the MSME model and the handling of the switching behaviour. As shown in Table 7.4, every simulation run needs about 1 hour to calculate the current-elongation behaviour with a current-step width of 0.01 A, which is also two times finer than the SBS and the calculation of one current step is nearly 14 times faster. Furthermore the computing time of any simulation run is very close. This is caused by the circumstance that the MSME is described with only one magnetisation curve in each simulation step and the required interaction between FEMM and Excel is limited.

Sample	Step size (A)	Time (min)	Time (per step)
C80_04	0.01	62 min	7.4 sec
C87_03	0.01	52 min	6.3 sec
C87_04	0.01	55 min	6.6 sec
C87_05	0.01	61 min	7.3 sec
C99_13	0.01	61 min	7.3 sec
C99_14	0.01	61 min	7.3 sec
C99_15	0.01	62 min	7.5 sec
C99_16	0.01	61 min	7.3 sec
	Average	59 min	7.1 sec

Table 7.4: Computing time of DMC approach of all samples

7.3.3 Evaluation

The DMC is faster, but less precise, compared to the other methods. The smaller calculation time is an advantage to test an actuator design qualitatively. Anyhow, the low precision is an issue, especially when several actuator concepts should be compared, based on the simulation prediction offered by the DMC.

7.3.4 Further Improvements

The main drawback of this method is the low precision. This is caused by the self-supporting effect, whereby every calculated sample reaches full elongation. This effect could be compensated by a modified stress calculation. In particular for this model, a damping factor or a separation of the MSME into several sections could be helpful, but this would be a drawback because the advantage of short calculation time will get lost. Another possible option is a different stress calculation, but this has to be researched. Although improvements of the computing time are possible, the precision offered by the DMC seems too low to be taken into consideration for simulation of MSM actuators.

7.4 Stress Dependent Magnetisation Curve (SDM)

The SDM method has the lowest computational complexity of all three methods but needs huge preparation in advance. This is caused by the stress and strain depended magnetisation curves described in Section 4.4.2. The computing time per simulation step is a little bit lower, compared to the DMC. But in contrast the SDM approach has the possibility to estimate the performance of an MSM actuator in only one simulation step. Therefore the step width can be chosen very small and particularly in this case an average predicted current-force curve is calculated by the SDM in less than 17 minutes. The sample C80_04 was excluded from this method, because the sample was damaged.

7.4.1 Precision

The coefficient of determination is in average 0.9 and the deviation with 10.3 % is comparable with the SPS approach (Figure 7.6). Also in this simulation run is one sample (C87_03) because of lower accuracy and higher deviation conspicuous. As shown in Figure 7.7, some simulations (green) are in a very good agreement to the measurement (black), while some are deviating. Also the reached elongation precision is, compared to the SPS method low however much but better than the DMC method.

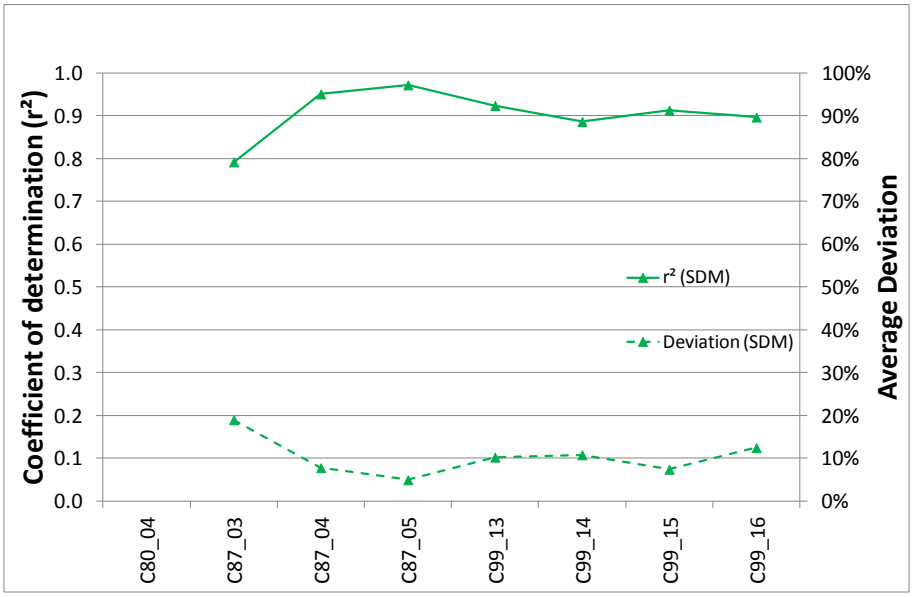

Figure 7.6: Coefficient of determination and average deviation of all SDM simulation runs

	SDM	
Sample	r²	Deviation
C80_04		
C87_03	0.79	18.9%
C87_04	0.95	7.7%
C87_05	0.97	4.9%
C99_13	0.92	10.2%
C99_14	0.89	10.7%
C99_15	0.91	7.4%
C99_16	0.90	12.4%
Average	0.90	10.3%

Table 7.5: Coefficient of determination and average deviation of all SDM simulation runs

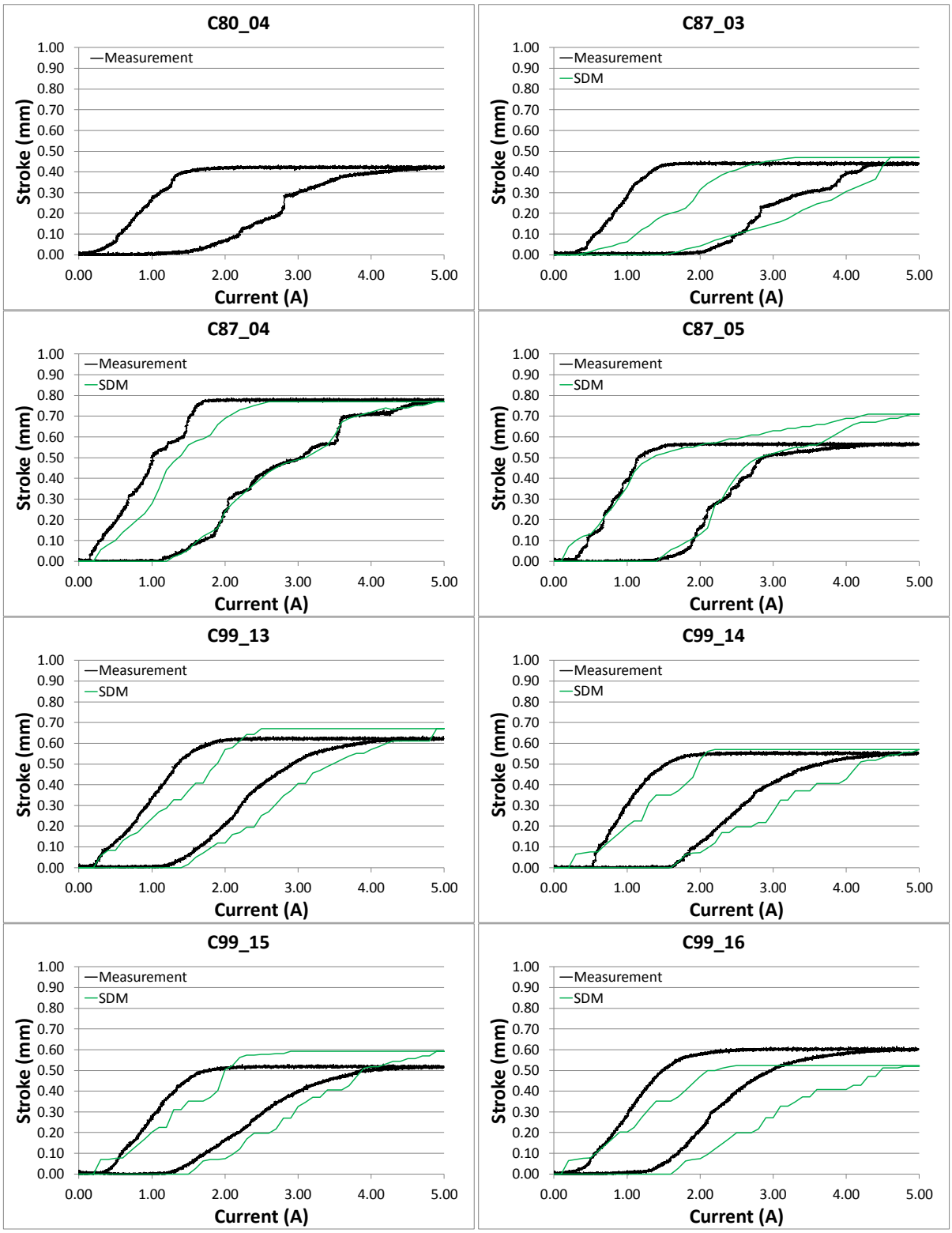

Figure 7.7: Measurement (black) and SDM simulation (green) of current-displacement curves

7.4.2 Computing Time

A comparison of the calculation time in this case is difficult. Since simulation steps are in fact not necessary to estimate the functionality, the needed computing time can be reduced to less than 10 seconds (Table 7.6). Anyhow, to obtain a meaningful current-elongation curve, a step size of 0.05 A was chosen and a single simulation step is about 30 % slower than one of the DMC but 10 times faster than the SPS.

Sample	Step size (A)	Time	Time (per step)
C80_04	0.05	-	-
C87_03	0.05	15 min	8.7 sec
C87_04	0.05	15 min	9.2 sec
C87_05	0.05	16 min	9.7 sec
C99_13	0.05	18 min	10.7 sec
C99_14	0.05	20 min	11.8 sec
C99_15	0.05	14 min	8.2 sec
C99_16	0.05	19 min	11.1 sec
	Average	16.7 min	9.9 sec

Table 7.6: Computing time of SDM for all samples

7.4.3 Evaluation

The SDM is as precise as the SBS. The circumstance that the SDM needs only one simulation run to estimate if the actuator is efficient to reach full elongation, makes this method attractive for optimisation tasks. The precision of this simulation approach is sufficient for designing actuators.

7.4.4 Further Improvements

As already shown, the measurement results of the pre-stressed magnetisation curve have low precision. This is caused by the low ratio of sample surface to measurement coil diameter, as well as inaccurate pre-stress adjustment. Furthermore it is an issue that the measurement device is designed to measure samples with constant geometrical behaviour. Finally it can be said that there is room for improvements on the magnetisation curve measurements that should lead to better data collection and thus to improved precision of the SDM as well as other simulation methods.

7.5 Conclusion

In magnetic FEM simulations for reluctance actuators a good agreement is achieved with a deviation of less than 5 % (ETO MAGNETIC GmbH, 2012). On the other hand, in the last centuries many researchers were working in this area and the experience in this class of actuators is very high, in contrast to actuators based on MSM. Furthermore the calculation of MSM is in principle a multi-physics problem and therefore more complex, which in turn reduces the prediction accuracy.

Results are presented showing that sufficient prediction of the response of MSMEs in an actuator is possible (Figure 7.8). Depending on the approach, good precision in adequate computational time is achievable. The SBS and the SDM have comparable precision. The SDM shows a performance advantage (Figure 7.9). Furthermore it would be possible to improve the quality by improved measurement techniques. Anyhow, it should not be neglected that the measurement of data like the stress dependent magnetisation curves is challenging and time consuming. The specific magnetisation curve, which is measured for the method, is only suitable for one particular stress situation. In the case

that the stress situation is changing dynamically, for instance in dependence on the Maxwell force, the simulation method will fail to predict the response of the MSME, unless additional measurements are taken into account by the user.

The SBS approach is interesting for research purposes for an ideal actuator and MSME interaction. Although it cannot rebuilt the physical phenomena in detail, it gets as close as reasonable for this type of simulation in combination with the complete actuator. Anyhow, it seems that this approach hits its borders; therefore further improvement in the measurement of magnetic properties is mandatory. On the one hand, the surface ratio between diameter of measurement coil and dimension of the specimen is less than 10 %, whereas it should be bigger than 50 %, on the other hand the measurement of these curves is a fundamental issue, because the circumstance that the measurement method itself affects the geometry, influences measurement result.

The DMC approach has the shortest current simulation time but the lowest precision of all three methods. The self-supporting effect plays a dominant role in this simulation and needs to be improved or compensated to make this method attractive. The proposed idea of a modified stress calculation would certainly contribute to an improvement, but would also increase the complexity of the model and thus would reduce the advantage of this method. It can be said that the SBS and SDM are good choices for most simulation issues. They are sufficient for optimisation of actuators with MSM and enable a deeper insight of the MSME behaviour in combination with an electromagnetic actuator.

Finally it has to be mentioned that in this work the time-dependent effects such as the training and the aging of the MSME, were neglected. These effects play a minor role in this thesis because the number of performed switching cycles during measurements is quite low.

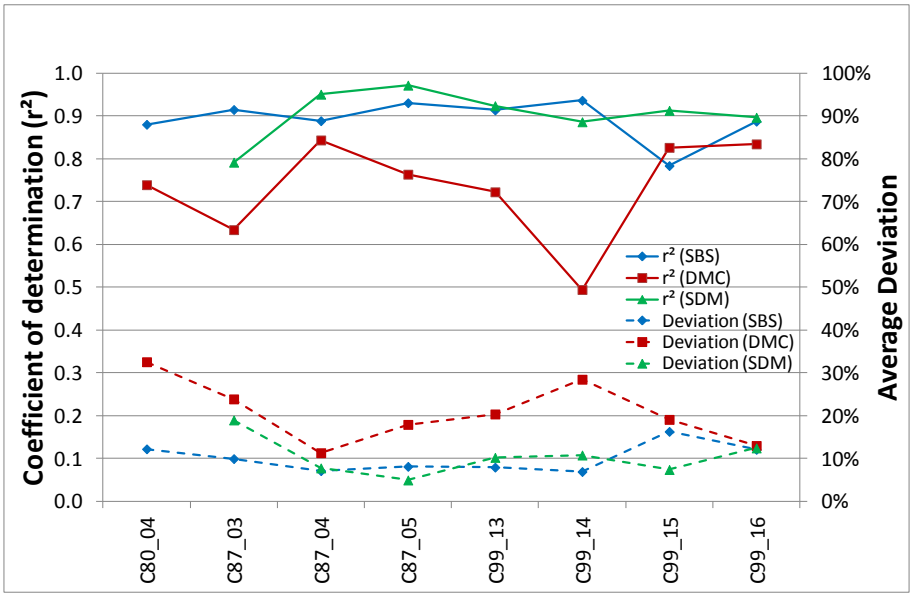

Figure 7.8: Simulation quality of all approaches

	SBS		DMC		SDM	
Sample	r^2	Deviation	r^2	Deviation	r^2	Deviation
C80_04	0.88	12.2%	0.74	32.6%		
C87_03	0.91	9.9%	0.63	23.9%	0.79	18.9%
C87_04	0.89	7.1%	0.84	11.3%	0.95	7.7%
C87_05	0.93	8.1%	0.76	17.9%	0.97	4.9%
C99_13	0.91	7.9%	0.72	20.3%	0.92	10.2%
C99_14	0.94	6.9%	0.49	28.5%	0.89	10.7%
C99_15	0.78	16.3%	0.83	19.1%	0.91	7.4%
C99_16	0.89	12.1%	0.83	13.0%	0.90	12.4%
Average	0.89	10.1%	0.73	20.8%	0.90	10.3%

Table 7.7: Simulation quality of all approaches

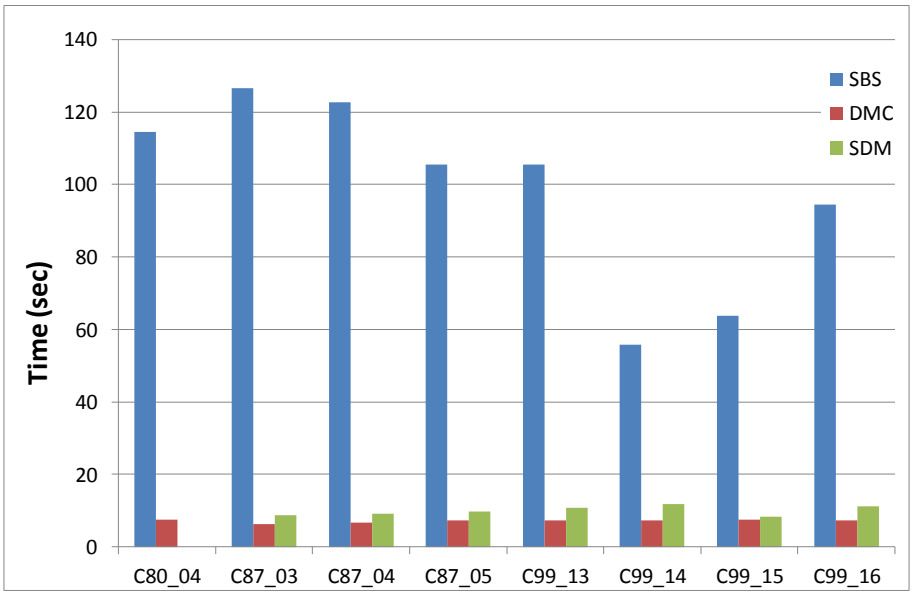

Figure 7.9: Computing time of one simulated current step of all approaches

8 Application of MSME simulation methods

In the following, examples are shown, in which the established simulation methods were used to gain insight, optimise actuators and improve fatigue. In some cases the methods are supporting assumptions, in others they have a central role and lead to a deeper understanding of the material behaviour and reveal neglected effects as important impact factors.

8.1 Interaction of MSME in an actuator

Since the pioneering publication of Kari Ullakko in 1996, over 1000 papers have been published in the MSM area citing his work. Some of these study how an MSME behaves in a magnetic field or concentrate on how single crystals can be produced, which composition could lead to better performance and so on. But direct interaction between an MSME and an actuator that generates a magnetic field with a minimised amount of electrical energy consumption is normally not in focus.

As discussed in Section 4.2.3, the direction of the magnetic field in the MSME is responsible for the reorientation of the martensitic variants. The SBS method is able to calculate the magneto-stress in every slice and is taking into account the *x* and *y* components of the magnetic field as well as external and internal stress individually. Figure 8.1 shows the magnetic FEM simulation of an exemplary MSME inside an external magnetic field. The field is directed vertically and the red areas represent martensitic twins with comparatively lowest twinning stress value so that these can switch with a low amount of current and therefore in an early actuation. After these first areas have switched the magnetic field is concentrated inside these areas, because their magnetic easy axis is already oriented parallel to the external magnetic field.

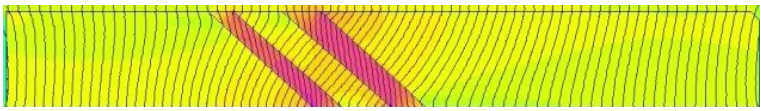

Figure 8.1: Magnetic interaction between switched areas (red) and non switched (yellow)

On the contrary, the field in non-switched areas reduces. Figure 8.1 also shows, that the flux lines nearby and especially between the two switched areas are tilted by 45° with respect to the external field. The result is a locally increased magnetic field component in *x*-direction (horizontal in Figure 8.1) that in turn causes a local compressive stress contribution in *x*-direction. As shown in Equation 4.2 the stress component in *x*-direction (σ_x^{ext}) has an impact on the switching behaviour and impedes the elongation in the *x*-direction.

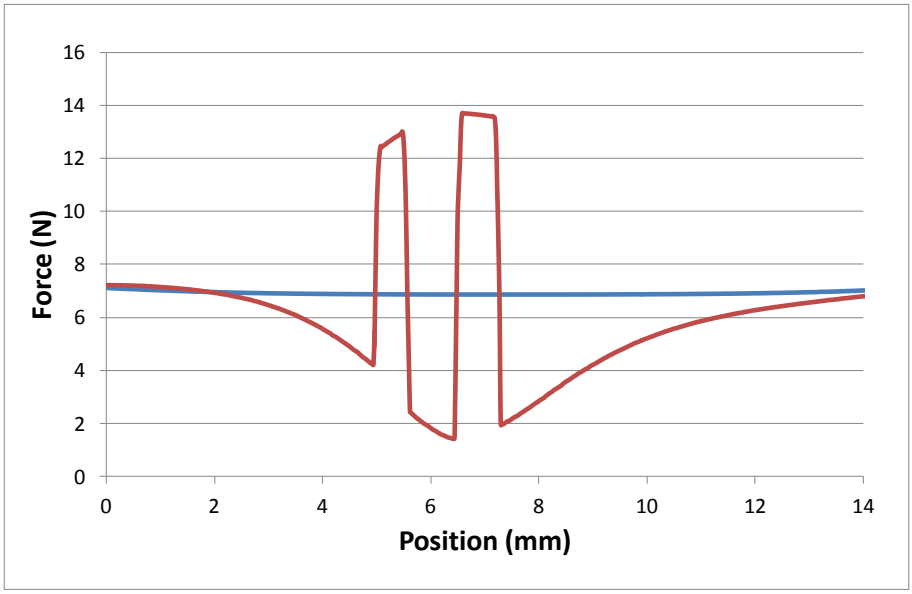

Figure 8.2: Calculated magneto-forces in MSME, with non-switched areas (blue) and two switched areas (red)

Figure 8.2 shows the calculated magneto-forces along the *x*-direction through the MSME. A non-switched MSME (blue) is taken as reference and compared with an MSME as shown in Figure 8.1, where two twin areas have already switched. As expected, the local forces for switched twin areas increase, they roughly double because of increased permeability. However, in the proximity of these areas a force drop is observed which affects even relatively distant areas of the element. This local force drop is explained with the local tilting of the field lines, as discussed before. The external field has to be increased to obtain a value inside the MSME, which is sufficient to induce further switching.

Furthermore it is known that the mobility of twin boundaries could increase over many switching cycles, because a finer twinning structure arises (Aaltio, Soroka, Ge, Söderberg, & Hannula, 2010). The amount of martensitic variants has a direct impact on the resolution of the elongation and could also have an impact on the current-elongation behaviour of an actuator. The SBS allows reproducing and observing this effect just by varying the number and the width of martensite slices. Additionally the distribution of twinning stress can be varied and effects of this variation can be observed. Thus, the SBS also allows estimating how a MSME would behave in the case of aging, or modification of twin microstructure.

It should be noted that the SBS only estimates what happens in reality. Nevertheless the simulation results allow a very important design insight about the response of a MSME during actuation, and have proven that SBS-based models depict the real phenomena adequately. A very important detail shown by the SBS simulation is that the orientation of the variants influences the magnetic field locally and distorts the magnetic field because of the anisotropic permeability. This distortion could be partially influenced by a certain design of the magnetic circuit. An idea is schematically shown in Figure 8.3. In the schematic two magnetic circuits are shown. The flux lines for the blue magnetic circuit are illustrated in red and the ones for the green circuit in black. Flux lines are closed loops that follow the path of lowest resistance. In such a situation, the diagonal path through the MSM is much longer than the path which goes directly to the other end of the magnetic circuit and therefore has higher magnetic resistance, so that the deviation of the flux lines should be lower. It can be assumed, that such a solution should reach full elongation with a lower magnetic field and therefore lower electrical energy.

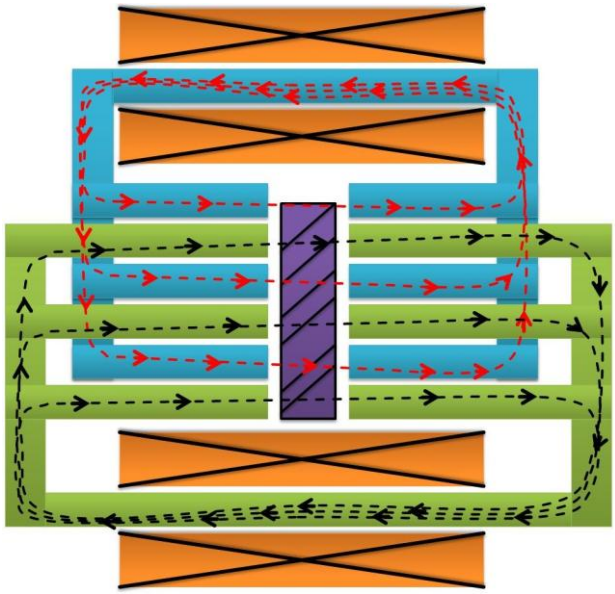

Figure 8.3: Schematic representation of magnetic circuits

8.2 Actuator optimisation with evolutionary algorithms

For a further improvement and consequent commercialisation of the MSM technology, effective simulation tools are required to identify optimised actuator designs in short time. However, the optimum is defined by individual requirements of particular applications, such as smallest space or lowest energy consumption or combinations of both. Due to the variety of requirements, the nonlinearity of electromagnetism and the large number of design parameters, an evolutionary algorithm (EA) has been tested for the optimisation of MSM actuators. Evolutionary algorithms are robust optimisation methods, for nonlinear problems with many decision variables and linear or nonlinear constraints. EA's are a class of stochastic metaheuristic optimisation methods which are inspired by the natural evolution of living beings and help to solve problems particularly for computer simulations and applications of computer science appropriate models. Based on the nature of candidate solutions to a given problem are artificially evolved, EA are so natural analogue optimisation methods (Rechenberg, 1994). The assignment to the class of stochastic and metaheuristic algorithms means, that an EA usually does not find the best solution for a problem, but a sufficiently good one. The different EAs differ primarily by the used selection, recombination and mutation operators, the genotype-phenotype mapping and the problem representation (Schäfer, 2012).

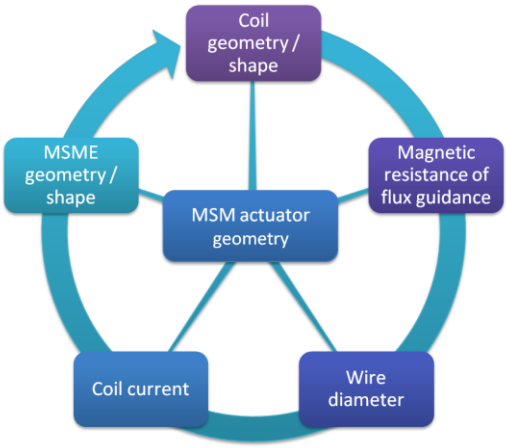

Figure 8.4: Interdependencies of design parameters

A modification of the (μ/μ, λ) EA of Rechenberg has been proven as a good choice for nonlinear magnetic problems (Rechenberg, 1994), (Schäfer, 2012).

8.2.1 Optimisation procedure

This method usually consists of an initialisation step and a first evaluation, as well as a succeeding loop, that is executed until a termination criterion is satisfied (Weicker, 2007). As shown in Figure 8.5, the optimisation process starts with the initialisation, where the first generation of candidate solutions to the problem is generated randomly. In the next step these candidates are evaluated and their properties are assessed by the so-called value function. The value function delivers finally a single value (or, in multi-objective EAs, a vector value) which allows evaluating if the tested parameters are a good solution or not. Based on the value function the best individuals, also called parents, are selected and subsequently recombined to the next generation and the optimisation loop starts again. Additionally a random variation of the descendants is performed (mutation). In the next step an evaluation of these individuals is performed. Again, depending on the value function, a selection and determination of a new generation is done, or the optimisation loop is stopped if the termination criterion is fulfilled.

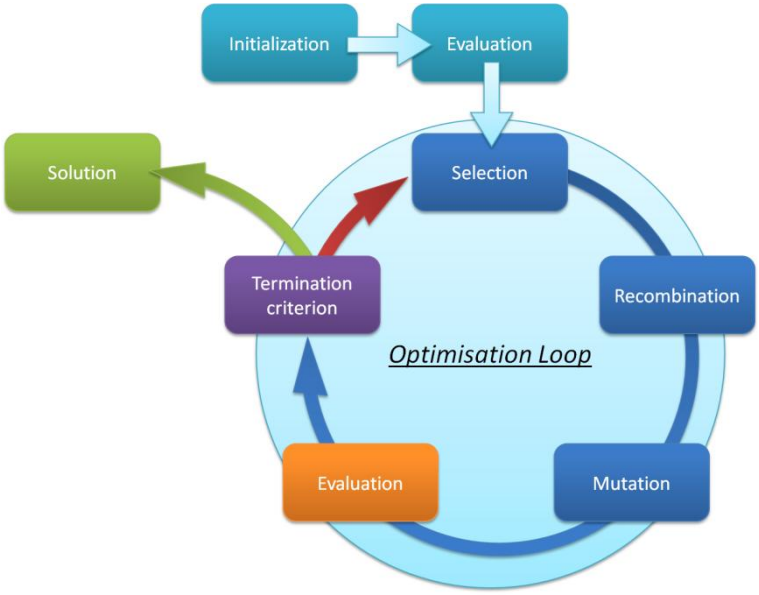

Figure 8.5: Optimisation procedure

This optimisation strategy thus is a kind of intelligent trial and error method. In the case of multi-parametric and nonlinear problems several local maxima exist. Therefore a high number of random samples are necessary to have a better chance to identify a sufficiently good solution. Based on the work of Rechenberg, in this thesis an EA with 5 parents, 8 parameters and 20 mutated children was implemented (Figure 8.6). In every generation only the best five individuals are considered for the next generation and 20 children imply also 20 simulations per generation. This suggests that the computing time of a single simulation run should be as fast as possible. For one optimisation attempt more than 100 generations are expected which finally means 2000 simulations. The SDM is able to estimate in one simulation step and with adequate precision if an actuator design is able to reach full elongation of the MSME, even under stress. Therefore the SDM approach is suitable for such optimisation purposes. In this case the termination criterion was chosen to be fulfilled, when no significant improvement occurs in about 50 generations.

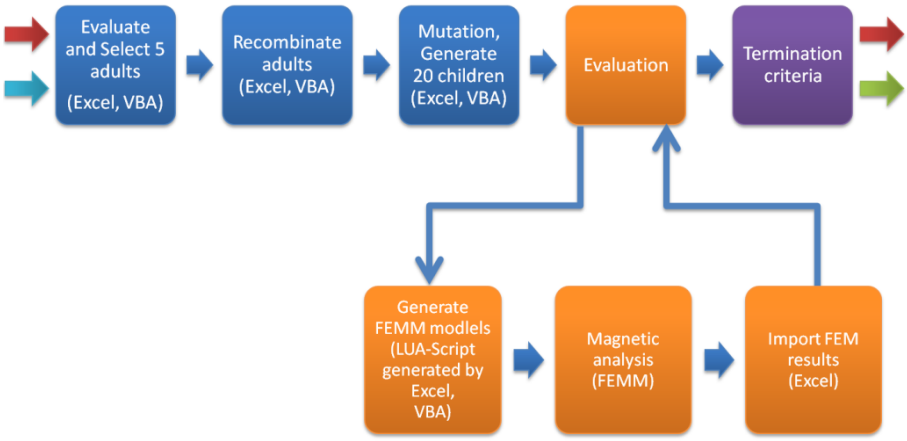

Figure 8.6: Workflow of the one optimisation loop in this particular case

8.2.2 Value function

The value function determines how good a solution is for the problem. At first the definition of "optimal" has to be found. Especially when the objectives, such as required electrical energy, actuator size, maximal current or voltage and operational temperature, are somehow in contrast, the final "optimal" solution can only be a compromise. Anyhow, during the optimisation a decision must be made, which states ultimately if the current solution is an improvement for the optimisation or not. In order to make this decision, it is necessary to have a single value that allows quick and easy evaluation of the grade of fulfilment of the objectives. This value is returned by a function that takes into account the different objectives, called value function (Miettinen, 1999). The different objective in the value function can also be properly weighted. An a priori weighting of the parameters in the value function performs only at good-natured problems to a meaningful solution, namely the compromise between the various objective attributes. (Weicker, 2007).

In this case the objectives for the MSM actuators were:

- minimisation of the size Q_S,
- minimisation of the power consumption Q_P,
- minimisation of the Maxwell forces Q_M that act on the MSME
- minimisation of the magnetic flux density Q_F required for full elongation
- minimisation of the mechanical instability Q_G (geometrical moment of inertia) of the MSME

To avoid unbalanced weighting, the quality indexes Q_x were normalised, and then depending on prioritisation weighted with the weights w_x, finally they are summed up to an overall quality index Q_{all}. The target of the optimisation is the minimisation of such a quality index:

$$Q_{all} = w_s \times Q_S + w_P \times Q_P + w_M \times Q_M + w_F \times Q_F + w_G \times Q_G \qquad \textbf{8-1}$$

Furthermore it has to be ensured that any improved objective leads to a decreased index so that an optimised criterion leads to lower Q_{all}; otherwise it is necessary to work with the reciprocal value. Here the weighs of Q_S, Q_P and Q_M were doubled, with respect to other indexes, with the goal to get a small actuator with low power consumption, as well as low Maxwell force acting on the sample.

8.2.3 Parameters

As shown in Figure 8.7, a full parametric model was created. Parameter P_1 to P_8 are geometrical attributes and parameter P_9 is the number of windings in dependence on the wire diameter, which is indirectly depending on the parameters P_2 and P_3. The reachable force of an MSME depends on the

cross section, as well as on the amount of the magnetic field. In this case the cross section was specified, so that the MSME width P_6 was adjusted as a parameter and the thickness P_7 was calculated to ensure that the MSME cross section remains equal. In general it was assumed that a symmetrical design is advantageous in terms of manufacturability and production costs. Therefore the actuator model is defined with these relevant parameters.

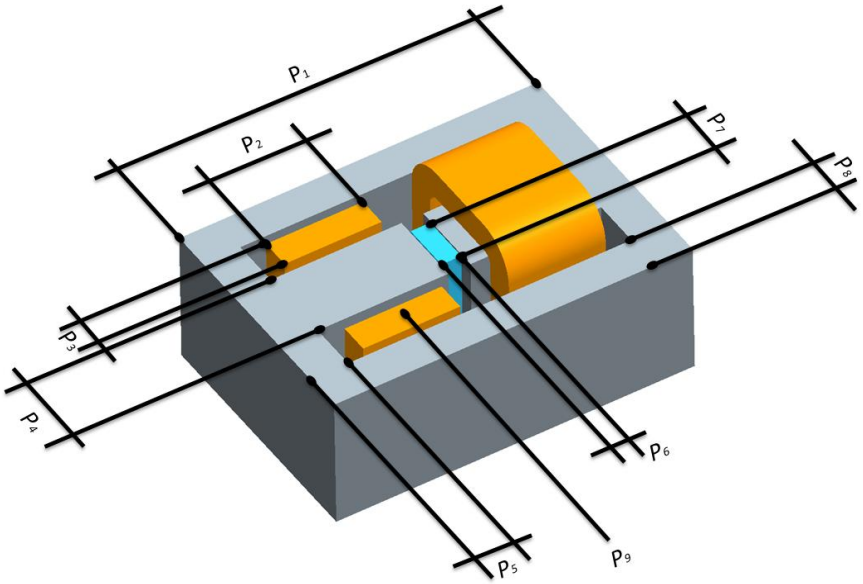

Figure 8.7: Parametric model of MSM actuator

8.2.4 Results

Due to the relative small number of parameters (8) the EA converges in less than 100 generations. The termination criterion is reached even though it can be seen that the required magnetic flux density Q_F as well as the power consumption Q_P show in some cases increased values. Anyhow, the termination criterion refers to the overall quality index (Q_{all}) and it can be seen in Figure 8.9 that a further reduction of power consumption (Q_P) has a negative effect on the needed magnetic field, i.e. the quality index Q_F increases. The increment of power results in an increased magnetic field and therefore increased Maxwell forces, i.e. Q_F and Q_M. However, in relation to Q_{all}, the effects are compensating, as can be seen in Figure 8.9. The optimisation time in this case was less than 6 hours.

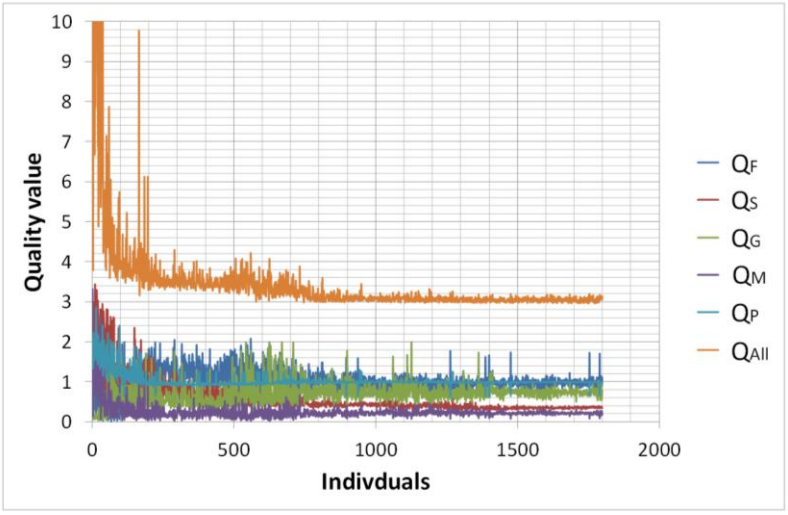

Figure 8.8: *Q* over all simulation cycles

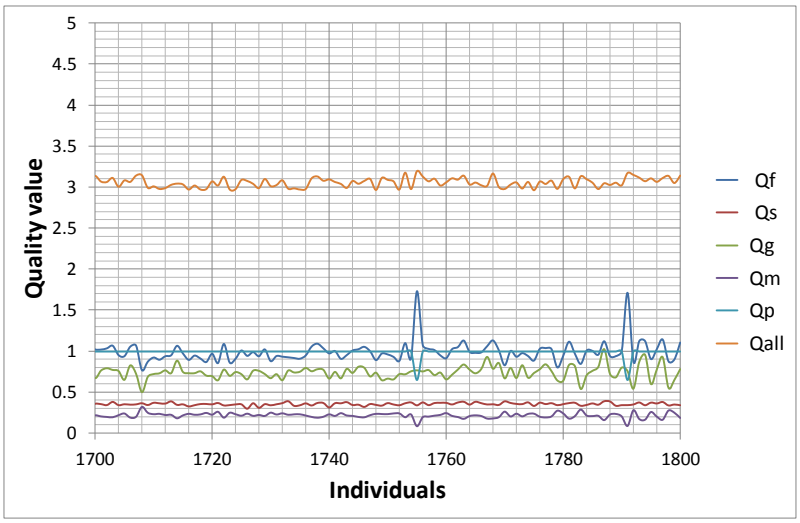

Figure 8.9: *Q* in the final 100 simulation cycles

8.2.5 Conclusion

The EA has been combined with a magnetostatic FEM tool. Based on value functions, that evaluate the quality of the magnetic and geometric design under different boundary conditions, hundreds of actuator variants are analysed in short time. The actuator volume optimised by the EA has been compared with the engineered solution. In conclusion the chosen FEM simulation approach is an advantageous tool for the complex and iterative development process, aiming to high efficiency MSM actuators. For a further commercialisation of the MSM technology effective simulation tools are required to identify an optimised actuator design in short time. An optimum MSM actuator design shall meet the requirements such as smallest space or lowest energy consumption or combinations thereof. Different optimisation objectives are thinkable, depending on the customer application. FEMM is not able to simulate transient, however a low static inductance can serve as an indicator for the electrical dynamics of the actuator, so that also this dynamics could be an objective with this method. Today´s MSME have an operation temperature limit of 80°C (Pagounis, Chulist, Szczerba, & Laufenberg, 2014). It is thus necessary to predict the maximum operating temperature of the MSM actuator in a particular application scenario. In some customer applications the MSME must withstand the introduced energy, which is converted to thermal energy. FEMM is also able to perform thermal simulation and therefore it is also possible to optimise the maximum steady-state temperature (Schiepp, Schlüter, Schäfer, Maier, & Laufenberg, 2014).

8.3 Fatigue investigations

Fatigue of engineering components is a major concern when considering their industrial applications. High-cycle fatigue seems to be one of the MSME technological advantages. The fatigue behaviour of MSME received considerable interest, when high cycle fatigue was demonstrated in 2004 (Müllner, Chernenko, Mukherji, & Kostorz, 2004). Additionally in some first attempts, an actuator fatigue life of 200 x 10^6 (Altio, Ge, Liu, Soderberg, & Hannula, 2008) and of 425 x 10^6 cycles (Pagounis, Maier, & Laufenberg, 2011) has been reported. In a comprehensive investigation Aaltio *et al.* studied the fatigue behaviour of MSME using a set-up which mechanically elongates and contracts the material (Aaltio, Soroka, Ge, Söderberg, & Hannula, 2010). They measured a fatigue life of more than 10^9 cycles, however without taking into account magnetic effects. Furthermore the strain amplitude was restricted to ± 1%. The situation, where the MSM material is placed in the air gap of an actuator with a strain output of > 4 %, is considerably different. However, to realise this high number of switching cycles is

not trivial. Therefore knowledge of the key factors influencing the fatigue of the actuator is indispensable.

8.3.1 Effects in an actuator

By implementing the MSME into an actuator, additional effects like friction induced by Maxwell forces on the ferromagnetic MSME and/or high local stresses can occur, which may affect the material as well as the actuator performance (Schiepp, Detkov, Maier, Pagounis, & Laufenberg, 2013). Therefore a type of actuator was designed, to study fatigue properties and investigate failure mechanisms, which also helps to improve simulation quality. In the actuator shown in Figure 8.10 the pre-stress and the air gap between the MSME and magnetic circuit parts can be adjusted in order to study geometrical influences on fatigue. In order to observe the motion of the MSME during actuation with a high speed camera, the magnetic circuit was designed asymmetrically with coils that were placed on the backside of the MSME.

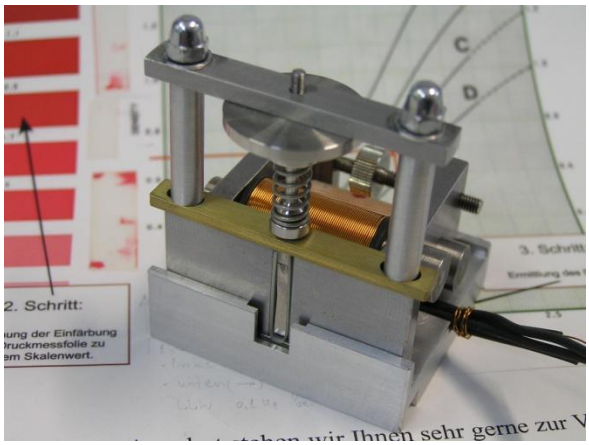

Figure 8.10: MSM actuators for studying the fatigue behaviour

The Maxwell forces in MSM actuators are often neglected. In particular in small actuators this effect can have a huge impact. As shown in Figure 8.11, the Maxwell forces twist and bend the MSME such that the magnetic resistance of the magnetic circuit is minimised. This mechanical stretching influences the switching behaviour as well as fatigue life. Even though the Maxwell forces, as well as the resulting torque, can be calculated easily with FEM software, in the case of MSME this is more difficult. The calculated force depends on the magnetic field, as well as on the magnetic permeability, and the permeability depends on strain. Using the SBS method it is possible to calculate the Maxwell forces, as well as the resulting stresses depending on internal as well as external loads of any individual slice in any elongation state of the MSME. The SDM approach is suitable to receive the resulting force of the complete MSME for optimisation purposes fast and easily.

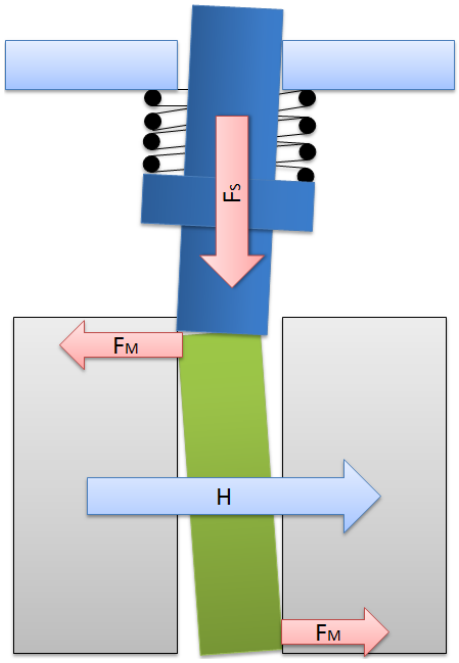

Figure 8.11: Maxwell forces (F_M) acting on the MSME (green)

As shown in Figure 8.11, the magnetic field that acts upon the MSME generates Maxwell forces (F_M) which bend and tilt the element. Additionally the force of return spring (F_S) acts upon the MSME. The mechanical resistance depends on the geometry of the MSME and the maximum mechanical stress σ_{max} resulting from the forces F_S and F_M is given by

$$\sigma_{max} = \frac{F_S}{w \times d} + 6\frac{F_M \times h}{w \times d^2}, \qquad \textbf{8-2}$$

where *w*, *d*, and *h* are width, depth and height of the MSME, respectively. But the situation is more complex, because depending on the strain the MSME has different stiffness and shows quasi-elastic behaviour.

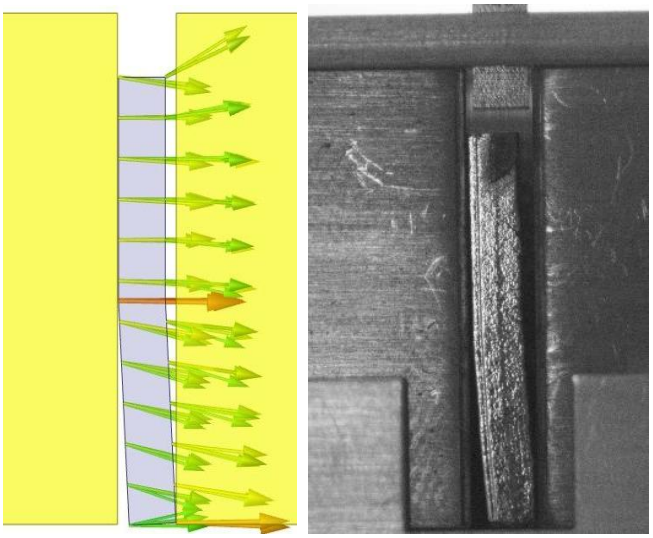

Figure 8.12: Bending of an MSME in an actuator, FEM analysis (left) and prototype (right)

For a first estimation simplified assumptions were made and magnetic calculations were performed with an MSME in fully elongated state. In order to determine the Maxwell forces acting on the

MSME, magnetostatic FEM simulations (Figure 8.12, left) were performed using the MSME aligned in its magnetically favoured position, as shown in Figure 8.12 on the right. A static simulation, using the SBS method in the single variant state, fully compressed and elongated, was performed. For intermediate states the DMC method was used to calculate the Maxwell forces that act upon the MSME. Additionally the Maxwell forces were measured using Fuji Prescale foils (Figure 8.13). These foils were placed in-between the MSME and the core pieces and the actuator was energised. The resulting forces cause a colour change of the foils and indicate, locally resolved the maximum pressure exposure during measurement.

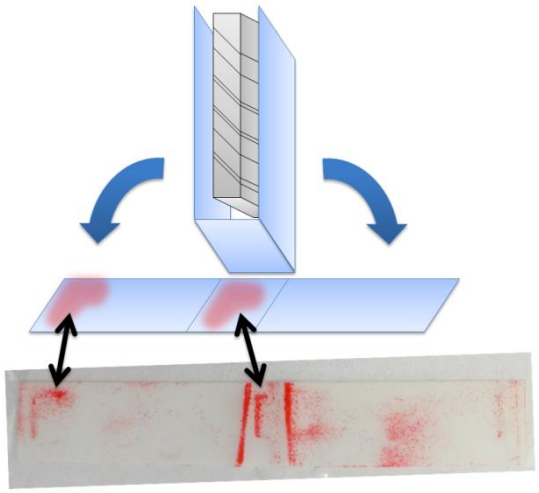

Figure 8.13: Measurement method with Fuji Film Prescale foils (bottom) show local stress up to about 10 N/mm²

These experimental results confirm the simulation results and show that the Maxwell forces may cause a torque of 15 Nmm and local stresses of up to about 10 MPa on a 2×3×15 mm³ MSME. The local stress can dramatically exceed the twinning stress of about 0.5 MPa by more than an order of magnitude. Therefore damage and fatigue problems are expected already in an early stage. It is obvious that the torque or the Maxwell forces are growing with the smaller gap, when the MSME is aligned in its magnetically favoured position. It could be advantageous that the element is guided so that it remains ideally in the middle between the core pieces, in such a way that the Maxwell force would be low (PCT/EP2014/065565).

Furthermore the Maxwell force contributes to the friction force between the MSME and the core pieces. This effect was confirmed to be most severe where the relative motion between the MSME and the adjacent magnetic cores is maximum, which is typically the case at the upper end of the element. MSM prototype actuators were built to study fatigue effects at operation frequencies above 50 Hz, so that many switching cycles can be realised and the fatigue behaviour can be tested in a short time. The design allows to adjust the pre-stress externally and to measure the elongation continuously in real time. To investigate the magneto-mechanical properties of the MSME itself, it is possible to remove the element easily. Furthermore a force sensor with a high sampling rate can be attached beneath the MSME, so that a dynamic force measurement, during elongation and compression of the MSME, operating up to 400 Hz can be observed. Five identical actuators were built and fitted into a test bench (Figure 8.14), so that statistically reliable test results can be obtained. The actuators where driven with a frequency up to 60 Hz in a water cooled test bench so that approximately 5×10^6 switching cycles can be realised per day without overheating the MSME.

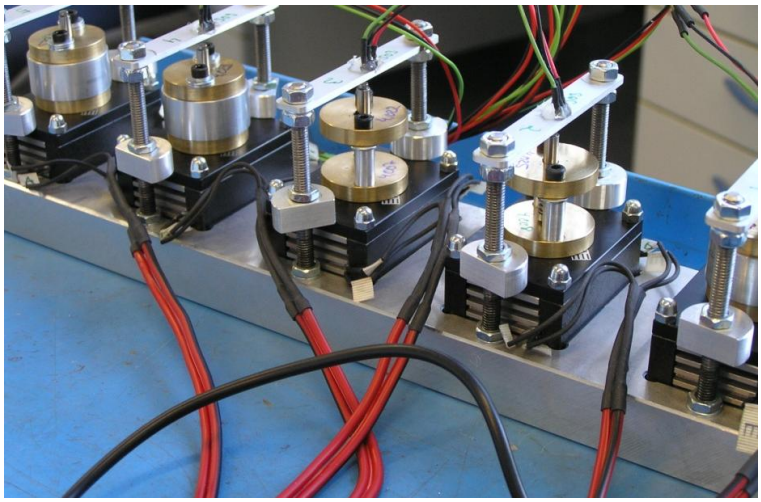

Figure 8.14: MSM actuator test bench with five fatigue test actuators

These actuators were not optimised for fatigue testing and the mechanical load was increased so that the discussed effects appeared early. As shown in Figure 8.15, abrasive wear appeared at the core pieces as well as on the surface of the MSME and caused damages of the twin structure which leads to higher twinning stress and higher magnetic fields for complete elongation. A degradation of the magneto-mechanical properties after less than 1×10^7 cycles (Figure 8.16) is visible.

Figure 8.15: Abrasive wear on the core pieces

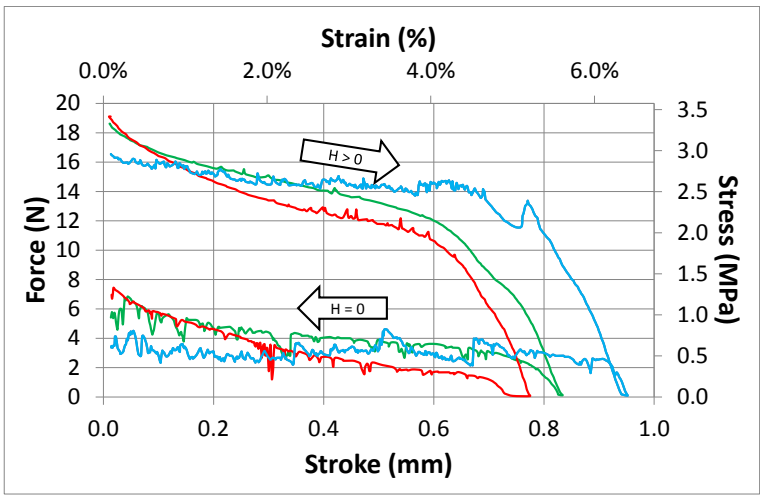

Figure 8.16: Force-stroke curves of MSME before testing (blue), after 8.5×106 (green), and after 13×10^6 cycles (red)

8.3.2 Dynamical effects

Short current pulses can cause overshoots of the mass spring system that finally can get into resonance or even an overshoot with spring back effect that could lead to damage in the MSME. FEM was used to reduce the acting Maxwell forces to a minimum and an additional fatigue test was performed. As shown in Figure 8.17, a MSME was destroyed after 23 10^6 cycles in the fatigue test by dynamical effects. The fracture of these samples is intracrystalline and looks similar to findings in already published work (Aaltio, Soroka, Ge, Söderberg, & Hannula, 2010). In order to further investigate the failure mechanism, the force was measured during a single switching operation.

Figure 8.17: Photograph of MSM element after 23 million switching cycles

In Figure 8.18 the force curve (blue) and the corresponding stroke (red) of the push rod, which is spring loaded to the MSME, are shown. As already mentioned the force sensor was mounted below the MSME and shortly before reaching the full elongation, the contact between the MSME and the mass-spring system is obviously lost for roughly 800 µs (plateau of blue curve with zero force). This overshoot presumably damaged the MSME during the test when the rod was thrown back onto the MSME with a certain kinetic energy. From the measured force a resulting peak stress on the MSME of about 1.3 MPa can be estimated. Remarkably all actuators still operated with reduced performance or even with broken elements.

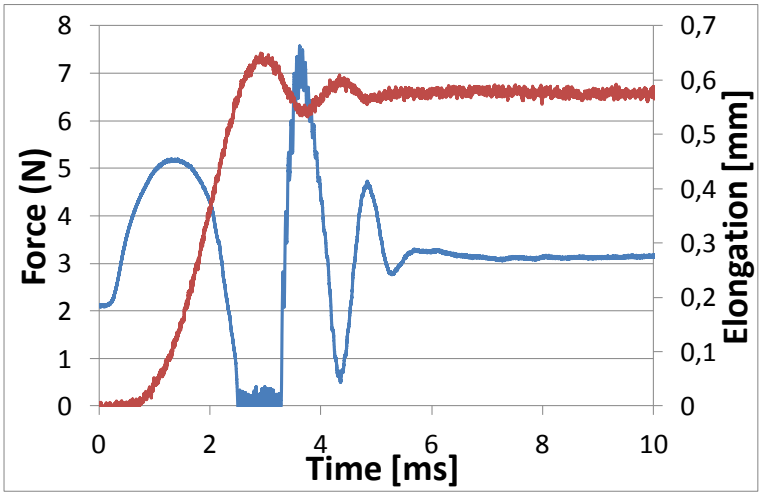

Figure 8.18: Switching behaviour of MSM actuator. Elongation (red) force (blue)

In a second test run, the excitation voltage was controlled with a pulse-width modulation (PWM) in such a way that the movement of the MSM is slower and the contact between the rod and the MSME is always ensured and the overshoot in the elongation measurement disappeared (Figure 8.19). Figure

8.19 shows the PWM profile (blue) and elongation (red), it can be seen that dynamics are reduced but could be optimised.

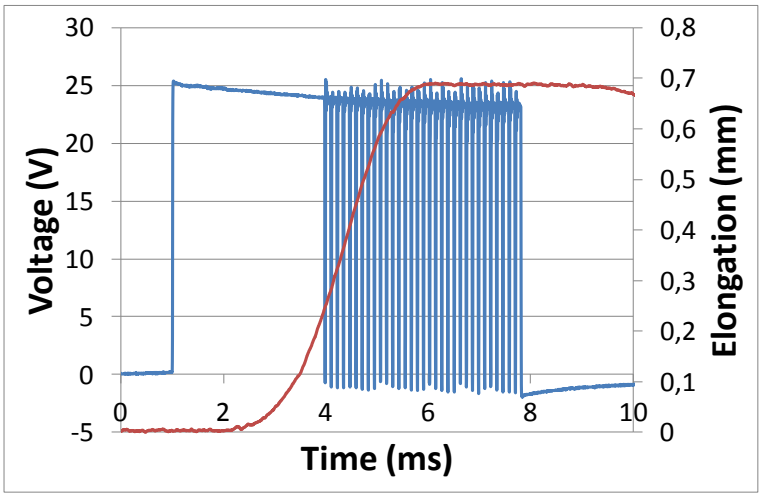

Figure 8.19: Switching behaviour of the MSM actuator excited by a PWM voltage (blue), elongation (red)

Even though the PWM profile avoided a destruction of the MSME, it can be seen in Figure 8.20 that the magneto-mechanical performance of the MSME was still degrading. The blue curve was measured directly after the production process (i.e. after electro polishing) and shows maximum force as well as lowest reset force (corresponding to lowest twinning stress). The green curve is measured after 40×10^6 cycles and shows that the performance of the MSME is further reduced. An investigation of the surface of the friction partner using energy dispersive X-ray spectroscopy (EDX) revealed abrasive wear because nickel, manganese as well as gallium were identified in the analysis. This clearly indicates that even the low friction forces were high enough to damage the MSME. Finally the MSME underwent an additional electro polishing treatment and the red curve in Figure 8.20 was measured. It can be seen that this process recovers the performance to a large extent, supporting that the abrasive wear damaged a surface layer of the element with a certain depth. It can be deduced that friction between the MSME and the adjacent iron cores needs to be reduced possibly close to zero in order to achieve lifetimes in the 10^8 or even 10^9 regimes.

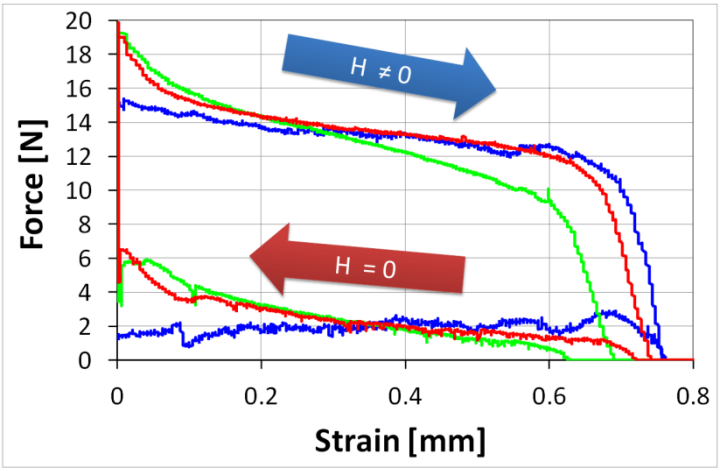

Figure 8.20: Magneto-mechanical behaviour of a MSM sample, before fatigue testing (blue), after 40 × 10^6 cycles (green) and recovered (red)

Figure 8.21 shows design suggestions that reduce Maxwell forces as well as friction between the MSME and the magnetic circuit. At the bottom of the MSME it can be guided by the magnetic circuit, because the relative movement of the sample is low, while at the top the MSME needs to be gripped by the pushrod, where the relative movement is big.

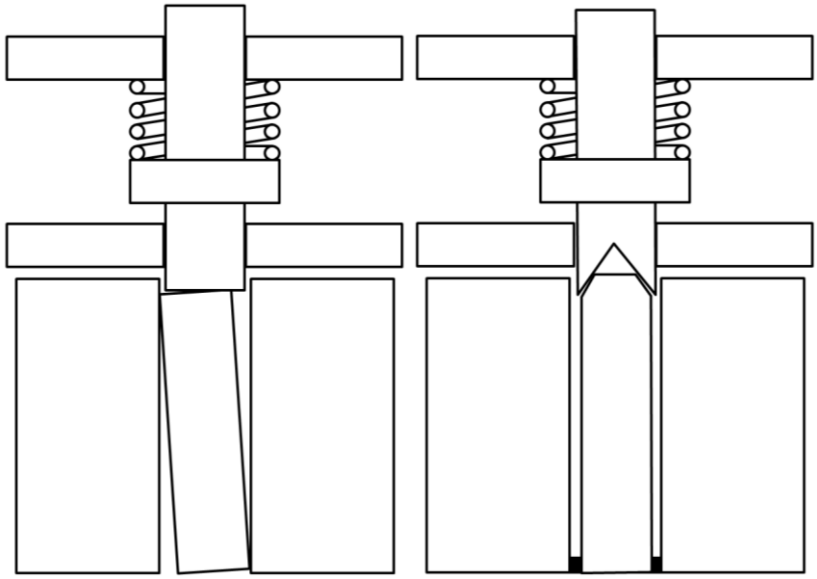

Figure 8.21: Frictionless design (Laufenberg & Schiepp, 2013)

8.3.3 Conclusion and outlook

To further improve the fatigue life and to guarantee a proper functionality of MSM actuators, also in various environments under series application conditions, a deeper understanding is required. These results help to understand failure mechanisms of MSM materials like:

- Maxwell forces
- Friction
- Torque
- Overshoot/ resonance

Based on these results it can be assumed, that Maxwell forces have to be carefully considered when designing an MSM actuator, because these forces can significantly exceed the twinning stress locally. With the SDM method an actuator can be designed, which takes into account the Maxwell forces. Additionally with the SBS method the MSM material twin structure can be considered, which could significantly improve the actuator fatigue life. Therefore it was visualised that the deviation angle of the MSME during actuation has a huge impact on the Maxwell forces. They contribute to the friction force between the MSME and the magnetic core of the actuator and reduce the material lifetime drastically. The result of 15 Nmm torque of the simulation was confirmed by the measurement and results in local stress of more than 10 MPa. This effect was confirmed to be most severe, where the relative motion between the MSME and the adjacent magnetic cores is maximum, which is typically the case at the upper end of the element.

Short rise times can be realised, but with an inappropriate, impulsive voltage excitation an overshoot of the mass-spring system can appear, which can lead to mechanical damages such as intracrystalline fracture of the MSME. Using a modified excitation profile and an optimised actuator design, a fracture of the MSME was prevented and the high cycle fatigue was improved. It has been observed that the

resonance of the spring-MSM-system can have an impact on fatigue and may destroy the system very fast. This behaviour also can be calculated by simulation in advance. To reach a high number of cycles in an actuator this failure mechanism has to be considered.

8.4 MSM Operation in Actuators

The actuators that were used for fatigue testing are combined with a spring as a restoring element. This is necessary to restore the MSME to its starting state when the field coils are not energised. As shown in the measurements (Figure 6.10), most of the elements did not reach full elongation because the pre-stress of the spring was (intentionally) too large. Furthermore the force progression along the elongation of an MSME is not ideal to work against such an element. As shown in Figure 3.5, the maximum force of the MSME is greatest at the beginning of elongation and reduces continuously with elongation. Therefore the described effect in Section 5.2 appears and the result is a reduced elongation as well as lower work output. This can be improved by optimising the interaction between the MSME and the restoring element.

8.4.1 Operating modes

B. Holz has established general operating modes for a bar shaped MSME (Holz & Janocha, 2010). These modes describe five basic possibilities of how to use an MSME in a functional device in combination of magnetic or mechanical stimulus. As shown in Figure 8.22, where a single MSM cell is considered, there are in general three types of external stimuli that can induce a shape change and two differ in their effective direction. Thermal energy is independent from direction because a phase transformation takes place and this will cause a change of the edge length of the unit cell from tetragonal to cubic. The mechanical stimulus is depending on the acting direction, so that finally it is divided in a push or pull stimulus. For the magnetic stimuli the axis is important, the direction is not.

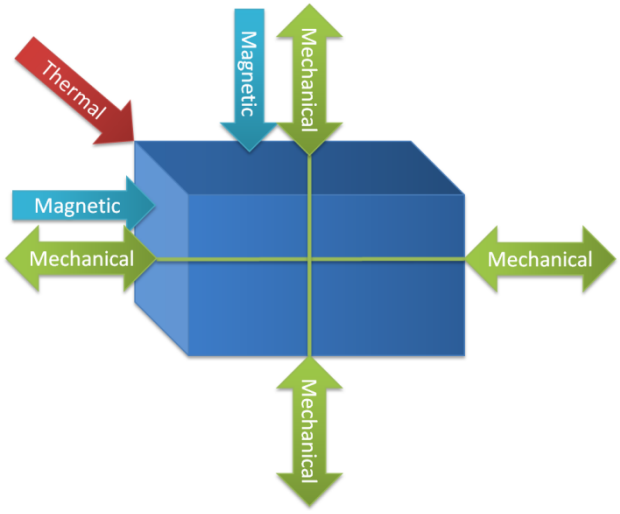

Figure 8.22: MSM unit cell and possible actuation stimuli

In the case that a phase change is excluded the remaining stimuli can be combined to possible operation modes. As shown in Figure 8.23, six operating modes can be distinguished.

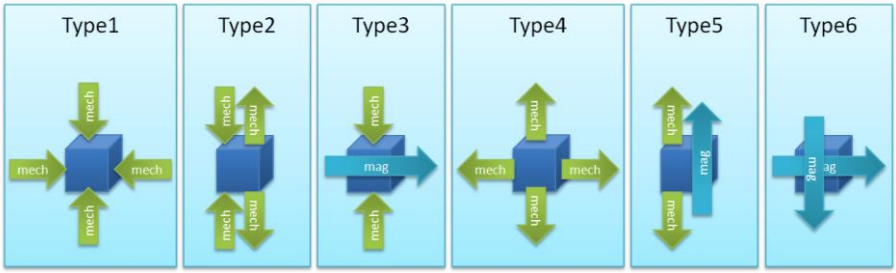

Figure 8.23: General operation types without thermal energy (according to Holz & Janocha, 2010)

8.4.2 Passive restoring of the MSME

Type 3 is one of the promising modes. A MSME will be stimulated by a magnetic field and afterwards it needs to be restored. This can be realised by a passive mechanical component, like a spring, which is working perpendicular to the magnetic field. It can also be realised with a "magnetic spring", where the mechanical spring element is replaced by a magnetic element, based on a permanent magnet. The advantage of such a magnetic spring is a restoring force, that improves the output ratio of such a MSM actuator (Laufenberg & Schiepp, 2014b). This magnetic spring can be tuned to give an output stress ideally slight above the twinning stress level so that the maximum elongation, restoring and therefore ratio can be achieved. Furthermore it is possible to calculate or to optimise both actuators sequentially in a simulation run to calculate the interaction of both devices. An example is shown in Figure 8.24, where a FEMM simulation of the magnetic spring is shown on the left and of the MSM actuator on the right in only one simulation run. Anyhow to realise this kind of simulation with the SDM approach, several drawbacks have to be accepted. On the one hand the complete current-elongation curve has to be calculated because the stress situation at a certain current, as well as the elongation state is unknown in advance and on the other hand the magnetisation curves of the samples with external load at any strain level have to be measured in advance. This increases the complexity and the advantage of simplicity gets lost but this allows the optimisation of a complete system.

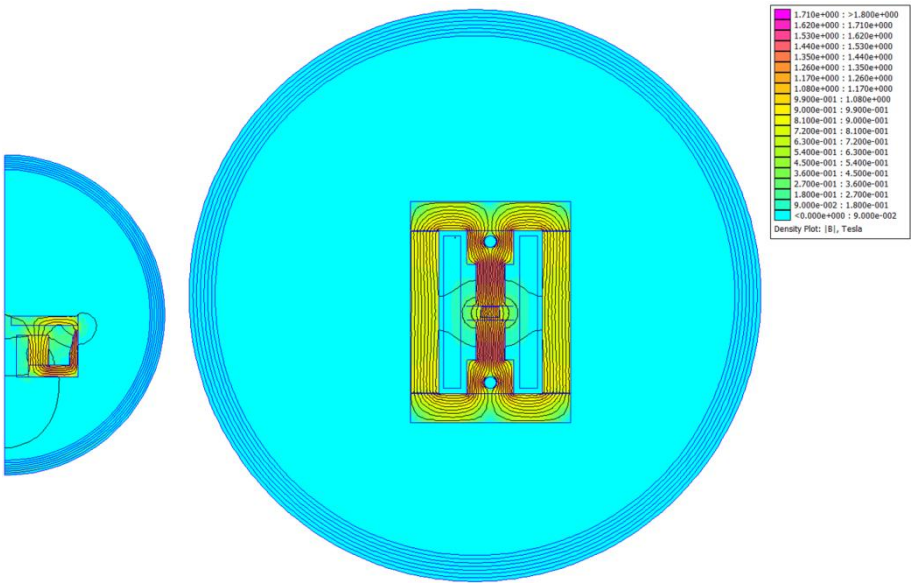

Figure 8.24: Simulation of magnetic spring (left) and MSM actuator (right)

8.4.3 Active restoring of the MSME

The restoring of the MSME further can be realised by an active component like a solenoid (Figure 8.25) or another MSME actuator. These are the so-called push-push actuators and have the advantage that during elongation the opposing force could be nearly zero, when mass moment of inertia, friction force and gravity are neglected. This leads to the advantage that the MSME can elongate with a minimum field in minimum time. Additionally the push rod of this actuator retains in the last state without consuming power, which is called multistability. An optimisation with the SDM approach can be performed fast and easily, because the MSME is nearly unloaded. Therefore the elongation state can be calculated again in only one simulation step and the optimisation procedure can be focused on the restoring element, which needs to work against the twinning stress of the MSME.

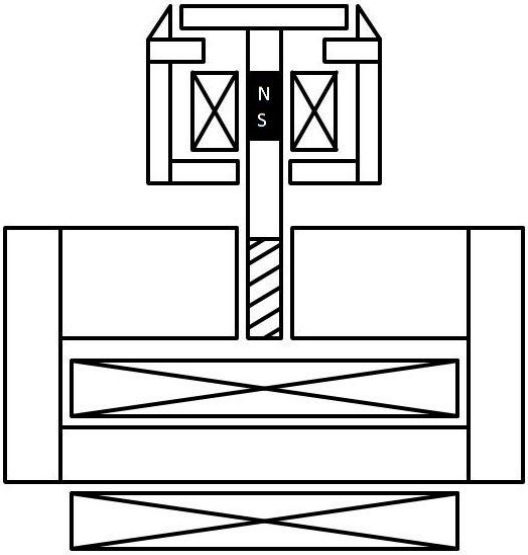

Figure 8.25: Principle of MSM hybrid actuator combined with a solenoid (Laufenberg & Schiepp, 2014a)

8.4.4 Conclusion

Considering the different operating modes, it can be said that the MSM technology has advantages in several applications. The type 3 operation mode has an influence on the ratio. A good design of the restoring element is of great importance for the success of this type of actuator system. Hence the functionality and the interaction of the MSM actuator as well as the restoring element have to be optimised. Especially for the passive restoring element the simulation method becomes more complex. The optimisation could be realised in sequences, so that a restoring element has to be designed and optimised in relation to a given and already improved MSM actuator. Nevertheless it can be said that an MSM actuator combined with an active restoring element, the so called MSM hybrid actuator, shows maximum benefit for the ratio, the elongation and furthermore it exhibits multistability. This kind of actuator can be easily optimised with the SDM method in combination of conventional FEM magnetostatic calculations.

9 Conclusion and Further Work

9.1 Conclusion

Smart materials are interesting for the design and development of actuators because of their unique properties. The specific characteristics of Magnetic Shape Memory (MSM) alloys make this class of material promising for several applications. Actuators based on MSM represent a new type of smart electromagnetic actuators where the MSM element can elongate and contract fast in a magnetic field. The MSM material is typically a monocrystalline Ni-Mn-Ga Heusler alloy, which has the ability to change its size and shape many million times repeatedly. The shape change is realised by a reorientation of variants in the martensitic state. This reorientation can be obtained by mechanical stress or by an applied magnetic field. Recently developed MSM alloys are able to achieve a magnetic field induced strain of up to 12% and work at temperature up to 80°C.

Over the last decades industrial development cycles have become considerably shorter, accompanied by a continuous demand for the reduction of development time and costs. So, fast and easy-to-handle engineering and simulation tools, especially tools based on finite element methods (FEM), have been widely applied for the product design and development. To analyse and evaluate applicability of the MSM actuator technology, this kind of tools and simulation strategies must be developed and established. Significant differences towards electromagnets have to be overcome. Several approaches have been established for simulating the magneto-mechanical behaviour of MSM materials. However, they are not suitable to effectively simulate the behaviour of a complete MSM actuator for engineering purposes. For instance, standard, commercially available FEM tools are not suitable to simultaneously calculate magnetic field, mechanical stress and resulting shape change in MSM. To improve and optimise actuator designs, it is indispensable to enable engineers to predict the challenging magneto-mechanical behaviour of a MSM-based actuator. In this thesis three simulation methods based on FEM analysis have been proposed, designed and developed. These methods can be effectively used for designing MSM actuators for various applications. These methods rely strongly on a priori magneto-mechanical characterisation of MSM elements, where the deformation as well as the magnetisation capability of each element must be analysed with respect to the possible magnetic and/or mechanical excitation of the sample. Thus, in this thesis several approaches for obtaining the desired element characterisation have also been proposed, designed and developed.

The main achievements of the PhD thesis are:

1) The systematic review of the literatures to analyse and evaluate the previous work about the study of MSM properties and their application to the design and development of actuators. Especially, the problems associated with the simulation methods for the design and development of MSM-based actuators have been critically discussed and evaluated.
2) A generic framework has been proposed for the simulation of MSM-based actuators, with the aim of better design and development.
3) New measurement approaches for measuring the unique magneto-mechanical characteristics of MSM alloys have been proposed.
4) Three new FEM-based simulation methods have been proposed, which are based on the measurement approaches and require different measurement and computational effort:
   - Stress based simulation method (SBS)
   - Dynamic magnetisation curve method (DMC)
   - Stress dependent magnetisation curve method (SDM)
5) Validation of the overall measurement and simulation process by the prototype MSM actuator

The proposed simulation methods have advantages and disadvantages, which are on the following briefly discussed. The SBS offers the opportunity to understand the interaction between an MSM element and the actuator. It is an attempt to imitate the phenomenological behaviour of MSM element on a macroscopic level: for the analysis, the MSM element is subdivided in several elementary volumes called slices. During the simulation the deformation, the magnetic properties and the stress level in each slice is calculated separately. The overall response of the slices gives the overall magneto-mechanical response of the MSM element. Thus, a unique advantage of this method is that it is possible to observe the local stress condition and the local reaction of the MSM element to the external stimuli. Although it cannot rebuilt the physical phenomena in detail it gets as close as reasonable to it, offering to the designer several important insights about the material behaviour as well as about any interaction between the element and the actuator. This makes the SBS very interesting from the scientific viewpoint. As advantage, the SBS rely on very few characterisations of the MSM element prior to simulation. However, a drawback of the SBS is the complex, time-consuming calculation of the stress in each slice and consequently in the MSM element.

In contrast to the SBS, the DMC does not attempt to get insight in the physical process underlying the variant reorientation, but rather describes it from a purely phenomenological viewpoint at a macro scale level. In this approach, several magnetostatic simulations are performed for different current values. In each simulation, the magnetic field value is used to determine the actual deformation. The magnetisation curve of the MSM element is than updated based on the actual deformation and is used for the calculation of the magnetic field in the MSM element at the next step. The main advantage of the DMC is that it needs a very small computing time with respect to the SBS and also the SDM. On the other hand, the DMC as proposed in this thesis does not reach a satisfactory simulation precision. In particular, the deformation predicted by the DMC simulation is generally too big with respect to the measurements. Some ideas which could fix this problem are proposed, but they would probably increase also the complexity of the method and thus reduce its main advantage.

The last method, the SDM, neither gives insight in the physics of the MSM element nor makes use of a stress calculation in the element to determine the final deformation. The method is based on the magnetisation curve measured in a specific stress condition. This magnetisation curve is then used in the FEM software as reference for the actuator evaluation. The main advantages, as demonstrated in this thesis, are the computational simplicity and the satisfactory precision in predicting the actuator behaviour. Nevertheless, the simulation gives a result which is valid in a very specific stress situation and will not give reliable results if, in the experimental case, the stress situation is time-varying or different from the estimation. Furthermore, it should be considered that the measurement of such a stress-dependent magnetisation is challenging and very time-consuming.

The measurements and simulation approaches proposed in this thesis can be used to perform a high-quality actuator design based on the magneto-mechanical properties of MSM alloys. The three simulation methods have been used for the rapid prototyping of several MSM actuators. In particular it is shown, how such methods could be interfaced with powerful, state-of-the-art optimisation algorithms such as evolutionary algorithms. The interaction allows the designer to find in relatively short time a design compromise which satisfies a given optimisation criterion.

For the validation of these methods a real prototype actuator was build. Eight MSM samples were characterised and then used to evaluate the precision of the simulation methods. The unavailability of standard measurement devices for MSM alloys made the adoption of innovative approaches for the characterisation necessary. The most important characteristic (on which all of the simulation methods rely) is the magnetisation curve of the MSM element. Therefore a significant modification had to be made, at the device that is used to measure the magnetisation and thus the permeability of MSM.

9.2 Contribution to the New Knowledge Generation

The core contribution of this thesis is the proposal of FEM-based simulation methods for the fast development of actuators based on the magnetic shape memory technology, in particular:

- The Stress Based Simulation Method (SBS) leads to a very precise model of the MSM alloy and of the actuator, offering a representation which allows gaining an interesting insight in the material behaviour and in the physical phenomena related to its magnetisation
- The Dynamic Magnetisation Curve method (DMC) is a very fast method, which needs few a priori measurements to be started, but at the same time leads to less precise results
- The Stress Dependent Magnetisation Curve method (SDM) can estimate the functionality of a MSM actuator in one simulation run

The methods are strongly dependent on the measurement of the magneto-mechanical characteristics of magnetic shape memory alloys. Thus, another important contribution of this thesis deals with the development of suitable measurement methods for the preparation of the simulations, as follows:

- Measurement of the magnetisation curves along the hard and easy axis of a MSM alloy
- Measurement of one magnetisation curve for one specific strain level
- Measurement of one magnetisation curve in combination with a specific external stress

The methods and techniques developed in this PhD thesis extend standard magnetostatic FEM simulations techniques to take into account the magneto-mechanical coupling and the magnetic anisotropy of the MSM materials. The experimental results demonstrate that the developed methods are relatively simple but very effective way to model and predict the behaviour of a MSM actuator.

9.3 Further Work

For commercial success of the MSM technology the implementation of such simulation tools is indispensable. To exploit the advantages of this class of material further steps are still to be done:

- Future works could in fact deal with the improvement of the simulation methods proposed here. For all three methods it could be advantageous to optimise the characterisation of the MSM samples, by improving the measurement equipment. The objective should be the reduction of measurement inaccuracies.
- On the other hand the simulation models can be improved and in particular the DMC. An improved version of this method could offer a fast and reliable simulation approach, which also relies on a small measurement/characterisation effort of the user.
- Furthermore, all the simulation models proposed in this thesis could be combined additionally with thermal simulations. This is an interesting aspect because several characteristics, such as permeability or mobility of the martensitic variants composing the MSM element are depending on temperature.
- A further step could also be to reduce the model order of these simulation methods. This could enable several advantages. On the one hand it could be possible to perform transient calculation in very short time, so that the switching speed of an MSM actuator could be calculated and optimised. On the other hand it would be possible to calculate the interaction of an MSM actuator with a complete system, thus simulating a complete MSM-based actuator solution. This would definitely lead to further analysis possibilities, for instance the design of control algorithms for MSM actuators in a wide variety of applications.

10 References

60404-4:2009-08, D. E. (2009). *Magnetic materials - Part 4: Methods of measurement of d.c. magnetic properties of magnetically soft materials (IEC 60404-4:1995 + A1:2000 + A2:2008).*

Aaltio, I., Soroka, A., Ge, Y., Söderberg, O., & Hannula, S. (2010, June 01). High-cycle fatigue of 10M Ni–Mn–Ga magnetic shape memory alloy in reversed mechanical loading. *Smart Materials and Structures, Vol. 19 No. 7* , pp. 1-10.

Addington, D., & Schodek, D. (2007). *Smart materials and technologies - for the architecture and design professions.* Amsterdam: Elsevier.

Aharoni, A. (2000). *Introduction to the Theory of Ferromagnetism, 2nd edition.* New York: Oxford University Press Inc.

Altio, I., Ge, Y., Liu, X., Soderberg, O., & Hannula, S.-P. (2008). Effect of Magnetomechanical Cycling on 10M Ni-Mn-Ga Magnetic Shape Memory Material. *International Conference on Martensitic Tranformations ICOMAT 2008* (pp. 487-491). Santa Fe, USA: G. B. Olson, D. S. Liebermann, A. Saxena.

APC International Ltd. (2011). *Piezoelectric Ceramics: Principles and Applications.* Mackeyville, Pennsylvania: APC International Ltd.

Atherton, D., & Borne, P. (1991). *Concise Encyclopedia of Modelling & Simulation (Advances in Systems, Control, and Information Engineering).* Pergamon Press: Oxford, New York, Seoul, Tokyo.

Bais, S. (2005). *Die Gleichungen Der Physik: Meilensteine Des Wissens.* Amsterdam: Amsterdam University Press.

Belahcen, A. (2004). *Doctoral thesis: Magnetoelasticity, Magnetic Forces and Magnetostriction in Electrical Maschines.* Helsinki, Finnland: Helsinki University of Technology, Laboratory of Electromechanics.

Benon, J. (2001). *Smart Materials and Structures: Technological Feasibility and Policy Assessment.* Cambridge, USA: Massachusetts Institute of Technology, Department of Materials Science and Engineering.

Bergmann, L., Schaefer, C., & Raith, W. (2006). *Lehrbuch der Experimentalphysik, Band 2 Elektromagnetismus.* Berlin, New York: Walter de Gruyter.

Boettinger, W., Warren, J., Beckermann, C., & Karma, A. (2002, August). Phase-Field Simulation of Solidification. *Annual Review of Materials Research Vol. 32* , pp. 163-194.

Bozorth, R. (1951). *Ferromagnetism.* Toronto: Van Nostrand.

Bravais, A. (1846). *Analyse mathématique sur les probabilités des erreurs de situation d`un point.* France: Mém. prés. par divers savants à l`Acad. des sciences de l`Inst. de France.

Buehler, W., Gilfrich, J., & Wiley, R. (1963). Effects of low-temperature phase changes on the mechanical properties of alloys near composition TiNi. *Journal of Applied Physics, Volume 34* , pp. 1475-1477.

Buesgen, T., Feydt, J., Hassdorf, R., Thienhaus, S., & Moske, M. (2004, July 29). Ab initio calculations of structure and lattice dynamics in Ni-Mn-Al shape memory alloys. *Physical Review B, Vol. 70* , p. PhysRevB.70.014111.

Bungartz, H.-J., Zimmer, S., Buchholz, M., & Pflüger, D. (2009). *Modellbildung und Simulation.* Berlin, Heidelberg: Springer-Verlag.

Chmielus, M. (2010). *Doctoral Dissertation: Composition, Structure and Magneto-Mechanical Properties of Ni-Mn-Ga Magnetic Shape-Memory Alloys.* Berlin: Logos Verlag Berlin GmbH 2010.

Claeys, P., & Vogel, A. (2006). *Patent No. DE 10 2004 056 279 A1*. Germany.

ETO Group. (2013). *MAGNETOSHAPE Brochure.* Stockach: ETO Group.

ETO MAGNETIC GmbH. (2012). *ETO Akademie: Magnetismus Aktorauslegung für Konstrukteure.* Stockach: ETO Stockach.

Faidley, L. (2006). *Doctoral Dissertation: Characterization and modeling of ferromagnetic shape memory Ni-Mn-Ga in a collinear stress-field configuration.* Columbus, Ohio, USA: Graduate School of The Ohio State University.

Feynman, R., Leighton, R., & Sands, M. (2007). *Feynman-Vorlesungen über Physik: Band II: Elektromagnetismus und Struktur der Materie.* Munich, Germany: Oldenbourg.

FUJIFILM Europe GmbH. (2007, October 18). Retrieved April 17, 2014, from http://www.fujifilm.eu: http://www.fujifilm.eu/fileadmin/products/prescale/media/Prescale_Film_Brochure_klein_e.pdf

Gauthier, J., Hubert, A., Abadie, J., Lexcellent, C., & Chaillet, N. (2006, June). Multistable actuator based on magnetic shape memory alloy. *Proceedings of the 10th International Conference on New Actuators, ACTUATOR'06, Bremen* , pp. 787-790.

Gruner, M., Entel, P., Opahle, I., & Richter, M. (2008, March 13). Ab initio investigation of twin boundary motion in the magnetic shape memory Heusler alloy Ni2MnGa. *Journal of Materials Science, Vol. 43* , pp. 3825-3831.

Gümpel, P. (2004). *Formgedächtnislegierungen: Einsatzmöglichkeiten in Maschinenbau, Medizintechnik und Aktuatorik.* Renningen: expert verlag.

Heczko, O. (2004, December 15). Determination of ordinary magnetostriction in Ni–Mn–Ga magnetic shape memory alloy. *Journal of Magnetism and Magnetic Materials* , pp. 846-849.

Heczko, O. (2005, April). Magnetic shape memory effect and magnetization reversal. *Journal of Magnetism and Magnetic Materials, Vol. 2* , pp. 290-291.

Heusler, F. (1903). Über magnetische Manganlegierungen. *Verhandlungen der Deutschen Physikalischen Gesellschaft 5* , p. 219.

Holz, B., & Janocha, H. (2010). MSM Actuators – Magnetic Circuit Concepts and Operating Modes. *Proc. 12th International Conference on New Actuators* (pp. 307-310). Bremen: Messe Bremen.

Hunt, F. (1947, July). A Survey of Magnetostriction Transducer Research at the Harvard Underwater Sound Laboratory 1941-1945. *The Journal of the acoustical society of America, Volume 19, Number 4* , p. 725.

James, R., & Wuttig, M. (1998). Magnetostriction of martensite. *Philosophical Magazine A, Vol. 77 No. 5* , pp. 1273-1299.

Janocha, H. (2013). *Unkonventionelle Aktoren.* München: Oldenbourg Verlag.

Jiles, D. (1998). *Introduction to Magnetism and Magnetic Materials, 2nd Edition.* London & New York: Chapman and Hall.

Jiles, D., & Devine, M. (1994, November). Recent developments in modeling of the stress derivative of magnetization in Recent developments in modeling of the stress derivative of magnetization in ferromagnetic materials. *Journal of Applied Physics, Vol. 76, No. 10* , pp. pp. 7015-7017.

Joule, J. (1847). On the Effects of Magnetism upon the Dimensions of Iron and Steel Bars. *The London, Edinburgh and Dublin philosophical magazine and journal of science (Taylor & Francis)* , pp. 225–241.

Kallenbach, E., Eick, R., Quendt, P., Ströhla, T., Feindt, K., Kallenbach, M., et al. (2012). *Elektromagnete.* Wiesbaden: Vieweg+Teubner Verlag.

Karaman, I., & Lagoudas, C. (2006, January 29). TEES Final Progress Report to ARO on the project, "Magnetic Shape Memory Alloys with High Actuation Forces". Texas, USA.

Keilig, R. (2007). *Doctoral Dissertation: Entwurf von schnellschaltenden (hochdynamischen) neutralen Elektromagnetsystemen.* Illmenau, Germany: Universität Illmenau.

Kiang, J., & Tong, L. (2009, Dezember 8). Nonlinear magneto-mechanical finite element analysis of Ni–Mn–Ga single crystals. *Smart Materials and Structures, Volume 19, Number 1* , p. 015017.

Kiefer, B. (2006). *Doctoral Dissertation: A Phenomenological Constitutive Model for Magnetic Shape Memory Alloys.* Texas: Texas A&M University, Department of Aerospace Engineering.

Kittel, C. (2006). *Einführung in die Festkörperphysik.* Munich: Oldenbourg Verlag.

Koch, J. (1988). *Piezoxide (PXE) – Eigenschaften und Anwendungen.* Heidelberg: Dr. Alfred Hüthig Verlag.

Kopitzki, K., & Herzog, P. (2007). *Einführung in die Festkörperphysik, 6. Auflage.* Wiesbaden: Vieweg+Teubner Verlag.

Koyama, T. (2008, March 13). Phase-field modeling of microstructure evolutions in magnetic materials. *Science and Technology of Advanced Materials, Vol. 9, No. 1* , pp. 1-9.

Krevet, B. (2010). FEM simulation of a Ni–Mn–Ga film bridge actuator. *3rd International Symposium on Shape Memory Materials for Smart Systems/E-MRS 2010 Spring Meeting* (pp. 154-161). Strasbourg, France: Elsevier.

Lagoudas, D. (2008). *Shape Memory Alloys: Modeling and Engineering Applications.* New York: Springer Science+Business Media.

Langbein, S., & Czechowicz, A. (2013). *Konstruktionspraxis Formgedächtnistechnik.* Springer Fachmedien: Wiesbaden.

Laufenberg, M., & Schiepp, T. (2014a). *Patent No. De 10 2013 107 744 A1.* Germany.

Laufenberg, M., & Schiepp, T. (2013). *Patent No. De102013110253A1.* Germany.

Laufenberg, M., & Schiepp, T. (2014b). *Patent No. WO 2014/019738.* Worldwide.

Lee, T., & Aksay, I. (2001, May 03). Hierarchical Structure-Ferroelectricity Relationships of Barium Titanate Particles. *Crystal Growth & Design, Vol.1, No.5* , pp. 401-419.

Liebermann, H., & Graham Jr., C. (1977, July). Plastic and magnetoplastic deformation of Dy single crystals. *Acta Metallurgica, Volume 27, Issue 7* , pp. 715-720.

Likhachev, A., & Ullakko, K. (2000). Quantitaive Model of Large Magnetostrain Effect in Ferronagnetic Shape Memory Alloys. *Physics Letters A, Vol. 275 No. 1-2* , pp. 142-151.

Linnemann, K. (2007). *Doctoral Dissertation: Magnetostriktive und piezoelektrische Materialien - Konstitutive Modellierung und Finite-Element-Formulierung.* Karlsruhe, Germany: Universität Karlsruhe (TH) Institut für Baustatik.

Liu, Y., & Xie, Z. (2007). Detwinning in Shape Memory Alloy. *Progress in Smart Materials and Structures* , pp. 29-65.

Majewska, K., Zak, A., & Ostachowicz, W. (2007, October 17). Magnetic shape memory alloys for forced vibration control of beam-like structures. *Smart Materials and Structures, Vol. 16* , pp. 2388-2397.

Maricourt, P. (1904). *The letter of Petrus Peregrinus on the magnet, A.D. 1269.* New York: McGraw publishing company.

Marioni, M., O'Handley, R., & Allen, S. (2003, November 3). Pulsed magnetic field-induced actuation of Ni–Mn–Ga single crystals. *Appl. Phys. Lett., Volume 83* , pp. 3966-3968.

Mayer-Kuckuk, T. (1997). *Atomphysik: Eine Einführung, Auflage: 5.* Stuttgart: Teubner Verlag.

Meeker, D. (2013). *FEMM Reference Manual.* Meeker, D.C.

Meeker, D. (2012). *Finite Element Method Magnetics.* Version 4.2 (11Apr2012 Build): http://www.femm.info.

Mennerich, C., Wendler, F., Jainta, M., & Nestler, B. (2011, June 19). A phase-field model for the magnetic shape memory effect. *Archives of Mechanics, Vol. 63, No 5-6* , pp. 549-571.

Miettinen, K. (1999). *Nonlinear Multiobjective Optimization.* Norwell, Massachusetts, USA: Springer Science & Business Media.

Mohammed, O., Demerdash, N., & Nehl, T. (1983, September). Nonlinear Three Dimensional Field Computation Methods in Laminated Iron Cores Under Saturated Conditions. *IEEE Transactions on Magnetics, Vol. 19, Iss. 5* , pp. 2091-2093.

Mohd Jani, J., Leary, M., Subic, A., & Gibson, M. (2013, November 16). A review of shape memory alloy research, applications and opportunities. *Materials and Design* , pp. 1078-1113.

Müllner, P., Chernenko, V., Mukherji, D., & Kostorz, G. (2004). Cyclic magnetic-field-induced deformation and magneto-mechanical fatigue of Ni-Mn-Ga ferromagnetic martensites. *MRS symposium Materials and devices for smart systems* (pp. 415-420). Boston: MRS Symp. Proc. 785.

Niskanen, A., & Laitinen, I. (2012, September). Design and Simulation of a Magnetic Shape Memory (MSM) Alloy Energy Harvester. *Advances in Science and Technology, Vol. 78* , pp. 58-62.

Nyce, D. (2003). *Linear Position Sensors: Theory and Application.* New Jersey: John Wiley & Sons.

Olabi, A., & Grunwald, A. (2007, January 11). Design and application of magnetostrictive materials. *Materials and Design* , pp. 469-483.

Otsuka, K., & Wayman, C. (1999). *Shape Memory Materials.* Cambridge, United Kingdom: Cambridge University Press.

Otsuka, K., Ohba, T., Tokonami, M., & Wayman, C. (1994, June 15). New description of long period stacking order structures of martensites in beta-phase alloys. *Scripta Metallurgica et Materialia, Volume 30, Issue 12,* , pp. 1605-1610.

Pagounis, E., & Schmidt, H. (2012). Progress in developing smart magnetic materials for advanced actuator solutions. *Actuator 2012* (pp. 317-322). Bremen: Messe Bremen.

Pagounis, E., Chulist, R., Szczerba, M., & Laufenberg, M. (2014, April 03). High-temperature magnetic shape memory actuation in a Ni–Mn–Ga single crystal. *Acta Materialia* , pp. 1-3.

Pagounis, E., Maier, M., & Laufenberg, M. (2011). Properties of large Ni-Mn-Ga single crystals with a predominant 5M-martensitic structure. *International Conference on Ferromagnetic Shape Memory Alloys* (pp. 207-208). Dresden: International Conference on Ferromagnetic Shape Memory Alloys.

Pearson, K. (1901). *On the Correlation of Characters not Quantitatively Measurable.* London: Philosophical Transactions Of The Royal Society Of London.

Physik Instrumente GmbH & Co. KG. (2012). *Piezoelektrische Aktoren.* Lederhose: PI Ceramic GmbH.

Rechenberg, I. (1994). *Evolutionsstrategie '94.* Stuttgart: Frommann-Holzboog.

Roos, S. (2015). *1-D simulation of MSM Actuators.* Konstanz, Germany: University of applied sciences, HTWG Konstanz.

Schäfer, S. (2012). *Master Thesis: Entwicklung von Optimierungsalgorithmen zur automatisierten Magnetkreisauslegung auf Basis der Evolutionsstrategie.* Stockach: ETO MAGNETIC.

Schiepp, T., Detkov, V., Maier, M., Pagounis, E., & Laufenberg, M. (2013). Failure mechanisms and high-cycle fatigue of MSM actuators. *ICFSMA13*, (pp. 48-49). Boise, Idaho.

Schiepp, T., Laufenberg, M., Maier, M., & Pagounis, E. (2011). Simulation of MSM actuators for engineering applications.

Schiepp, T., Laufenberg, M., Pagounis, E., & Maier, M. (2011). Simulation of MSM actuators for engineering applications. *ICFSMA11* (pp. 147-148). Dresden, Germany: IFW Dresden.

Schiepp, T., Maier, M., Pagounis, E., Schlüter, A., & Laufenberg, M. (2013). FEM-Simulation of Magnetic Shape Memory Actuators. *COMPUMAG2013*, (pp. PB6-10). Budapest.

Schiepp, T., Maier, M., Pagounis, E., Schlüter, A., & Laufenberg, M. (2014, February 26). FEM-SIMULATION OF MAGNETIC SHAPE MEMORY ACTUATORS. *IEEE Transactions on Magnetics, Vol. 50, No.2* , p. 10.1109/TMAG.2013.2279205 .

Schiepp, T., Schlüter, A., Schäfer, S., Maier, M., & Laufenberg, M. (2014). Optimization of Magnetic Shape Memory Actuators using Evolutionary Algorithms. *CEFC Annecy.* France: to be published.

Schneider, P. (2000). FEM-gestützte Ableitung von Magnetkreismodellen für elektromagnetische Aktoren. *18. CAD-FEM User´s Meeting* (pp. 1-8). Graf Zeppelin-Haus, Friedrichshafen: Fraunhofer-Gesellschaft, München.

Schöppner, C. (2011). *Diplomarbeit: Untersuchung einkristalliner magnetischer Formgedächtnislegierungen mittels Ferromagnetischer Resonanz.* Duisburg: Fakultät für Physik der Universität Duisburg-Essen.

Sclater, N. (2011). *Mechanisms and Mechanical Devices Sourcebook, 5th Edition.* New York, Chicago, San Francisco, Lisbon, London, Madrid, Mexico City, Milan, New Delhi, San Juan, Seoul, Singapore, Sydney, Toronto: McGraw-Hill Professional.

Smith, R. (2005). *Smart Material Systems: Model Development.* Philadelphia: Society for Industrial and Applied Mathematics.

Sozinov, A., Lanska, N., Soroka, A., & Zou, W. (2013, January 14). 12% magnetic field-induced strain in Ni-Mn-Ga-based non-modulated martensite. *Applied Physics Letters, Vol. 102, Iss. 2* , pp. 1-5.

Sozinov, A., Likhachev, A. A., & Ullakko, K. (2002). Crystal Structures and Magnetic Anisotropy Properties of Ni-Mn-Ga Martensitic Phases with Giant Magnetic-Field-Unduced Strain. *IEEE Trans. Magn., vol.38, no. 5* , pp. 2814-2814.

Steingroever, E., & Ross, G. (2009). *Messverfahren der Magnettechnik.* Köln: MAGNET-PHYSIK Dr. Steingroever GmbH.

Stephan, J., Pagounis, E., Laufenberg, M., Paul, O., & Ruther, P. (2011, Mai 23). A novel concept for strain sensing based on the ferromagnetic shape memory alloy NiMnGa. *Sensors Journal, IEEE* , pp. 2683-2689.

Straka, L. (2007). *Doctoral Dissertation: Magnetic and Magneto-Mechanical Properties of Ni-Mn-Ga Magnetic Shape Memory Alloys.* Helsinky, Finnland: Helsinki University of Technology.

Suorsa, I. (2005). *Doctoral Dissertation: Performance and Modeling of Magnetic Shape Memory Actuators and Sensors.* Espoo, Finland: Aalto University of Technology.

Suorsa, I., & Pagounis, E. (2004, May 01). Magnetic field-induced stress in the Ni–Mn–Ga magnetic shape memory alloy. *Journal of Applied Physics, Vol. 95* , pp. 4958-4961.

Tellinen, J. (1998). A Simple Scalar Model for Magnetic Hysteresis. *IEEE Trans. on Magnetics, Vol. 34 No. 4* , pp. 2200-2206.

Tichý, J., Erhart, J., Kittinger, E., & Prívratská, J. (2010). *Fundamentals of Piezoelectric Sensorics: Mechanical, Dielectric, and Thermodynamical Properties of Piezoelectric Materials.* Berlin, Heidelberg: Springer-Verlag.

Tickle, R., James, R., Shield, T., Wuttig, M., & Kokorin, V. (1999). Ferromagnetic shape memory in NiMnGa system. *IEEE Trans. on Magnetics, Vol. 35 No. 35* , pp. 4301-4310.

Tipler, P., & Mosca, G. (2004). *Physik Für Wissenschaftler und Ingenieure*. Munich, Germany: Elsevier.

Ullakko, K. (1996). Magnetically controlled shape memory alloys: A new class of actuator materials. *Journal of Materials Engineering and Performance, Vol. 5* , pp. 405-409.

Ullakko, K., Huang, J., Kantner, C., & O'Handley, R. (1996, September). Large magnetic-field-induced strains in Ni MnGa single crystals. *Appl.Phys. Lett., Vol. 69, No. 13* , pp. 1966–1968.

Ullakko, K., Huang, J., Kokorin, V., & O'Handley, R. (1997). Magnetically Controlled Shape Memory Effect in Ni2MnGa Intermetallics. *Scripta Materialia, Vol.36* , pp. 1133-1138.

Ullakko, K., Jakovenko, P., & Gavriljuk, V. (1996, August). High-strength shape memory steels alloyed with nitrogen. *Scripta Materialia, Volume 35, Issue 4* , pp. 473-476.

von Hippel, A. (1950, July 1). Ferroelectricity, Domain Structure, and Phase Transitions of Barium Titanate. *Reviews of Modern Physics, Volume 22, Issue 3,* , pp. 221-237.

Watkins, F. (1833, January 1). On the Magnetic Powers of Soft Iron. *Philosophical Transactions of the Royal Society of London* , pp. 333-342.

Weicker, K. (2007). *Evolutionäre Algorithmen.* Leipzig: Vieweg+Teubner Verlag.

Yang, J., Chen, H., & Wayman, C. (1992, May 01). Development of Fe-based shape memory alloys associated with face-centered cubic-hexagonal close-packed martensitic transformations: Part I. shape memory behavior. *Metallurgical Transactions A, Vol. 23, Iss. 5* , pp. 1431-1437.

Ziske, J., Ehle, F., Neubert, H., Price, A., & Lienig, J. (2014). A Simple Phenomenological Model for Magnetic Shape Memory Actuators. *IEEE Transactions on Magnetics* , pp. 1-9.

Zupan, M., Ashby, M., & Fleck, N. (2002, December 12). Actuator Classification and Selection - The Development of a Database. *Advanced Engineering Materials, Volume 4, Issue 12* , pp. 933-940.

APPENDICES

In this appendix some diagrams have been presented to demonstrate the procedures of the three simulation methods proposed, designed and developed in this thesis. A numerical example is also provided for each simulation method.

APPENDIX A Stress Based Simulation (SBS)

A/1 Input Data

The input data for SBS are: Actuator geometry, MSME type, twin width, magneto stress behaviour, MSME size, minimum and maximum current, twinning stress and magnetisation curves, as shown in Figure A.1.

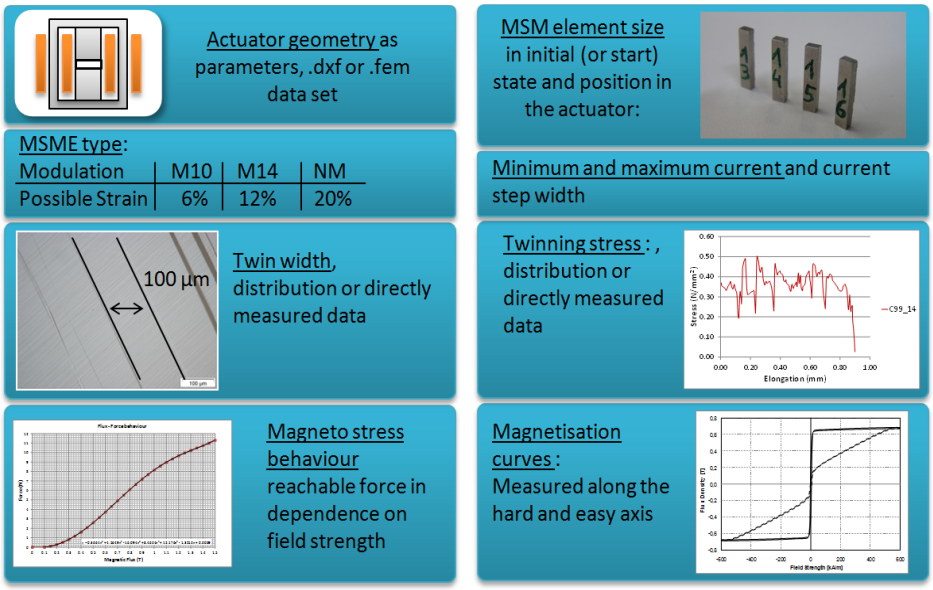

Figure A.1: Needed input data for the SBS method

A/2 Simulation procedure

There are seven steps in the SBS simulation as shown in Figure A.2:

1) Enable the Master-slave connection between Excel and FEMM
2) Load the actuator geometry and create the MSME based on the input data
3) Solve the Maxwell equations (performed by FEMM)
4) Process the magnetic fields from FEMM to Excel
5) Calculate the stress in each individual slice
6) Evaluate if this is sufficient to initiate reorientation in this slice
7) Save data of this simulation run

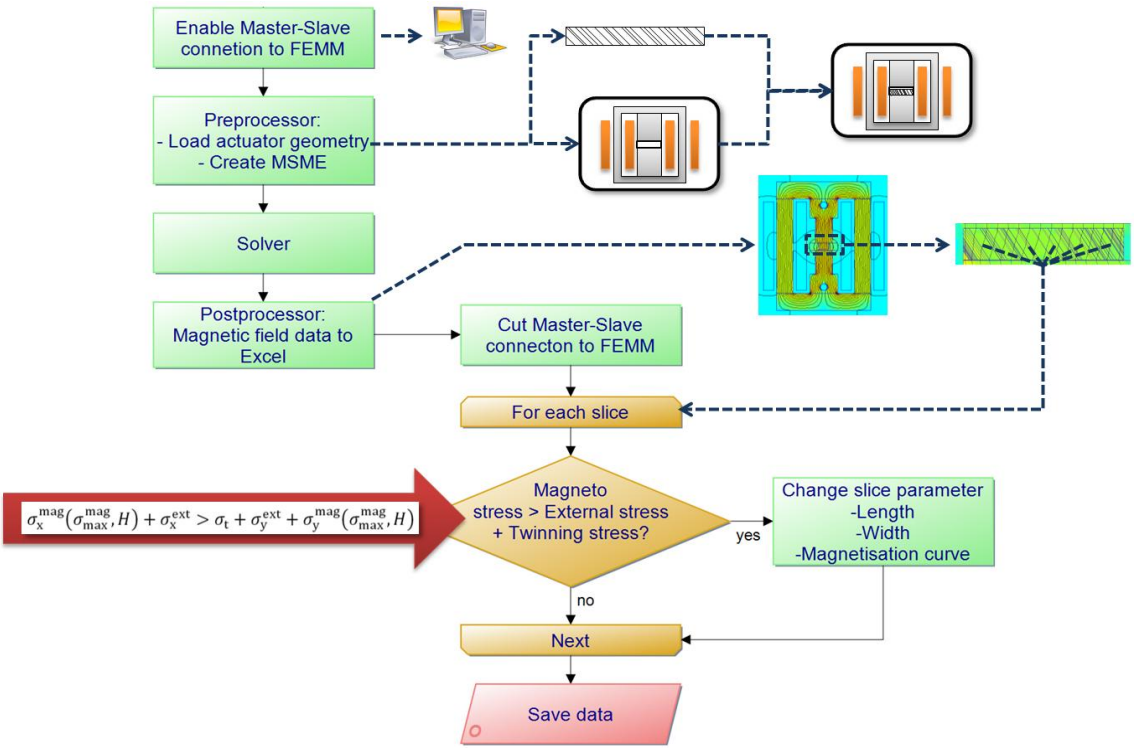

Figure A.2: The steps of the SBS simulation procedure

The first step is to enable the master-slave connection between Excel and FEMM. After this is initiated in a second step, the actuator geometry is imported into FEMM. This geometry data should include the magnetic circuit of the complete actuator, including core pieces and coils. Then the MSME is generated, where the twin boundaries are tilted by 45° with respect to the sample edges as shown in the centre of Figure A.3. This also includes the choice of the number of "slices", which should represent the behaviour of the MSME.

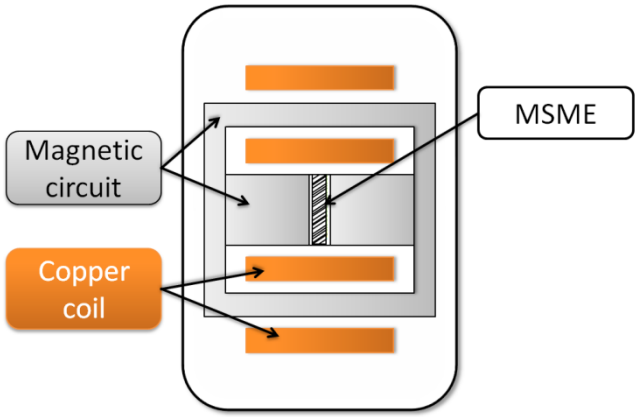

Figure A.3: Schema of an MSM actuator with MSME

In the third step the field strength is calculated by FEMM. In the fourth step the calculated magnetic fields in the inner of the MSME are transferred into Excel. In the fifth step the magneto stress in each MSM slice is individually calculated by using the Equation 4-2 also shown in Figure A.2. A exemplary calculation is shown at the bottom of Figure A.4. In this appendix a simplified example is shown; where the MSME only has three slices in the models described in this thesis, several hundred slices were used). A particular twinning stress is then assigned to each slice. In this example the twinning stress value is 0.46 N/mm² for the upper slice, 0.41 N/mm² for the middle one and 0.53

N/mm² for the lower slice. The FEM magnetic simulation is performed to calculate the resulting magnetic flux, as shown in the upper part of Figure A.4.

As long as the left part of the equation is not fulfilled, the slice will not reorient. At higher magnetic fields the reorientation occurs, when the stress in y-direction is larger than in x-direction, particularly when the magneto stress exceeds the external and internal (twinning) stress of a slice (e.g.: the middle slice on the right meets the switching condition and will be considered as switched for the next simulation step).

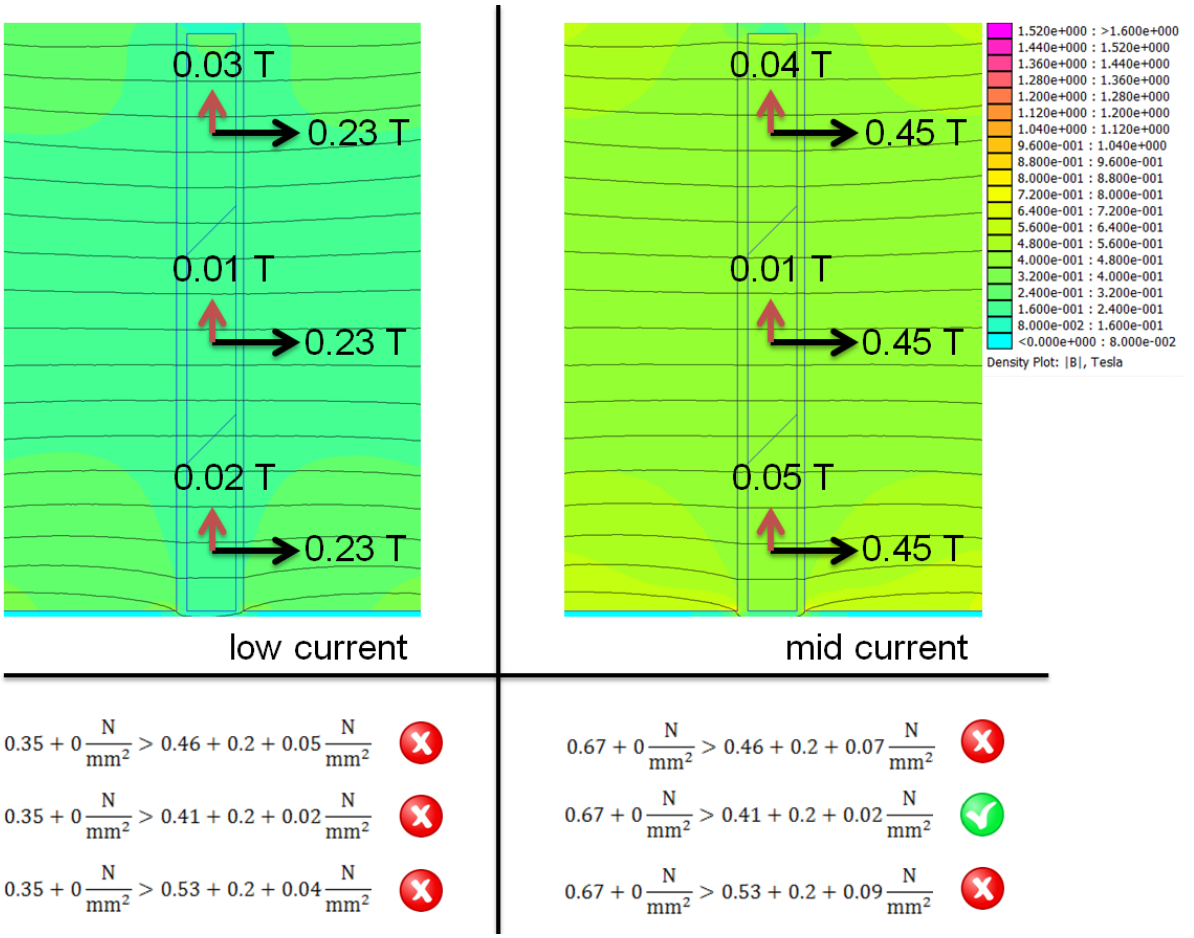

Figure A.4: Detail simulation screenshot and a typical stress calculation example

The sixth step is evaluating for every individual slice if it reorients or not. In the final step these statuses e.g. orientation, width and twinning stress of the MSME is stored in Excel so that in a following simulation this particular data can be used as a MSME history.

APPENDIX B Dynamic Magnetisation Curve (DMC)

B/1 Data Input

The input data for DMC are: actuator geometry, MSME type, twin width, magneto stress behaviour, MSME size, minimum and maximum current, twinning stress and dynamic magnetisation curves, as shown in Figure B.1. This method is less complex but the amount of mandatory data is bigger because, in contrast to the SBS, the magnetisation curves have to be measured at several strain levels, as discussed:

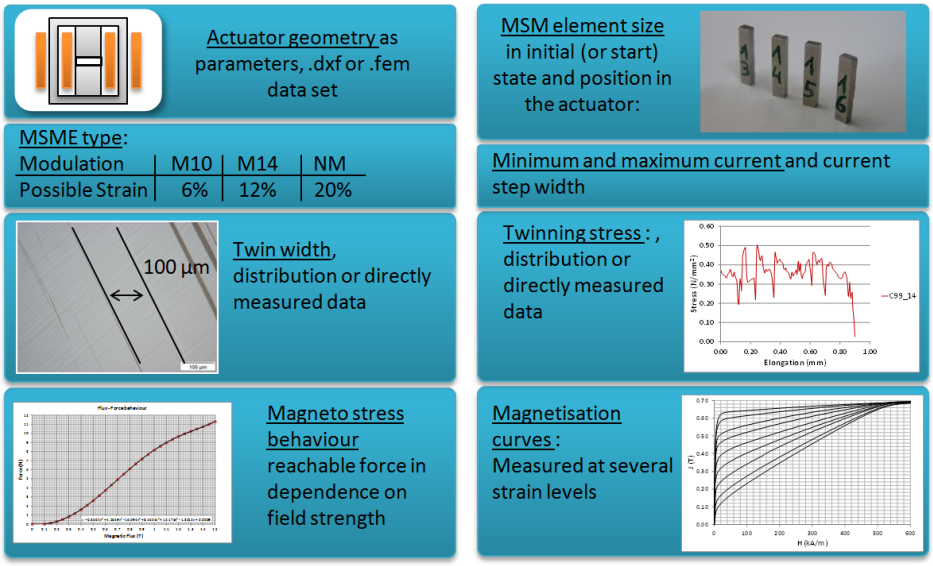

Figure B.1: The input data for the DMC approach

B/2 Simulation procedure

There are seven steps in the DMC simulation as shown in Figure B.2:

1) Enable the Master-slave connection between Excel and FEMM
2) Load the actuator geometry and create the MSME based on the input data
3) Solve the magnetic equations
4) Process the magnetic fields from FEMM to Excel
5) Calculate the stress situation in every individual slice
6) Evaluate if this is sufficient to initiate reorientation in this slice
7) Save data of this simulation run

Also the DMC method starts with the master-slave connection between Excel and FEMM and in the second step the actuator geometry is imported into FEMM, like it is done in the SBS. Also the MSME is generated in the DMC method, but this time it is treated as a black box, which means that the twin areas are not considered as slices in the FEM simulation model. The permeability of the MSME is represented with a single magnetisation curve, which describes the strain-dependent magnetic properties of the MSME. In the third step the field strength is calculated by FEMM and in the next step the calculated magnetic field value is transferred from FEMM to Excel.

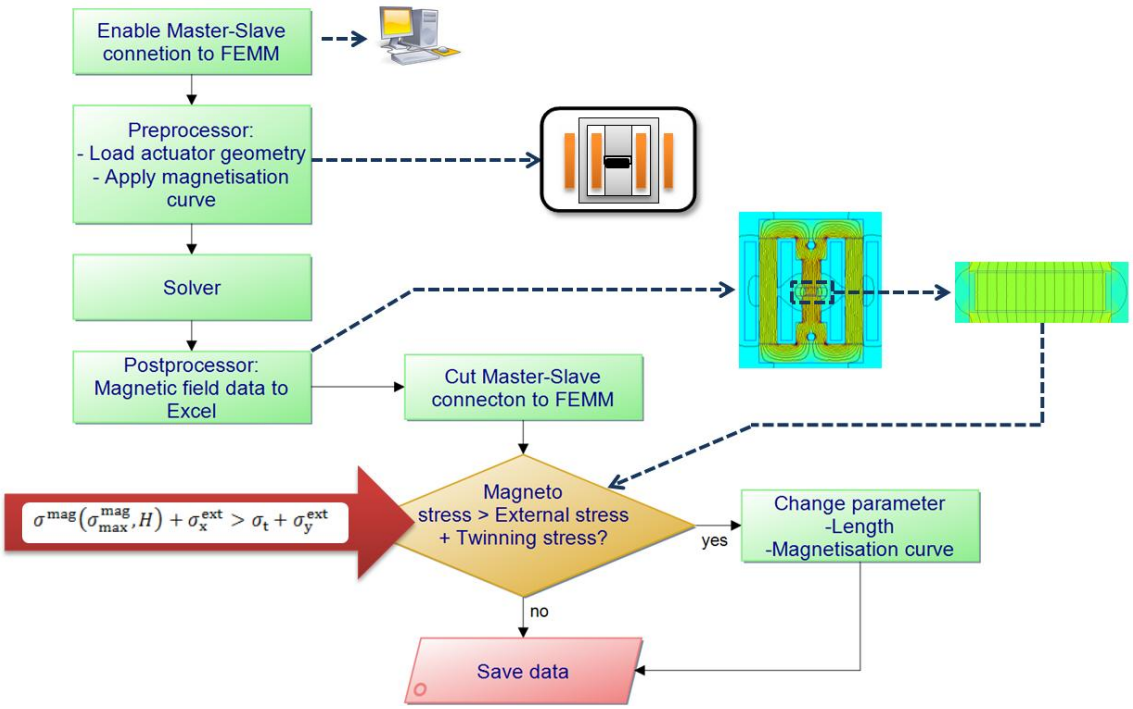

Figure B.2: Steps of the DMC simulation procedure

After the connection between FEMM and Excel is cut, the magneto stress in the MSM is calculated by using the Equation 4-3 that is the simplified form of Eq. 4-2 by neglecting the perpendicular field (also shown in Figure B.2). In the DMC method the twin structure is considered only in the Excel tool, here each twinning area is assigned a particular twinning stress value as well as geometry (width, height), to allow the calculation of the elongation of the MSME in the case that the specific slice reorients. Figure B.3 shows an example of magnetic simulation for the DMC. As discussed the simulation does not show slices, while the Excel tool considers the same number of slices of the previous example, with the same values of the twinning stress to get a better understanding of the difference of those two methods.

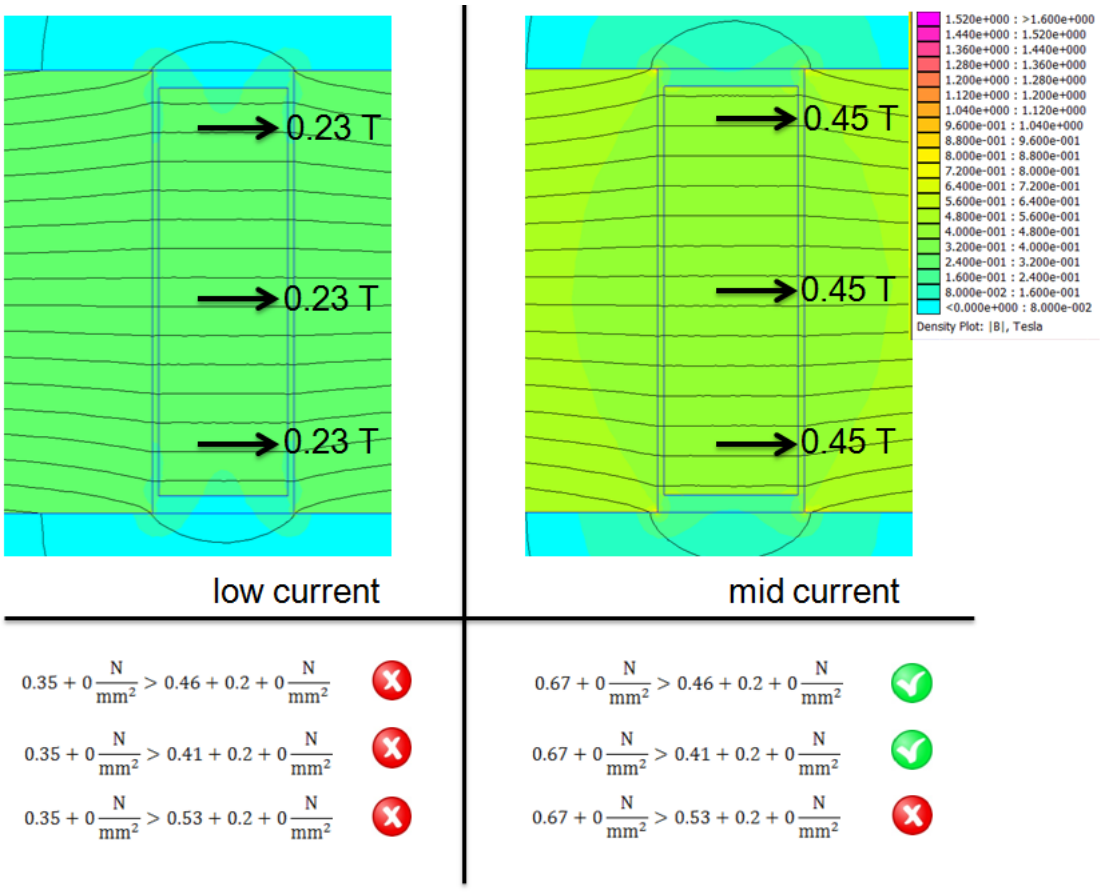

Figure B.3: Detail screenshot and exemplary stress calculation for three typical stress values

The stress situation decides which slice switches and thus the amount of strain obtained at that simulation step. Subsequently a new magnetisation curve is generated, based on the strain and fed back to the magnetic FEM simulation for the next step.

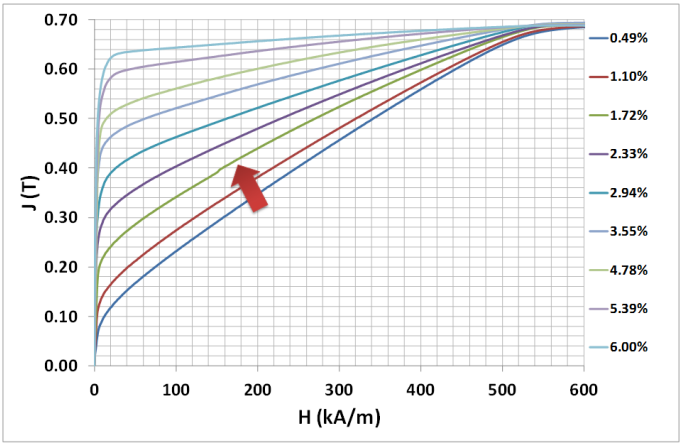

Figure B.4: Strain dependent magnetisation curves of MSM

APPENDIX C Stress Dependent Magnetisation Curve (SDM)

C/1 Data Input

The focus of this method is on the measurement data. The necessary measurements are challenging, because the permeability of MSME has to be measured under a certain pre-stress, while the MSME is elongating due to a sufficient magnetic field. The input data in SDM simulation are: MSME size, minimum and maximum current (as shown in Figure C.1):

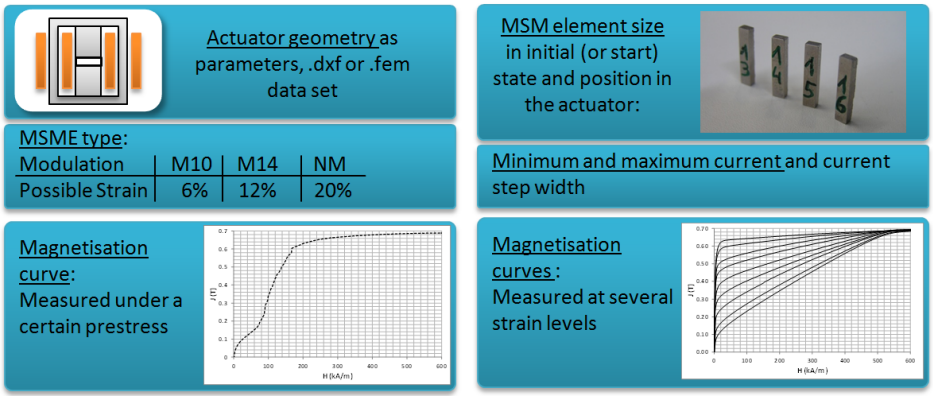

Figure C.1: Input data for the SDM approach

C/2 Simulation procedure

There are six steps in the SDM simulation as shown in Figure C.2:

1) Enable the Master-slave connection between Excel and FEMM
2) Load the actuator geometry and create the MSME based on the input data
3) Solve the magnetic equations
4) Process the magnetic fields from FEMM to Excel
5) Evaluate if the magnetic field is sufficient to initiate reorientation of the MSME
6) Save data of this simulation run

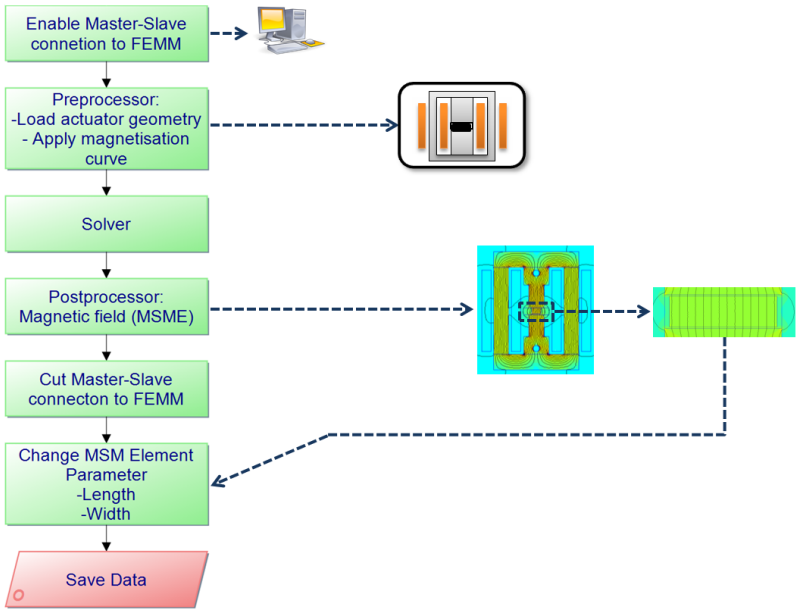

Figure C.2: Steps of the DMC simulation procedure

As shown in Figure C.2, the simulation procedure starts with the master-slave connection between Excel and FEMM and the import of the actuator geometry. Similar to the DMC method, the MSME is represented as a black box. The permeability of the MSME is described with the magnetisation curve that is measured under a certain stress during elongation in the measurement device. In the third step the FEM simulation is started and the resulting magnetic flux is calculated by using FEMM. In the fourth step the average field strength is transferred to Excel and in the fifth one is used to estimate the resulting elongation. In this simulation method all the stress calculation is integrated in the behaviour of this magnetisation curve, under a defined pre-stress; therefore it does not need to be calculated separately. The permeability of the MSME is represented with a single magnetisation curve, which describes the strain-dependent magnetic properties of the MSME and, as shown exemplary in Figure C.3, reachable elongation can be directly taken by the elongation state of the strain dependent magnetisation curve of the DMC.

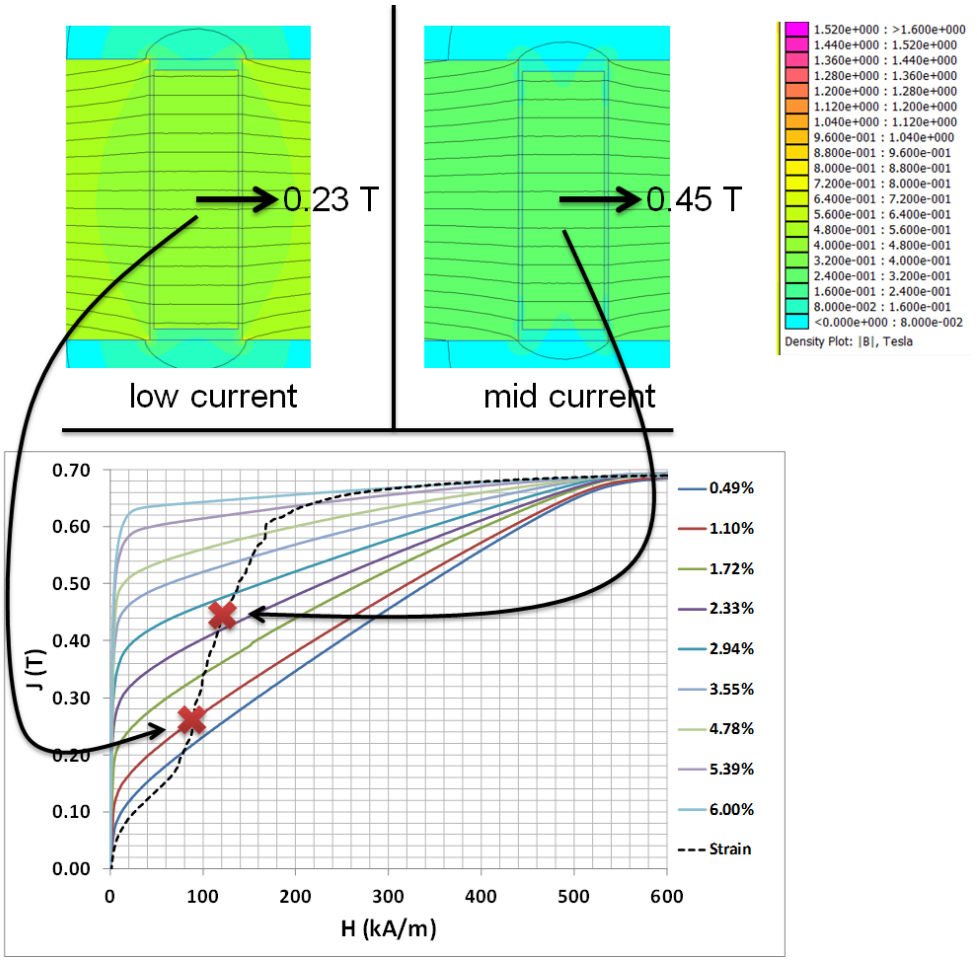

Figure C.3: Stress dependent magnetisation curve vs. several magnetisation curves at different strain levels